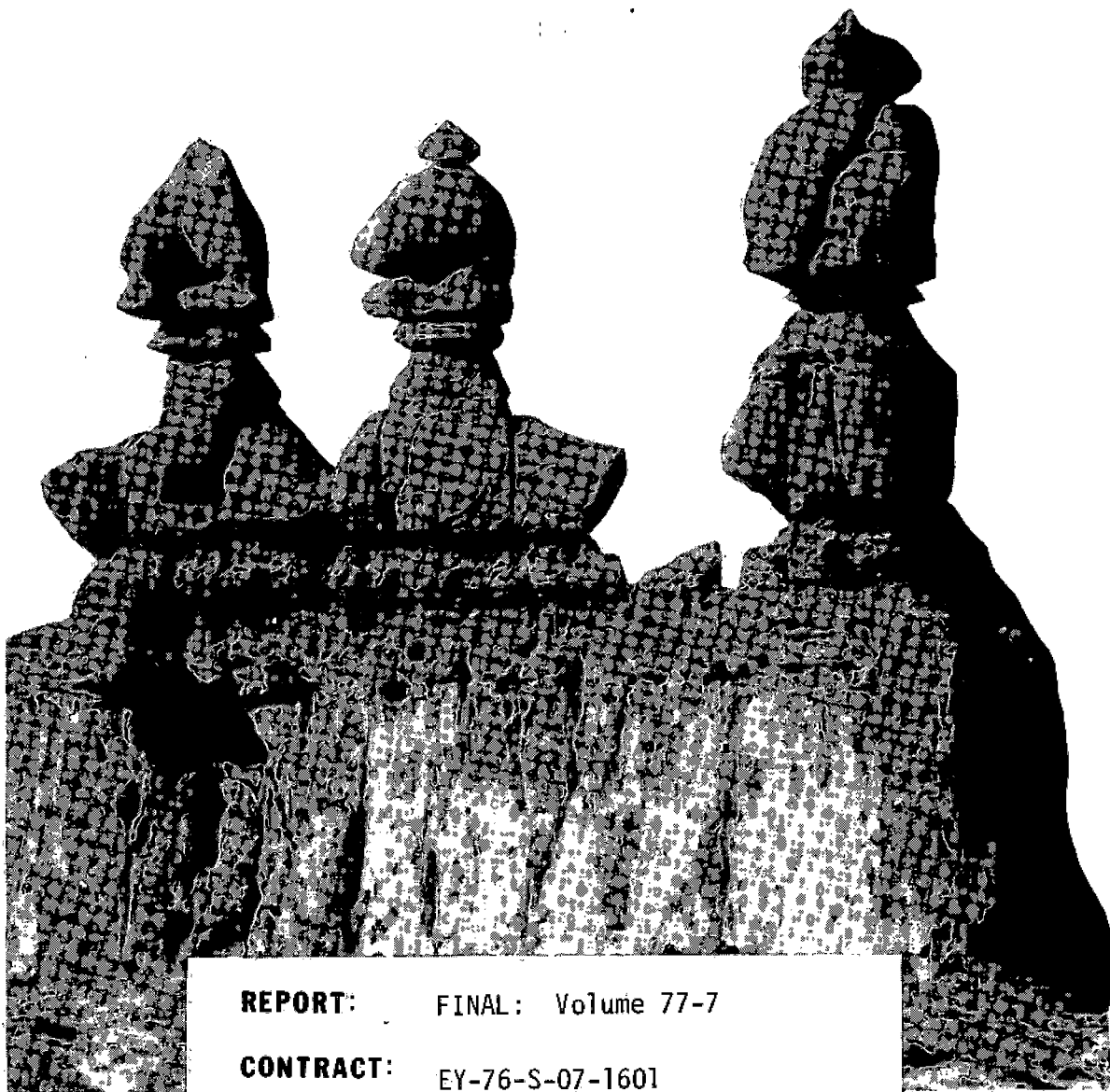


GLOII46

DEPARTMENT OF
GEOLOGY AND GEOPHYSICS



REPORT: FINAL: Volume 77-7

CONTRACT: EY-76-S-07-1601

AGENCY: DOE/DGE

TITLE: Gravity and Ground Magnetic Surveys in
the Monroe and Joseph KGRA's and Surrounding
Region, South Central Utah.

AUTHORS: Mark E. Halliday and Kenneth L. Cook

DATE: June 1978

NOTICE

This report was prepared to document work sponsored by the United States Government. Neither the United States nor its agent, the United States Department of Energy, nor any Federal employees, nor any of their contractors, subcontractors or their employees, makes any warranty, express or implied, or assumes any legal liability or responsibility for the accuracy, completeness, or usefulness of any information, apparatus, product or process disclosed, or represents that its use would not infringe privately owned rights.

NOTICE

Reference to a company or product name does not imply approval or recommendation of the product by the University of Utah or the U.S. Department of Energy to the exclusion of others that may be suitable.

GRAVITY AND GROUND MAGNETIC SURVEYS
IN THE MONROE AND JOSEPH KGRA'S
AND SURROUNDING REGION, SOUTH CENTRAL UTAH

by

Mark E. Halliday and Kenneth L. Cook

PREFACE

The attached report was submitted by Mark E. Halliday in partial fulfillment of the requirements for the degree of Master of Science in Geophysics, Department of Geology and Geophysics at the University of Utah. The work was performed under the direction of Dr. Kenneth L. Cook.

ABSTRACT

During the summer of 1977, regional gravity data were collected in portions of the Pavant Range, Tushar Mountains, northern Sevier Plateau, the Antelope Range, and throughout Sevier Valley approximately between the towns of Richfield and Junction, Utah. Additionally, detailed gravity and ground magnetic data were collected in the vicinity of hot springs in both the Monroe and Joseph Known Geothermal Resource Areas (KGRA's).

The regional gravity data were terrain corrected out to a distance of 167 km from the station and 948 gravity station values were compiled into a complete Bouguer gravity anomaly map of the survey area. Major features of this map include: 1) a pronounced regional gravity gradient associated with the Pavant thrust along which dense Paleozoic carbonate rocks structurally emplaced over Mesozoic sedimentary rocks are exposed not far from low-density volcanic rocks of the Marysvale volcanic field; 2) gravity lows over the alluvial-filled grabens of Sevier Valley and Marysvale Valley; 3) strong gravity gradients associated with the Sevier, Elsinore, Dry Wash, and Tushar faults; 4) gravity lows over the Mount Belknap, Red Hills, and Big John calderas; and 5) east-northeast-trending gravity contours in alignment with a belt of Tertiary intrusive rocks and the Wah-Wah-Tushar mineral belt of southern Utah.

Modeling of four regional gravity profiles throughout the survey

area indicates that: 1) the Sevier Valley graben has an alluvial-fill about 1300 m in depth and Marysvale Valley graben has an alluvial-fill about 1200 m in depth; 2) the regional gravity gradient in the southern Pavant Range may be largely due to changes in densities of sedimentary rocks across the Cordilleran hingeline, and only partly the result of changes in the depth to the Moho across the Basin and Range-Colorado Plateau transition; and 3) the Mount Belknap caldera gravity low may be due to low-density Tertiary volcanic fill in the caldera surrounded by sedimentary and intrusive rocks. Polynomial residual gravity anomaly maps were helpful in delineating a closed gravity low in the Pavant Range which may be related to a volcanic source area.

A total of 840 ground magnetic stations established along 19 profiles in the Monroe KGRA were compiled into a diurnal-corrected total magnetic intensity anomaly map. Major features of this map include: 1) a magnetic anomaly of about 700 gammas relief across the Red Hill Hot Spring with the magnetic high on the Sevier Valley side of the hot spring; and 2) a linear magnetic low along the Monroe Hot Springs area. These magnetic features are believed to be due to alteration of magnetite in the alluvium by thermal waters rising along the Sevier fault zone. Modeling of gravity and magnetic profiles in the Monroe KGRA shows the faulting to consist of many individual en echelon faults along the Sevier fault zone instead of one large fault.

Detailed gravity and ground magnetic data were also collected along two profiles in the Joseph KGRA. Modeling of gravity and magnetic data along one of these profiles indicates: 1) relatively

little throw along the Dry Wash fault, which controls the Joseph Hot Springs; and 2) the existence of a larger fault of about 800 m throw (down on the east) farther west in the valley near the Sevier River.

The results of this work have provided valuable information regarding large-scale faults throughout the survey area and particularly about faults which control hot springs in the Monroe and Joseph KGRA's. Such information should be of significant help in properly locating future test or production drill holes designed to tap the geothermal energy resources of this region.

ACKNOWLEDGMENTS

I wish to thank Dr. K. L. Cook, Dr. R. L. Bruhn, and Dr. D. S. Chapman, members of my supervisory committee, for their numerous consultations and critical reviews of this manuscript. Charles Mase, Brad Taylor, and Jean Chu, students at the University of Utah, assisted in the acquisition of field data.

The friendly people of Sevier and Piute counties helped to make the field work an enjoyable experience. Mayor Norris Jensen of Monroe, Utah and Ms. Lucy DeLuke of Marysvale, Utah helped with special logistical problems.

Members of the U. S. Geological Survey provided special assistance. Donald Plouff was helpful in solving terrain correction problems. C. G. Cunningham and T. A. Steven helped to expand my geological knowledge of the survey area.

Dr. Jerry R Montgomery of ASARCO generously provided the polynomial fitting program used in processing of the gravity data. My appreciation is expressed to those students preceding me who have developed the computer software used throughout this project.

Financial support was provided by the U. S. Department of Energy under contract number EY-76-S-07-1601. I am also appreciative of the support provided as recipient of the ASARCO Fellowship in Geophysics at the University of Utah during the Autumn and Winter quarters of the academic year 1976-1977 and the summer of 1977.

TABLE OF CONTENTS

	Page
ABSTRACT	iv
ACKNOWLEDGMENTS	vii
LIST OF ILLUSTRATIONS	x
INTRODUCTION	1
Purpose	4
Location	4
Physiography	6
Previous Investigations	6
GEOLOGY	13
Stratigraphy	13
Structure	17
Geologic Control Data	23
DATA ACQUISITION	30
Instrumentation	30
Regional Gravity Data	30
Detailed Gravity Data	31
Detailed Ground Magnetic Data	32
DATA REDUCTION	36
Gravity Data Reduction	36
Gravity Terrain Corrections	37
Ground Magnetic Data Reduction	42
Error Analysis	44
DATA PROCESSING	51
Preparation of Data	51
Polynomial Surface Filtering	54

TABLE OF CONTENTS (CONTINUED)

	Page
INTERPRETATION.	64
Methods of Interpretation.	64
Regional Gravity Survey.	69
1) Complete Bouguer Gravity Anomaly Map	69
2) Polynomial Surface and Residual Gravity Anomaly Maps	72
3) Interpretive Geologic Cross Sections	74
a) Sevier Valley Profile	74
b) Pavant Range - Marysvale Valley Profile . . .	76
c) Mount Belknap Caldera Profile	79
d) Tushar Mountains - Sevier Plateau Profile . .	81
Detailed Gravity and Ground Magnetic Surveys	83
1) Monroe Hot Springs Area.	83
a) Total Magnetic Intensity Anomaly Map.	83
b) Red Hill Magnetic Profile (M77-1)	84
c) Red Hill Gravity Profile ("RH")	86
d) SS Canyon Magnetic Profile (M77-14)	88
e) Sand Canyon Gravity Profile ("SC")	90
2) Joseph Hot Springs Area.	90
a) Joseph Magnetic Profile (J2).	90
b) Joseph Gravity Profile (J2)	93
SUMMARY AND CONCLUSIONS	96
APPENDIX 1 - Description of Field Base Stations	101
APPENDIX 2 - Gravity Base Station Ties.	102
APPENDIX 3 - Geologic Control Data Relevant to the Regional Gravity Survey	103
APPENDIX 4 - Geologic Control Data Relevant to the Detailed Gravity and Ground Magnetic Surveys.	105
APPENDIX 5 - Principal Facts of Gravity Data.	107
APPENDIX 6 - Principal Facts of Ground Magnetic Data.	143
REFERENCES.	154
VITA.	164

LIST OF ILLUSTRATIONS

Figures

<u>Figure</u>	<u>Figures</u>	<u>Page</u>
1	Map of Utah showing area covered by regional gravity survey	2
2	Map of survey area showing major geographic features and location of Monroe and Joseph Known Geothermal Resource Areas (KGRA's)	3
3	U.S.G.S. 15-minute topographic quadrangle of Monroe showing detailed gravity and ground magnetic survey areas	5
4	Total ground magnetic intensity anomaly map of the Red Hill Hot Spring detailed grid. From 1976 Gravity and Magnetics class, Univ. of Utah, under supervision of Dr. K. L. Cook.	9
5	Total ground magnetic intensity anomaly map of the Joseph Hot Springs detailed grid. From 1976 Gravity and Magnetics class, Univ. of Utah, under supervision of Dr. K. L. Cook.	10
6	Total intensity aeromagnetic map of a portion of Utah, from Zietz and others (1976). Area of regional gravity survey is outlined	11
7	Generalized stratigraphic column for rocks within the survey area	14
8	Generalized lithologic map of the survey area	15
9	Explanation of symbols used in geologic structure map	18
10	Geologic structure map of the survey area	19
11	Map of survey area showing locations and densities (gm/cc) of rock samples collected. See Appendix 3 for description of samples.	24

LIST OF ILLUSTRATIONS (Continued)

<u>Figure</u>		<u>Page</u>
12	Map of Monroe Hot Springs area showing location of detailed gravity and ground magnetic profiles . . .	33
13	Map of Joseph Hot Springs area showing location of detailed gravity and ground magnetic profiles. . .	34
14	Complete Bouguer gravity anomaly map of the survey area	38
15	Total magnetic intensity anomaly map of the Monroe Hot Springs area.	43
16	Complete Bouguer gravity anomaly map of the Mount Belknap caldera region. Density of 2.67 gm/cc was used for Bouguer and terrain corrections	48
17	Complete Bouguer gravity anomaly map of the Mount Belknap caldera region. Density of 2.50 gm/cc was used for Bouguer and terrain corrections	49
18	Complete Bouguer gravity anomaly map of the survey area. Machine-contoured from 1-km digitized data.	53
19	R.M.S. residual vs. order of polynomial surface determined for gridded gravity data. Arrows show order of surfaces and residual maps selected for analysis.	55
20	3rd-order polynomial surface gravity anomaly map. . .	56
21	5th-order polynomial surface gravity anomaly map. . .	57
22	7th-order polynomial surface gravity anomaly map. . .	58
23	10th-order polynomial surface gravity anomaly map . .	59
24	3rd-order polynomial residual gravity anomaly map . .	60
25	5th-order polynomial residual gravity anomaly map . .	61
26	7th-order polynomial residual gravity anomaly map . .	62
27	10th-order polynomial residual gravity anomaly map	63

LIST OF ILLUSTRATIONS (Continued)

<u>Figure</u>		<u>Page</u>
28	Map of survey area showing location of gravity profiles.	68
29	Interpretive geologic cross section along Sevier Valley gravity profile. Densities shown in gm/cc	75
30	Interpretive geologic cross section along Pavant Range - Marysvale Valley gravity profile. Densities shown in gm/cc.	77
31	Interpretive geologic cross section along Mount Belknap caldera gravity profile. Densities shown in gm/cc.	80
32	Interpretive geologic cross section along Tushar Mountains - Sevier Plateau gravity profile. Densities shown in gm/cc.	82
33	Interpretive geologic cross section along Red Hill ground magnetic profile (M77-1). Magnetic susceptibilities shown in c.g.s. units.	85
34	Interpretive geologic cross section along Red Hill gravity profile (RH). Densities shown in gm/cc	87
35	Interpretive geologic cross section along SS Canyon ground magnetic profile (M77-14). Magnetic susceptibilities shown in c.g.s. units.	89
36	Interpretive geologic cross section along Sand Canyon gravity profile (SC). Densities shown in gm/cc.	91
37	Interpretive geologic cross section along Joseph ground magnetic profile (J2). Magnetic susceptibilities shown in c.g.s. units.	92
38	Interpretive geologic cross section along Joseph gravity profile (J2). Densities shown in gm/cc.	94

LIST OF ILLUSTRATIONS (Continued)

Tables

<u>Table</u>		<u>Page</u>
1	Summary of geologic control data.	26
2	Comparison of terrain corrections	41

INTRODUCTION

During the summer of 1977, regional gravity data were collected throughout the portion of Utah shown in Figure 1. In addition, detailed gravity and ground magnetic data were collected near hot springs within the Monroe and Joseph KGRA's (Known Geothermal Resource Areas). Figure 2 shows the boundaries of the two KGRA's (John Reeves, U.S.G.S. geothermal supervisor's office, 1978, oral communication) in the survey area.

This research was conducted as part of a variety of investigations into geothermal resource evaluation being performed by members of the University of Utah Department of Geology and Geophysics. Two factors have been of importance to the full realization of this project. First, increasing interest in geothermal exploration from both private and government agencies created a need for additional work to help evaluate the possible geothermal resources within the survey area. The impending development of a commercial geothermal resource near Milford, Utah has certainly strengthened interest in further exploration. Second, the availability in early 1977 of U.S.G.S. preliminary 7-1/2 minute topographic quadrangle maps provided a source of accurate horizontal and vertical control. This allowed the collection of regional gravity data of sufficient density to accurately define the major gravity features.

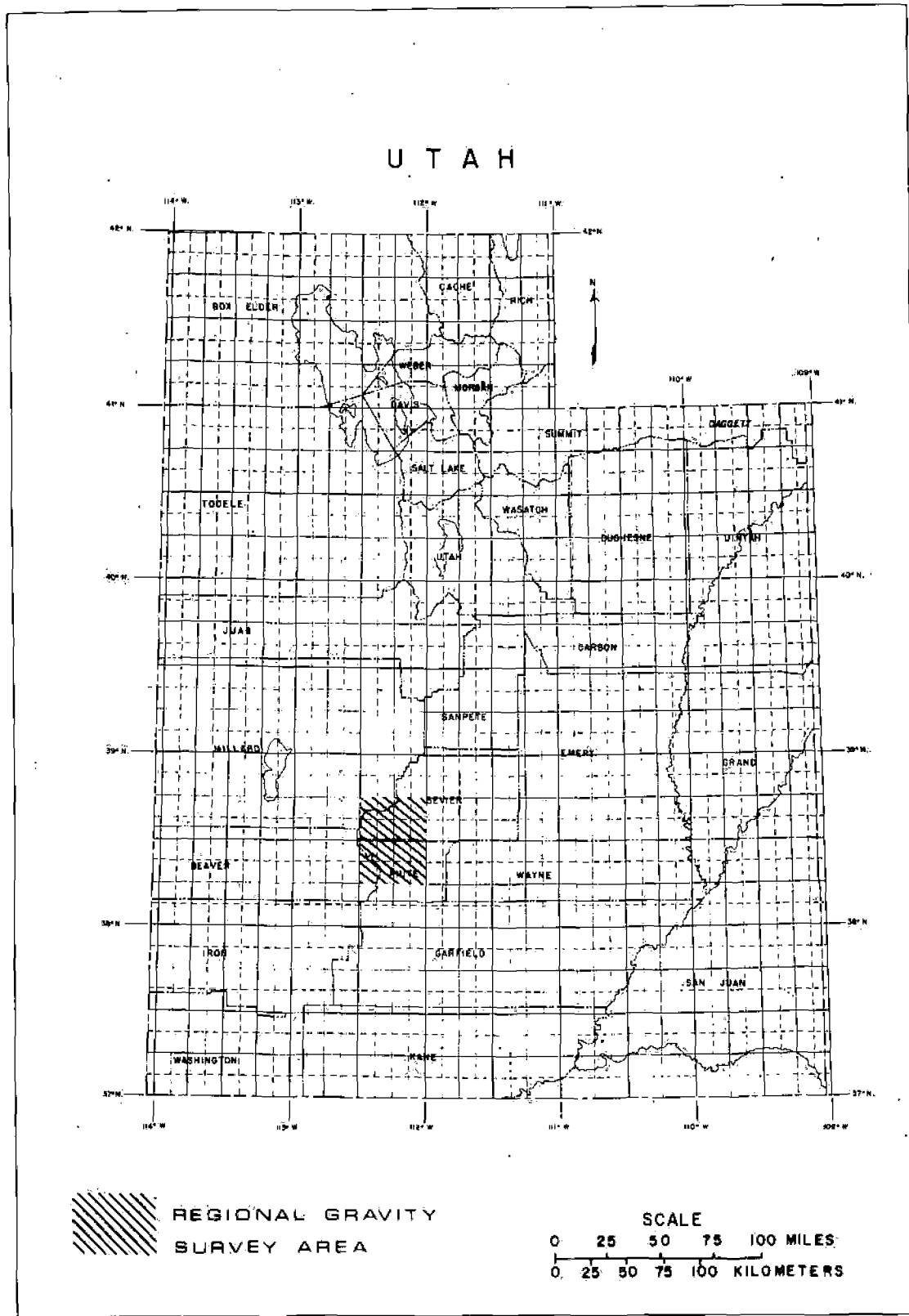


Figure 1. Map of Utah showing area covered by regional gravity survey.

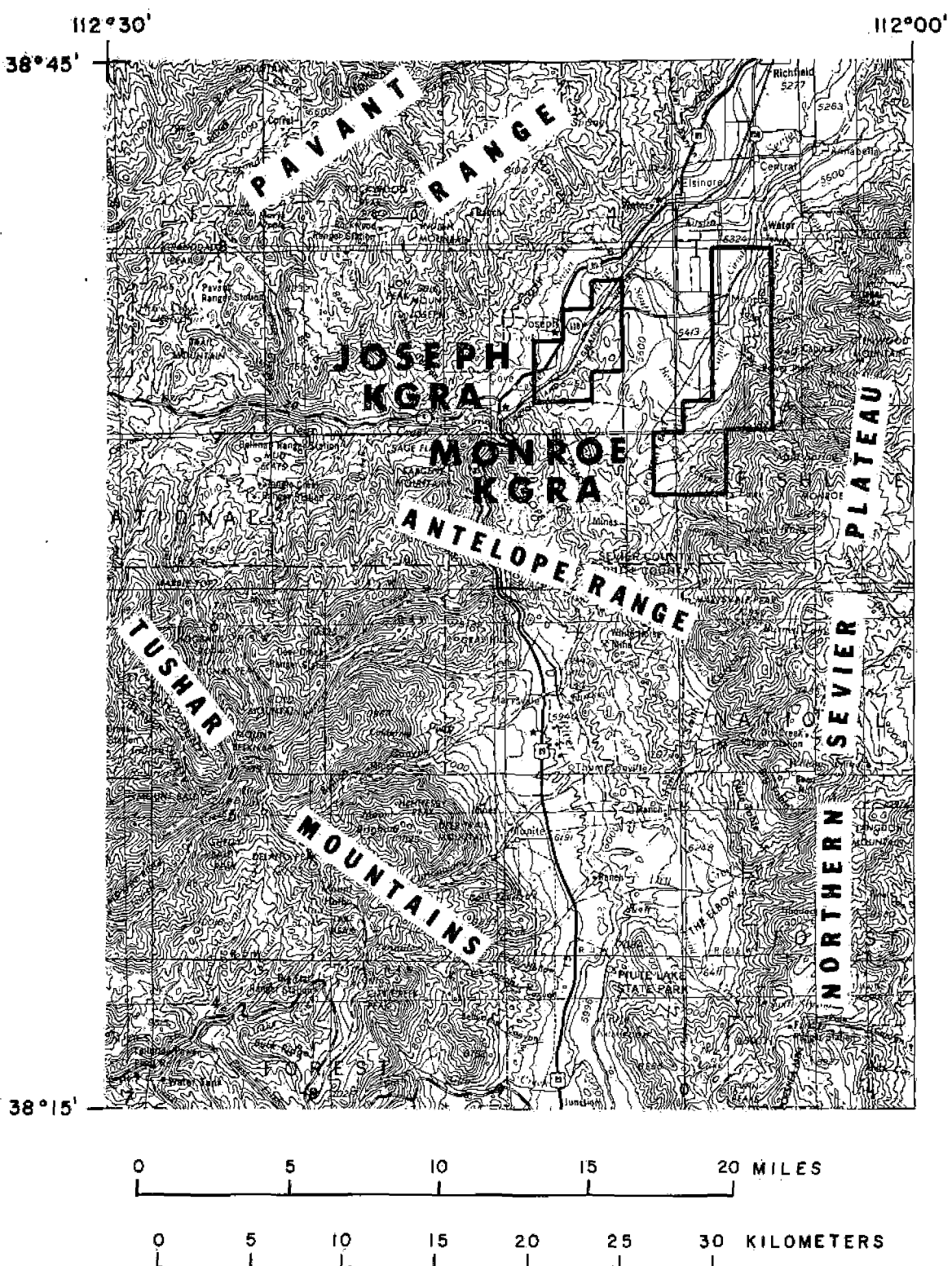


Figure 2. Map of survey area showing major geographic features and location of Monroe and Joseph Known Geothermal Resource Areas (KGRA's).

Purpose

The purpose of this research is to aid both the immediate and long-range evaluation of potential geothermal resources within the survey area. The objective of the detailed gravity and ground magnetic surveys is to assist immediate development of known geothermal resources in those areas near hot springs which will probably be targets of further exploration and development activity in the near future. Specifically, these surveys were designed to help locate faults controlling the hot springs and to constrain models of subsurface geology as a guide to exploratory and development drilling.

The purpose of the regional gravity survey is to improve our understanding of regional geologic aspects of the survey area. Specifically, the regional survey should provide information regarding the throw and location of major faults, estimates of depths of valley fill, and possibly help further delineate intrusive bodies and caldera structures.

Location

The regional gravity survey covers the area between latitudes 38° 15' N. and 38°45' N. and between longitudes 112°00' W. and 112°30' W. Located within portions of Millard, Piute, and Sevier counties, the survey covers a total area of about 2600 km² and comprises the four U.S.G.S. 15-minute topographic quadrangles of Monroe, Marysvale, Sevier, and Delano Peak.

The detailed gravity and ground magnetic profiles are located within the Monroe and Joseph KGRA's which are both in the U.S.G.S.

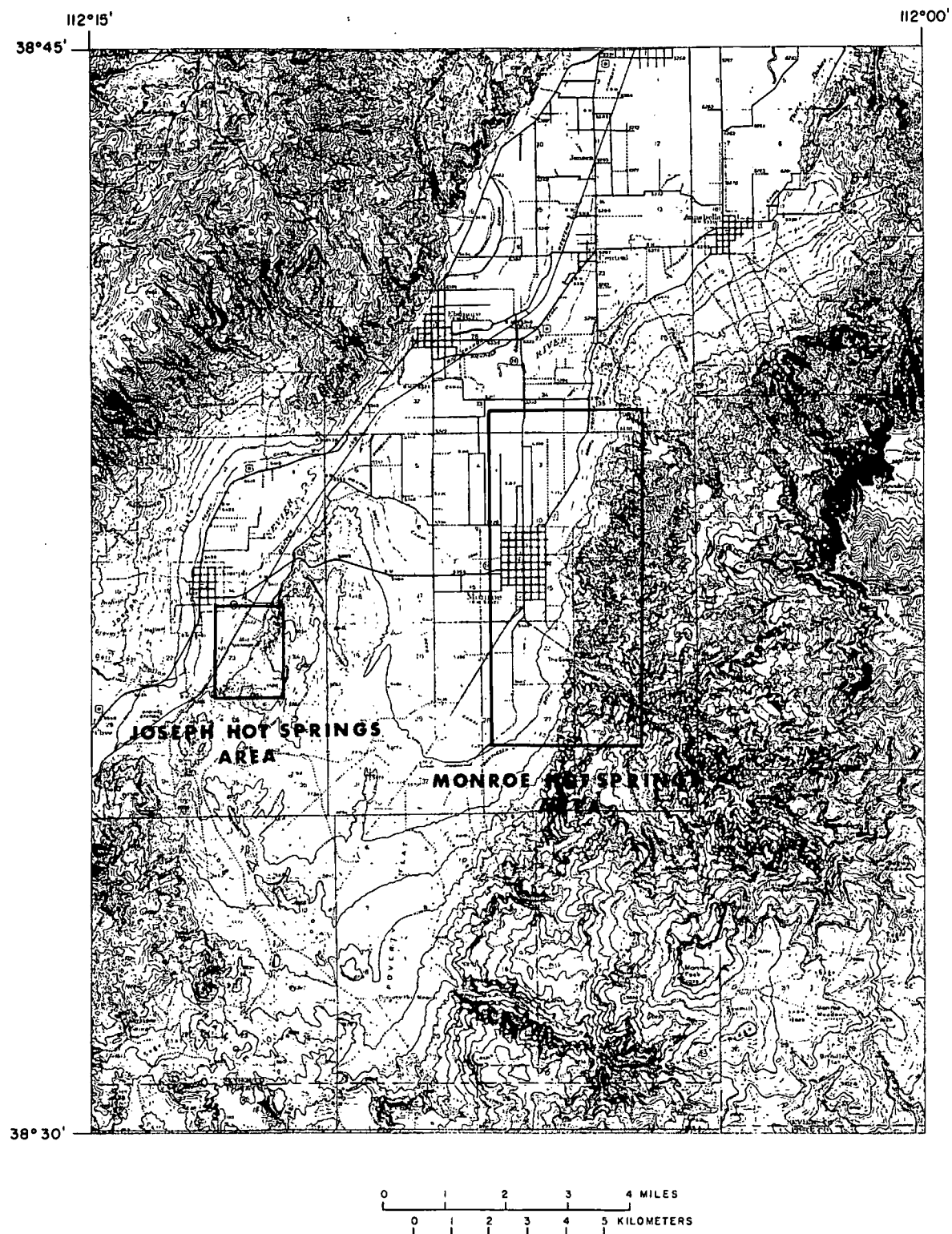


Figure 3. U.S.G.S. 15-minute topographic quadrangle of Monroe showing detailed gravity and ground magnetic survey areas.

15-minute topographic quadrangle of Monroe. Figure 3 shows the general areas covered by detailed gravity and ground magnetic data.

Physiography

The survey area lies in the transition zone between the Basin and Range physiographic province to the west and the Colorado Plateau province to the east. Topographically the area is extremely rugged, with elevations ranging from 1550 m in the valleys to over 3700 m in the Tushar Mountains.

Major geographic features of the survey area are shown in Figure 2. Sevier Valley extends south to north through the survey area. The northern Sevier Plateau lies east of Sevier Valley, and the Tushar Mountains and Pavant Range are on the west side. The Antelope Range trends east-west directly across Sevier Valley in the central portion of the survey area. The Sevier River, which provides the primary drainage for the entire survey area, has cut a deep gorge through the Antelope Range named Marysvale Canyon. Clear Creek, a tributary of the Sevier River, drains a large area lying between the Pavant Range and Tushar Mountains.

Previous Investigations

Geologic studies within the survey area have been conducted for about the last 100 yr and continue today. The impetus for this work has come from both academic interest in the thick accumulation of volcanic rocks of Tertiary age and economic interest in the variety of mineral deposits found here.

Dutton (1880) was one of the earliest investigators to study the

High Plateaus of Utah section of the Colorado Plateau. Butler (1920) covered subjects of economic interest, including precious metal, massive sulphide, and alunite deposits. Callaghan (1939) provided the first detailed description of volcanic stratigraphy in this region. The results of field work by Callaghan and others through 1952 were published as four U.S.G.S. geologic quadrangle maps, one covering each of the 15-minute quadrangle maps within the survey area (Callaghan and Parker, 1961a, 1962a, 1962b; Willard and Callaghan, 1962). Discovery of uranium mineralization in the Antelope Range near Marysvale in 1949 stimulated exploration and led to a study of the central uranium area by Kerr and others (1957).

Recently, geologists of the U.S. Geological Survey remapped parts of the survey area and have made progress in regional correlation of volcanic stratigraphy in southern Utah. Rowley and others (1975) studied areas south and west of the survey area. Steven and others (1977) suggested a revised stratigraphy for the volcanic rocks of the Marysvale area based on detailed field work and recent age-dating information. Based on the same work, Cunningham and Steven (1977) described two major collapse caldera structures in the region and interpreted the evolution of these features. Steven and others (1978) describe the most recent information available regarding the geology of the Marysvale volcanic field.

A regional gravity survey by Sontag (1965) overlaps with much of the region studied in this survey. Although his data were sparse in mountainous areas, they did indicate the presence of major gravity anomalies and thus served as a guideline in planning the field work

for the present survey. Brown (1974) conducted a gravity survey to the north in Sevier and Sanpete valleys, and the gravity survey by Fishman (1976) covers a large area east and south of this survey. Brumbaugh (1977) studied regional gravity features west of the area of this report area and considers specifically the use of gravity surveys in exploration for geothermal resources.

Limited gravity and ground magnetic data were available from field work of the 1976 Gravity and Magnetics class at the University of Utah under the supervision of Dr. K. L. Cook. The results of detailed ground magnetic surveys conducted in the vicinity of the Red Hill and Joseph Hot Springs are shown in Figures 4 and 5, respectively. The large anomalies across these features prompted the collection of additional ground magnetic data which is discussed and interpreted in this report.

Aeromagnetic data covering the survey area are available from the aeromagnetic map of Utah (Zietz and others, 1976). A portion of the data around the regional gravity survey area of this report is included as a contour map in Figure 6. Eppich (1973) discusses and interprets major features of this aeromagnetic data.

Since the present survey area contains a number of collapse caldera features within a volcanic field, previous investigations of the gravity signature over major volcanic fields and volcanic subsidence structures elsewhere were reviewed. Investigations by Yokoyama (1958) show gravity results over selected calderas in the Japanese island-arc. Gravity lows of more than 20-mgal closure were observed over the Kuttyaro and Aso calderas, whereas a gravity high of

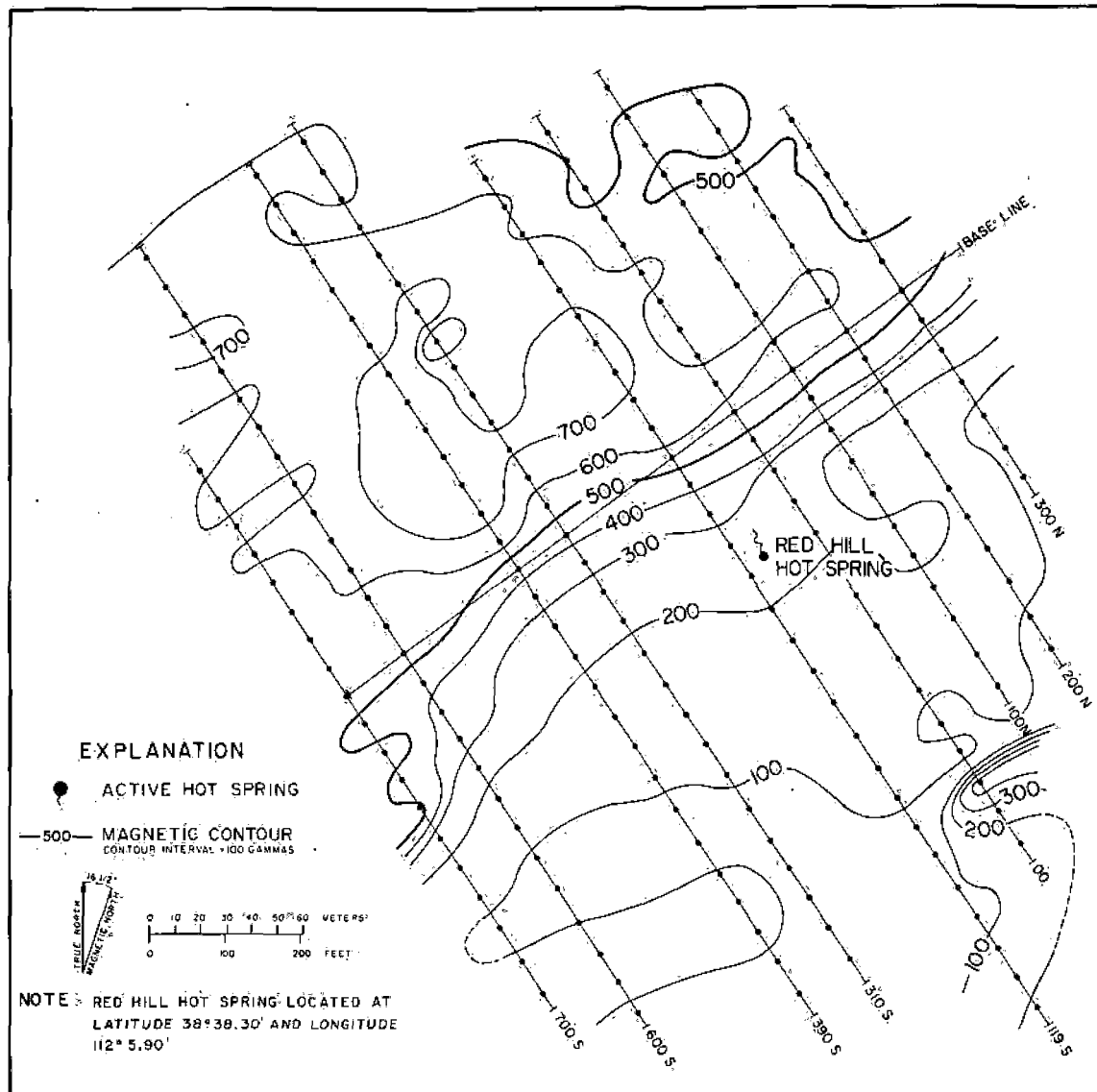


Figure 4. Total ground magnetic intensity anomaly map of the Red Hill Hot Spring detailed grid. From 1976 Gravity and Magnetics class, Univ. of Utah, under supervision of Dr. K. L. Cook.

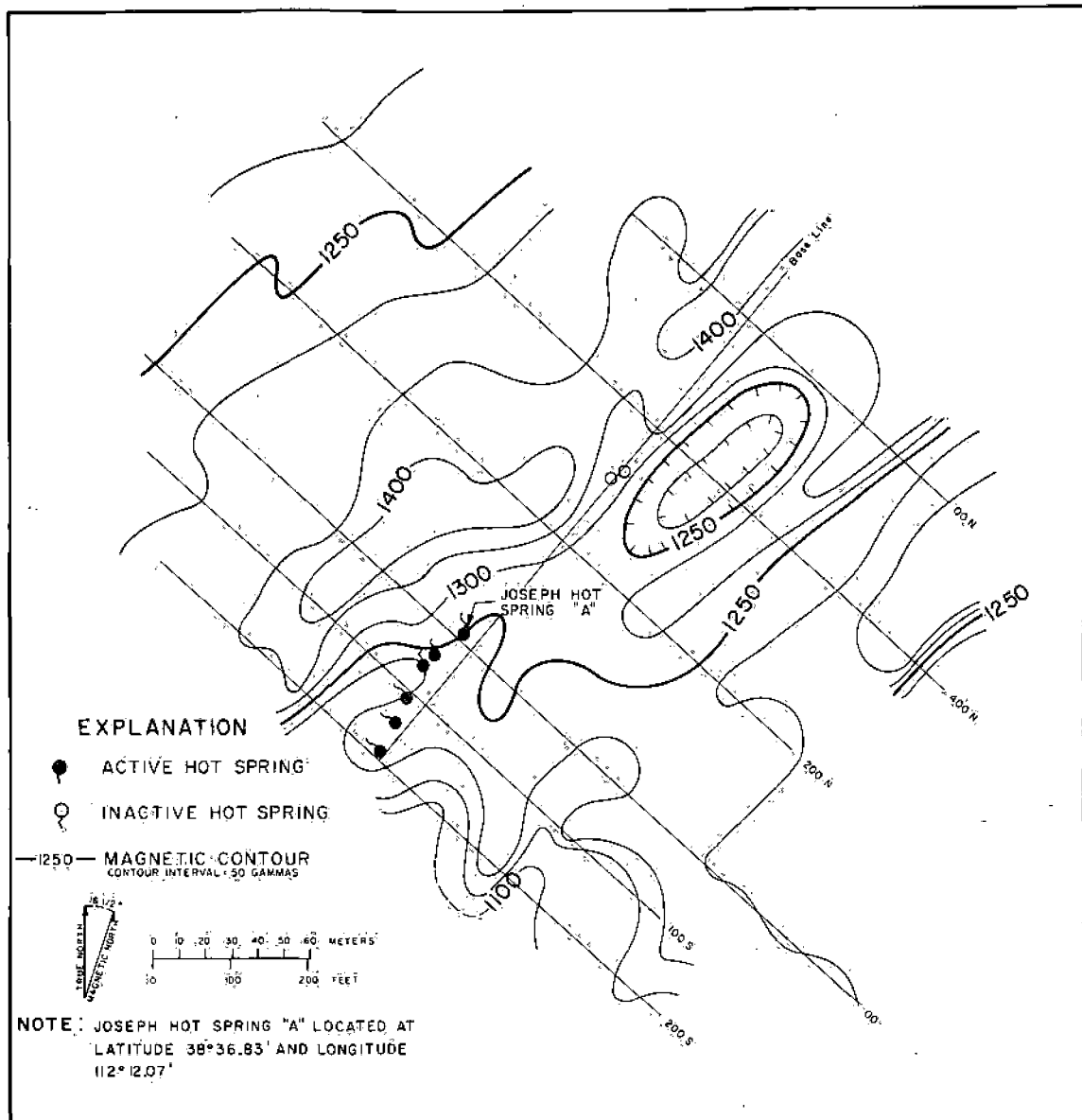


Figure 5. Total ground magnetic intensity anomaly map of the Joseph Hot Springs detailed grid. From 1976 Gravity and Magnetics class, Univ. of Utah, under supervision of Dr. K. L. Cook.

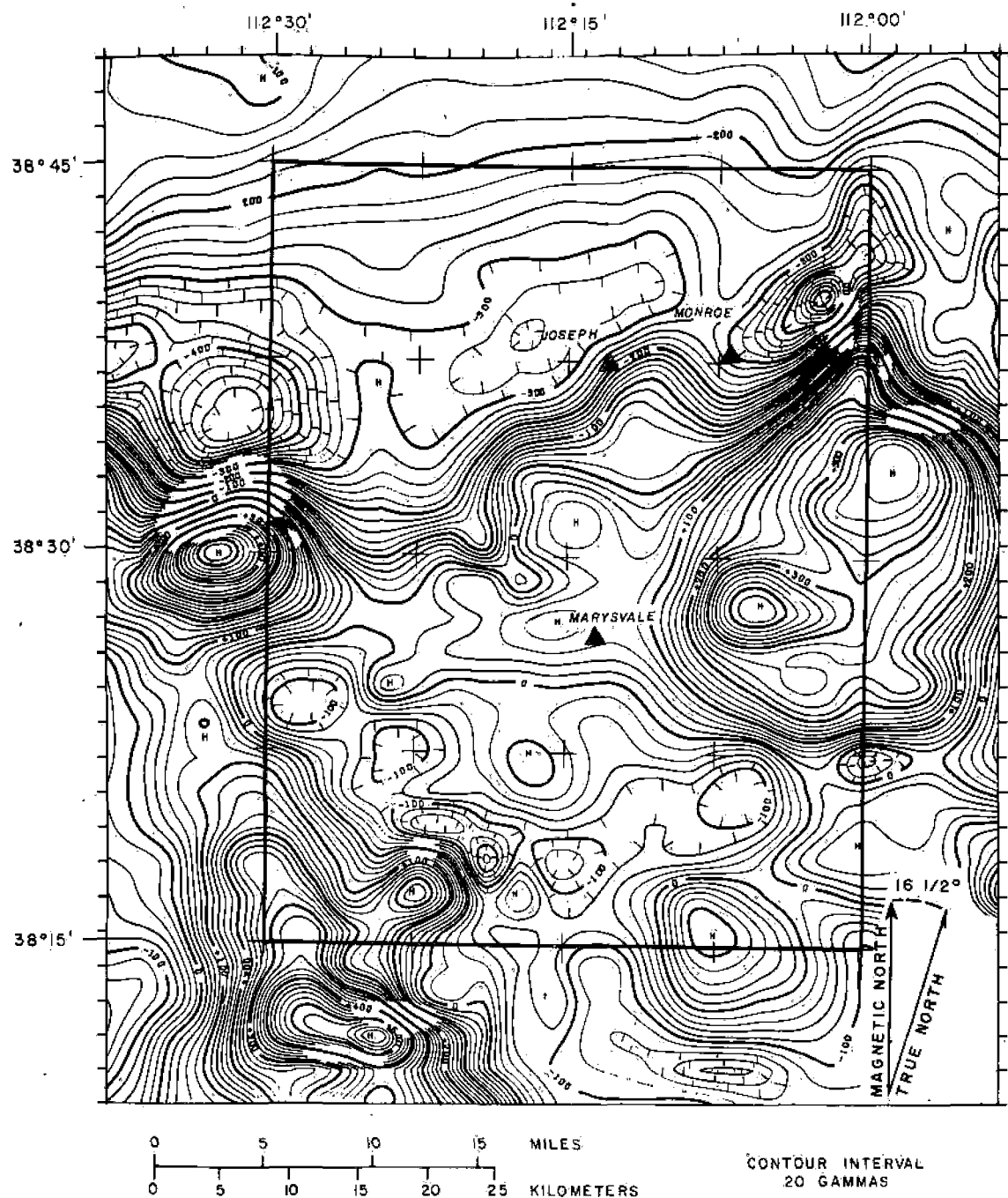


Figure 6. Total intensity aeromagnetic map of a portion of Utah, from Zietz and others (1976). Area of regional gravity survey is outlined.

about 15 mgal closure was observed over the Volcano Mihara. Pakiser (1964) noted a gravity low of about 70-mgal amplitude in the southern Cascade Range near Lassen Peak in California. Kane and others (1976) discuss a gravity low of about 50-mgal closure over the Long Valley caldera, California, which is interpreted to be the result of about 3 km of volcanic material in the caldera assuming a density contrast of 0.45 gm/cc. Studies by Eaton and others (1975) show a large gravity low of about 50-mgal closure in Yellowstone National Park. Here the gravity low was interpreted as due not to low-density volcanic fill but rather to a crystalline or molten batholith.

The San Juan volcanic field in southwestern Colorado consists of numerous caldera structures associated with widespread silicic volcanism (Steven and Lipman, 1976). A gravity survey over the Bonanza caldera in the northeastern part of the field (Karig, 1965) revealed a gravity low of at least 12-mgal closure. This low was interpreted as due to 2500 m of volcanic tuffs and lava flows assuming a density contrast of 0.2 gm/cc. Plouff (1972) made a gravity study of the entire San Juan volcanic field. A large gravity low of over 25-mgal closure was associated with the volcanic field, although individual gravity anomalies within the low were not obviously associated with the principal calderas. The regional gravity low was interpreted as due to a crystalline batholith underlying the San Juan volcanic field.

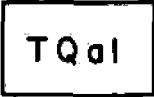
GEOLOGY

Stratigraphy

A lithologic map (Fig. 8) was prepared using the generalized stratigraphic column shown in Figure 7. The column is based principally on the work of Steven and others (1977), and contains some major changes from the stratigraphy as interpreted by Callaghan (1939). Since units of the stratigraphic column are described below in general terms only, the above sources should be consulted for more detailed description of the rocks involved.

Rocks of Precambrian age are not recognized within the survey area. The lowest stratigraphic unit consists of sedimentary rocks of Paleozoic, Mesozoic, and Tertiary age. Rocks of Cambrian and Ordovician age are found in the northern portion of the Sevier 15-minute topographic quadrangle, where they form the southernmost extremity of the Pavant thrust described by Maxey (1946). Sedimentary rocks of Paleozoic and Mesozoic age are exposed both near the Pavant thrust and along the base of Deer Trail Mountain south of Marysvale. Major formations within this unit include the Kaibab Limestone, Moenkopi and Chinle formations, Navajo sandstone (quartzite), and the Arapien shale. Sedimentary rocks of Tertiary age are found primarily in the north-central part of the survey area and consist of limestone, siltstone, shale, sandstone, and conglomerate.

Above the sedimentary rocks lie the Bullion Volcanics.



TQa1

TERTIARY AND QUATERNARY ALLUVIUM - poorly to moderately consolidated fluvial and lacustrine deposits of the Sevier River formation and all younger deposits.



TQb

TERTIARY AND QUATERNARY BASALT - thin vesicular olivine basalt flows of Miocene, Pliocene, and Pleistocene age. Closely associated with the Sevier River formation.



Tm

MOUNT BELKNAP VOLCANICS - rhyolitic lava flows and tuffs of Miocene age.



Tmj

Joe Lott Tuff Member of Mount Belknap Volcanics - poorly to moderately welded silicic ash-flow tuff.



Ti

TERTIARY INTRUSIVE ROCK - granitic to monzonitic intrusive bodies of Oligocene and Miocene age.



Tb

BULLION CANYON VOLCANICS - intermediate lava flows and volcanic breccias of Oligocene and Miocene age.



S

SEDIMENTARY ROCK - limestone, siltstone, shale, sandstone, and conglomerate of Paleozoic, Mesozoic, and Tertiary age.

Figure 7. Generalized stratigraphic column for rocks within the survey area.

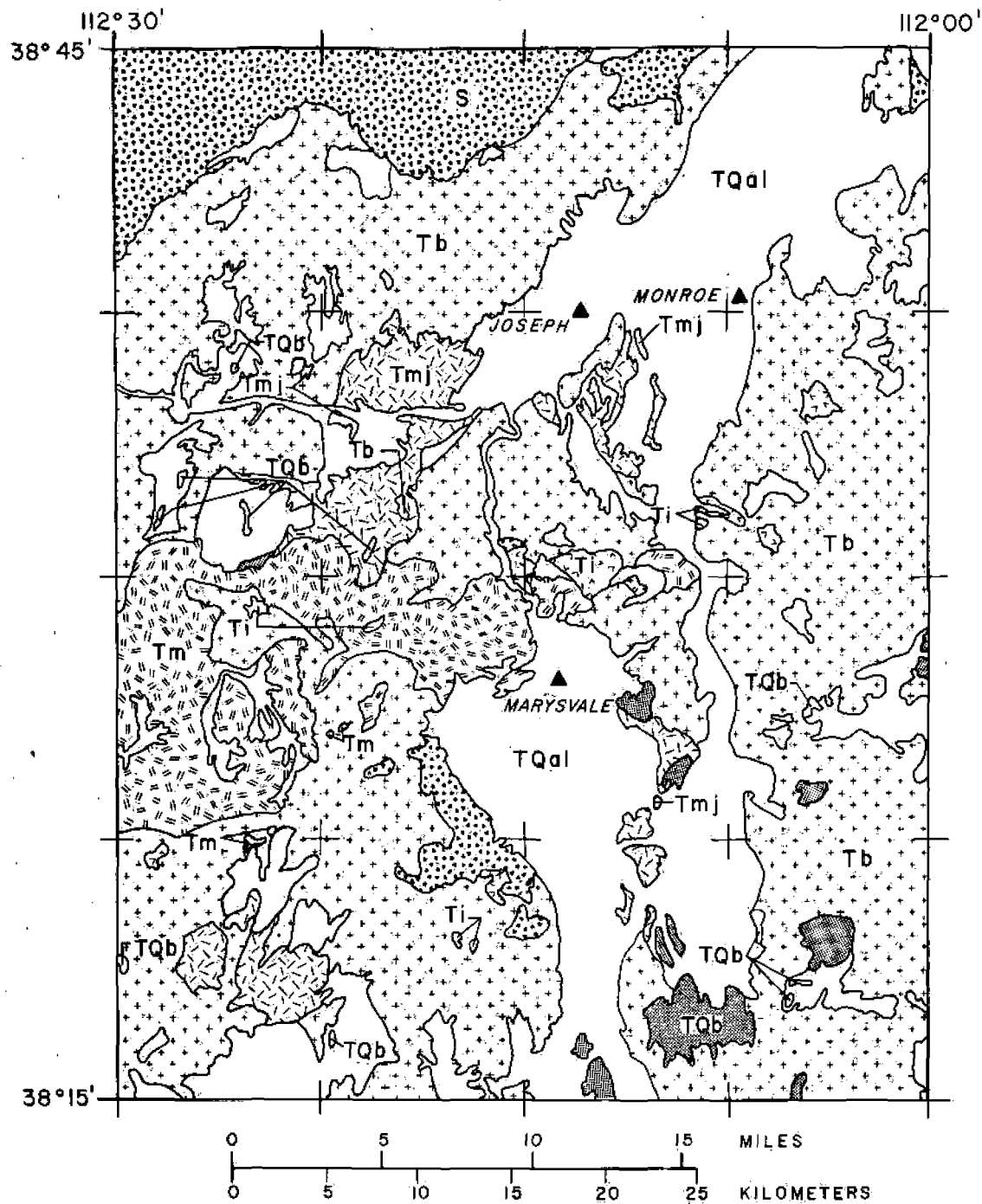


Figure 8. Generalized lithologic map of the survey area.

This unit comprises a major portion of the Marysvale volcanic field and is described by Steven and others (1977) as follows:

"The Oligocene and Miocene Bullion Canyon Volcanics is a complex assemblage of near source and outflow facies lava flows, volcanic breccias, and volcanic mudflow breccias that accumulated around a cluster of generally intermediate composition volcanoes centered in the Tushar Mountains, Antelope Range, and Northern Sevier Plateau."

Although progress has been made in distinguishing various members of the Bullion Canyon Volcanics, it will remain undivided for the purpose of interpreting gravity data. The lithologic map (fig. 8) includes as Bullion Canyon Volcanics all units previously mapped as Bullion Canyon, Dry Hollow, or Roger Park formations, following the suggestion of Cunningham (1978, oral communication).

Intrusive igneous rocks of Tertiary age are associated with both the Bullion Canyon Volcanics and the Mount Belknap Volcanics. The intrusions range from monzonitic to granitic in composition, are of variable texture, and trend east-northeast across the central portion of the survey area. The largest exposures of this unit are the "central intrusive" of Kerr and others (1957) located in the Antelope Range, and the Dry Creek and Monroe Canyon intrusives in the northern Sevier Plateau.

The Mount Belknap Volcanics is an important unit which resulted from a change from intermediate to silicic volcanism in the Miocene and the development of major collapse caldera structures. This unit consists primarily of rhyolitic lava flows and ash-flow tuffs of Miocene age. Eruptions apparently migrated southwestward from the

Antelope Range toward the Mount Belknap caldera over a period of a few million years. Cunningham and Steven (1977) have established a detailed stratigraphy for the Mount Belknap Volcanics, including both an outflow and intracaldera facies. In this compilation, however, the only subunit will be the Joe Lott Tuff member of the Mount Belknap Volcanics. The Joe Lott Tuff member is a poorly to moderately welded silicic ash-flow tuff which spread north, south, and east of the source area as the result of a series of catastrophic eruptions. It represents the largest-volume eruption of the Mount Belknap caldera and was followed by collapse of the caldera. In some places the Joe Lott Tuff member is up to 300 m thick.

Basalt of Tertiary and Quaternary age is intercalated with the alluvial unit of the same age lying above it and consists of generally thin vesicular olivine basalt flows. The basalt may be correlated with late Cenozoic extensional faulting and is therefore included in the stratigraphy.

Alluvium of Tertiary and Quaternary age includes the Sevier River formation of Callaghan (1939) and all younger alluvial deposits. The Sevier River formation consists of poorly to moderately consolidated fluvial and lacustrine deposits, and therefore is not expected to show a significant density contrast with recent alluvium of the major basins such as Sevier Valley.

Structure

Data shown on the structural geology map in Figure 10 were compiled from the work of Hintze (1963) and Cunningham and Steven

EXPLANATION

Normal fault, U on upthrown side,
D on downthrown side



Inferred normal fault, U on upthrown
side, D on downthrown side



Thrust fault, barbs on upper plate
of thrust sheet



Outline of caldera or wall of cauldron



Figure 9. Explanation of symbols used in geologic structure map.

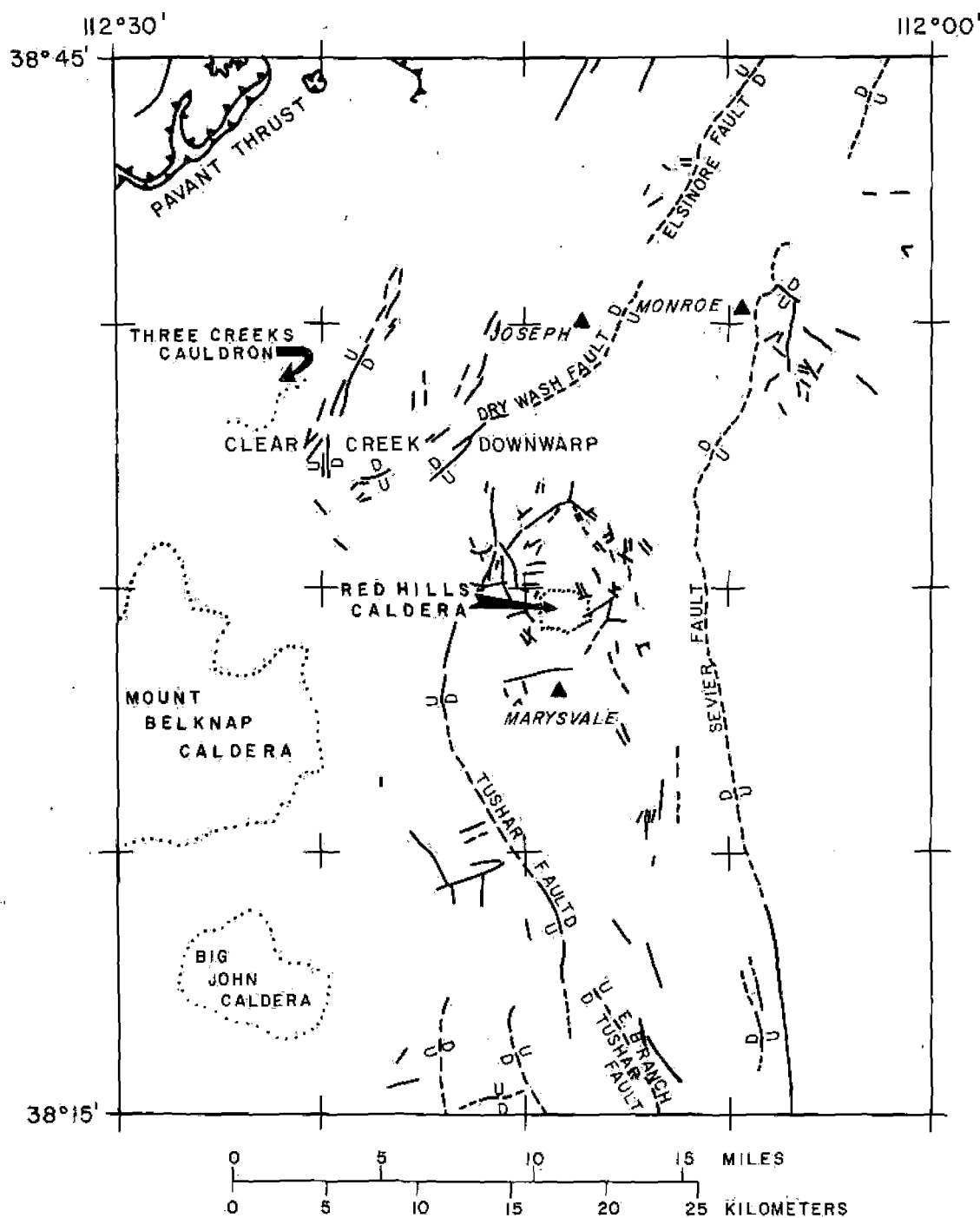


Figure 10. Geologic structure map of the survey area.

(1977). Structural features consist of normal faults, thrust faults, and collapse calderas or cauldrons.

The survey area lies within the structural transition zone between the Colorado Plateau and the Basin and Range physiographic provinces. Rowley and others (1978) discuss the age of structural differentiation of these two provinces, and apparently they were topographically differentiated by 24 m.y. ago. The main phase of basin-range faulting in the High Plateaus began less than 22 m.y. ago and continues today.

Normal faults are the dominant structural feature of the High Plateaus, and are responsible for many of the topographic features. Often there are zones of en echelon faulting as opposed to a single fault. Normal faults and associated horsts and grabens generally trend northerly, although some faults striking east-west occur locally. Rowley (1968, p. 137) has compiled a rose diagram of strikes of major faults near the southern Sevier Plateau. A bimodal distribution oriented at N. 25° W. and N. 35° E. is clearly indicated. Such a distribution with modes at 60° to each other has been interpreted by Moody (1966) as possible evidence for late Cenozoic wrench faulting. All field evidence, however, indicates entirely normal movement on the faults with no component of strike-slip motion (Rowley, 1968).

The Sevier fault is the most extensive normal fault in the survey area. Dutton (1880, p. 31) described this fault as extending from the Vermillion Cliffs to the northern High Plateaus of Utah and says:

The maximum displacement is apparently attained a few miles south of the Mormon village Monroe, and from that point northward it rather rapidly diminishes. Between Glenwood and Salina the apparent shear has become zero.

The Sevier fault scarp exceeds 1600 m in relief, which represents the minimum throw on the fault (Rowley, 1968).

Although the eastern edge of Sevier Valley is marked by the Sevier fault alone, the western side of the valley is marked by four individual faults. The Elsinore fault marks the boundary between the Pavant Range and Sevier Valley. This fault terminates just north of the town of Joseph, and from there south to the northern flank of the Tushar Mountains lies the Dry Wash fault. The Elsinore and Dry Wash faults form a relatively colinear pair, yet have opposite directions of displacement. Although direct evidence is not available, it is possible these two faults evolved together with "scissors" motion.

The Tushar fault originates on the southern flanks of the Antelope Range and extends southward, increasing to a maximum throw of over 1000 m near Cottonwood Creek (Callaghan and Parker, 1962a). The Tushar fault then diminishes abruptly and meets the East Branch Tushar fault near Piute Reservoir. The Tushar and East Branch Tushar faults are of opposite throw, and present the same relationship to each other as the Dry Wash and Elsinore faults to the north.

Normal faults striking east-west can be found in the area called the Clear Creek downwarp by Callaghan and Parker (1962b). The entire drainage of Clear Creek is rather complicated structurally and contains many small faults and folds.

Thrust faults are limited to those associated with the Pavant

thrust (Maxey, 1946) in the northern portion of the Sevier 15-minute topographic quadrangle. Although the Pavant thrust is rather complicated in detail, the gross relations are simple. Above the thrust plane lie sedimentary rocks of early Paleozoic age, and below it lie sedimentary rocks of Permian to Jurassic age. Red Ridge is a large hogback of resistant Navaho sandstone of Jurassic age which structurally underlies the Pavant thrust. This feature is so pronounced topographically that it can be easily recognized in ERTS satellite imagery.

The Mount Belknap and Red Hills calderas have been recently described by Cunningham and Steven (1977). The Mount Belknap caldera (18 m.y. old) is a major subsidence structure located in the central Tushar Mountains. The Red Hills caldera is a related smaller structure located in the southern Antelope Range. Both calderas are interpreted to have existed over high-level magma chambers above a common source. Depth to the high-level magma chambers is interpreted as 3 to 4 km based on thermodynamic calculations and analysis of the Mount Belknap Volcanics. Two calderas related to the older Bullion Canyon Volcanics are the Three Creeks cauldron and the Big John caldera. The Three Creeks cauldron is a volcanic subsidence structure (27 m.y. old) in the upper part of the Clear Creek drainage (T. A. Steven, 1978, oral communication). This feature apparently collapsed on one side only and is referred to as a cauldron instead of a caldera, which, by definition, must be a somewhat circular depression. The Big John caldera is located in Big John Flat in the Tushar Mountains just south of the Mount Belknap caldera (C. G. Cunningham,

1978, oral communication). This caldera was the source of an ash-flow tuff member of the Bullion Canyon Volcanics found in the vicinity of Delano Peak. Later eruptions filled the Big John caldera with Joe Lott ash-flow tuffs of the Mount Belknap volcanics (Steven and others, 1978).

Geologic Control Data

Rock density and magnetic susceptibility data were compiled to aid the interpretation of the geophysical data. Measurements of density and magnetic susceptibility were made on samples collected during the summer of 1977. Also, information was compiled from available drill hole descriptions in the literature.

Although no deep drill holes exist within the survey area, Ritzma (1972) describes three nearby deep wildcat oil wells. Two wells in the Sigurd area north of Richfield (Standard Oil of California No. 1 unit and Champlin Petroleum No. 13-31 USA) indicate a great thickness of the Jurassic Arapien formation lying beneath Sevier Valley. The Arapien is composed largely of salt and extends to a depth of 2.5 km below the valley floor. Another deep well in Antimony Canyon south of the survey area (Tenneco No. 1 Unit) shows about 200 m of Bullion Canyon Volcanics underlain by a thick sedimentary section. A search of drilling records at the Utah Geological and Mineral Survey yielded one additional drill hole located a few kilometers east of Richfield. This well showed volcanics down to a total depth of 200 m.

Drill holes within the survey area are limited to 11 shallow thermal gradient holes drilled in the Monroe KGRA by the University of

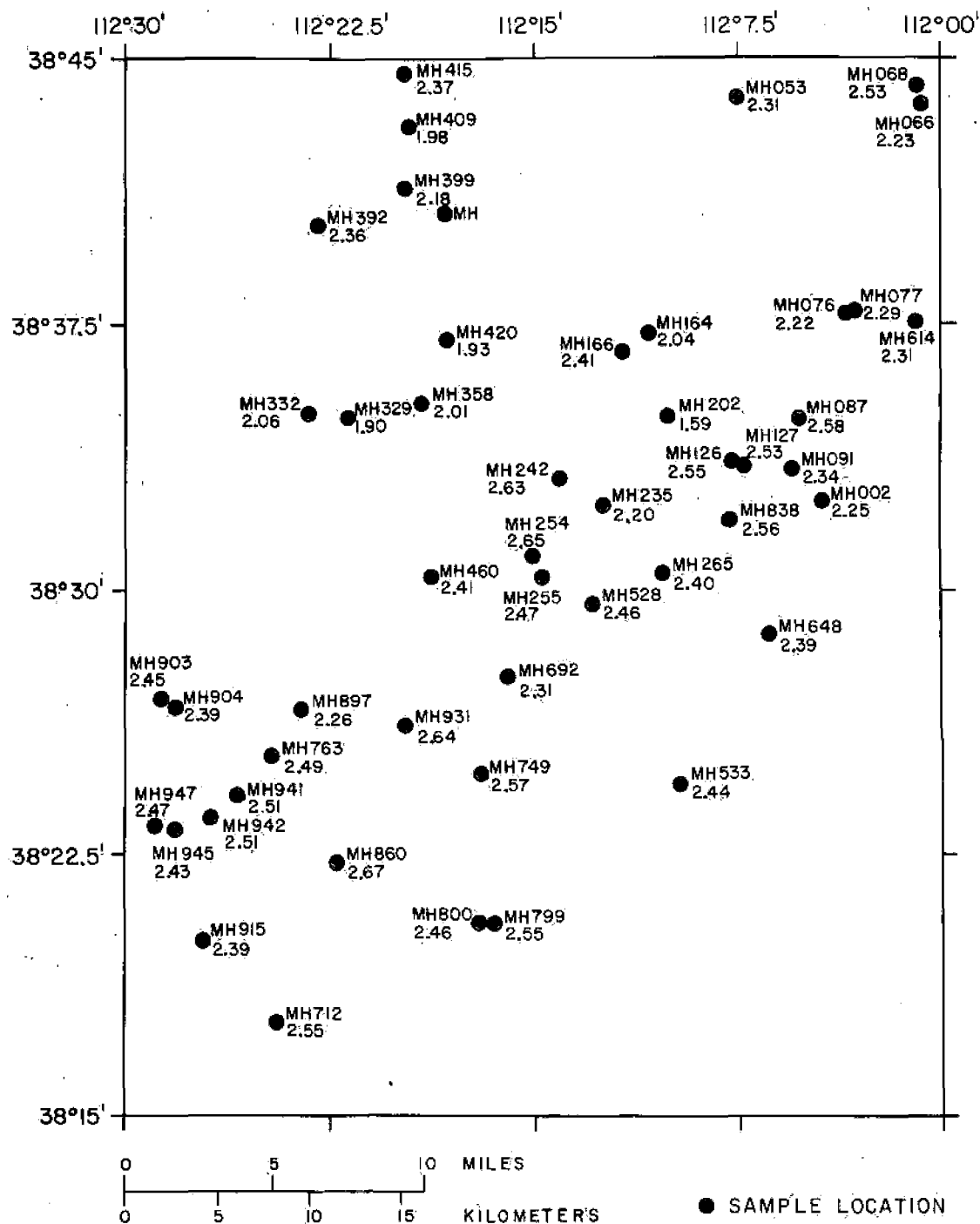


Figure 11. Map of survey area showing locations and densities (gm/cc) of rock samples collected. See Appendix 3 for description of samples.

Utah during 1977. Locations of these holes are shown in Figure 12. 11 core samples were measured for density and 37 samples (core, alluvium, or outcrop) were measured for magnetic susceptibility. Appendix 4 lists the results of these measurements and gives descriptions of the drill holes. Densities were determined by weighing each sample both in and out of water on a single beam balance. Magnetic susceptibility was measured with a Geophysical Specialties Co. Model MS-2 magnetic susceptibility bridge. Core and outcrop samples were crushed to pea-size before measurement, and a volume correction was made for the porosity of each sample. Density measurements were also made on 49 surface rock samples collected during the field season. Location and densities of these samples are shown in Figure 11, and a listing and description of the samples is given in Appendix 3.

A summary of the density and magnetic susceptibility measurements is given in Table 1. Regional rock samples were assigned to the proper unit of the generalized stratigraphic column (Fig. 7), and all sample densities in that unit were averaged to give a representative value. Data relevant to the detailed gravity and ground magnetic surveys have been grouped according to drill hole, with one additional group for two samples of outcrop basaltic andesite measured for magnetic susceptibility. The data of Table 1, as well as density measurements reported by previous investigators, were used to choose reasonable densities for modeling gravity and magnetic profiles.

Sedimentary rock densities are difficult to determine due both to

Table 1. Summary of Geologic Control Data

Densities Relevant to Regional Gravity Survey

<u>Rock Unit</u> ¹	<u>No. Samples</u>	<u>Range (gm/cc)</u>	<u>Average (gm/cc)</u>
TQa1	0	-----	-----
TQb	1	2.44 - 2.44	2.44
Tm	13	2.26 - 2.51	2.42
Tmj	6	1.59 - 2.06	1.92
Ti	2	2.56 - 2.65	2.61
Tb	23	2.18 - 2.67	2.41
S	4	1.98 - 2.57	2.36
All Samples	49	1.59 - 2.67	2.36

Densities Relevant to Detailed Gravity Surveys

<u>Drill Hole</u> ²	<u>No. Samples</u>	<u>Range (gm/cc)</u>	<u>Average (gm/cc)</u>
M2	3	2.19 - 2.29	2.26
M3	3	2.29 - 2.51	2.41
M6	2	2.43 - 2.52	2.48
RH1	3	2.46 - 2.50	2.48
All Samples	11	2.19 - 2.52	2.40

Magnetic Susceptibilities Relevant to Detailed Magnetic Surveys

<u>Sample Group</u> ²	<u>No. Samples</u>	<u>Range (c.g.s. units)</u>	<u>Average (c.g.s. units)</u>
M2	3	0.0001 - 0.0006	0.0003
M3	3	0.0001 - 0.0005	0.0003
M4	3	0.0003 - 0.0006	0.0005
M5	1	0.0001 - 0.0001	0.0001
M6	2	0.0000 - 0.0001	0.0001
RH1	8	0.0000 - 0.0001	0.0001
RH2	5	0.0009 - 0.0013	0.0011
RH3	3	0.0011 - 0.0017	0.0015
RH4	4	0.0000 - 0.0003	0.0002
RH5	3	0.0004 - 0.0024	0.0013
Outcrop	2	0.0026 - 0.0042	0.0034
All Samples	37	0.0000 - 0.0042	0.0007

¹See Figure 7 for rock unit description

²See Figure 12 for location of drill hole. All samples were either alluvium (TQa1) or Bullion Canyon Volcanics (Tb).

the variable nature of the sedimentary sequence, and the small number of surface samples collected from the relatively limited exposures of sedimentary rock. The average density for sedimentary rocks indicated in Table 1 is not considered a representative value due to the small number of samples and the fact that none of the samples are Paleozoic rock. Snow (1978) differentiated between Paleozoic and Mesozoic sedimentary rocks, assigning densities of 2.8 gm/cc and 2.6 gm/cc, respectively. His high density for Paleozoic rocks is based on seismic refraction data and surface density measurements by other investigators (Snow, 1978). Since the Paleozoic section in this portion of Utah consists largely of limestones and dolomites, the densities for those pure minerals, which range from 2.71 gm/cc to 2.85 gm/cc (Berry and Mason, 1959), could be considered maximum values. Carter (1978) reports 11 measurements of limestone densities in the Mineral Mountains which range from 2.55 gm/cc to 2.97 gm/cc, and average about 2.72 gm/cc. Brumbaugh (1977) reports 13 density measurements of dolomitic limestones from the Cove Fort area just west of this present survey. His measurements range from 2.29 gm/cc to 2.79 gm/cc, and average 2.64 gm/cc. Case and Joesting (1972) report densities ranging from 2.3 gm/cc to 2.5 gm/cc for Mesozoic sedimentary rocks in the central Colorado Plateau. Carter (1978) reports an average density of 2.62 gm/cc for sandstone and quartzite of unspecified age in the Mineral Mountains. Brumbaugh (1977) reports an average density of 2.58 gm/cc for sandstone and quartzite of unspecified age in his area. Brown (1975) reports mean densities from gamma-gamma bulk density logs of a wildcat oil well located 40 km

east-northeast of Richfield. Densities for Mesozoic sedimentary rocks were found to range from 2.52 gm/cc to 2.67 gm/cc, except for the Arapien formation which ranges from about 2.0 gm/cc to 2.1 gm/cc. Considering all the above data, we might expect most sedimentary rocks to fall in the density range of 2.5 gm/cc to 2.8 gm/cc, with even wider variations possible in some cases. Additionally, there seems to be an indication that Paleozoic sedimentary rocks are denser than Mesozoic rocks, particularly since the Paleozoic section consists mostly of limestones and dolomites.

Extrusive volcanic rock densities are relatively well determined by the data in Table 1 due to the large number of samples, but densities for intrusive igneous rocks are poorly determined since only two samples were collected. Extrusive volcanic rocks (Bullion Canyon Volcanics and Mount Belknap Volcanics) show wide ranges of densities with an average density very close to 2.4 gm/cc. One exception is the Joe Lott Tuff Member of the Mount Belknap Volcanics, which averages less than 2.0 gm/cc, and therefore can be expected to present a density contrast with other extrusive volcanic rocks. The two intrusive samples shown in Table 1 average close to 2.6 gm/cc, which agrees well with 11 density measurements on granite averaging 2.6 gm/cc as reported by Brumbaugh (1977). However, Case and Joesting (1972) report a range of 2.6 gm/cc to 3.2 gm/cc for Precambrian intrusive rocks, and Snow (1978) assumed a density of 2.8 gm/cc for intrusive rocks based primarily on seismic data. Carter (1978) reports 34 samples of granite measured which range in density from 2.45 gm/cc to 2.77 gm/cc, with an average value close to 2.6 gm/cc.

Considering the above data, extrusive volcanic rocks might be expected to range from 2.3 gm/cc to 2.5 gm/cc, whereas intrusive igneous rocks show a wide range of densities with most values in the 2.6 gm/cc to 2.8 gm/cc range.

The density of Tertiary and Quaternary alluvium is particularly difficult to determine since it cannot be sampled directly. A reasonable value of 2.0 gm/cc is suggested by Crebs (1976) based on a density profile across alluvium west of the Mineral Mountains.

DATA ACQUISITION

Instrumentation

All observed gravity values were obtained with LaCoste and Romberg Model G geodetic gravimeter No. 264. This instrument has a precision capability of 0.001 mgal. At both the beginning and end of the field work, the calibration of the gravimeter was checked by occupying the Salt Lake City calibration loop. The results of this test agreed well with those of previous surveys and the gravimeter was judged to be operating properly.

Ground magnetic data were obtained using a Geometrics Model G816 proton precession magnetometer, which measures the earth's total magnetic field intensity with a precision of ± 1 gamma.

Regional Gravity Data

To conduct the regional gravity survey, field base stations were established at both Monroe and Marysvale. Observed gravity values for these bases were determined by tying them in a "ABABA" looping technique to the Utah Gravity Base Station Network (Cook and others, 1971) stations in Beaver, Loa, and Richfield. Complete descriptions of the field base stations are given in Appendix 1. Descriptions of observed and computed gravity base station ties are given in Appendix 2.

A total of 953 regional gravity stations were established during

the summer of 1977. A standard looping procedure was used to collect these data, with each loop beginning and ending at a field base station. Although loops were closed as often as possible, it was sometimes necessary to take an entire day for one loop due to the rugged and remote terrain throughout the survey area. Access was usually by four-wheel drive vehicle, although it was occasionally necessary to backpack the gravimeter to a location. One overnight trip was necessary to establish stations along a remote ridge in the Tushar Mountains.

Horizontal and vertical control was obtained from U.S.G.S. preliminary 7-1/2 minute topographic quadrangle maps. Since the 40-ft contour interval of these maps was too coarse to provide control at arbitrary locations, stations were established only at benchmarks and spot elevations.

Detailed Gravity Data

A total of 88 detailed gravity stations were established along five profiles in the vicinity of hot springs within the Monroe and Joseph KGRA's. Each gravity station was read twice and the readings averaged in order to insure accurate data. Loops were closed to base station about every hour to minimize the effects of the earth tides and instrument drift. Horizontal and vertical control were provided by surveying with a Hewlett-Packard model 3810 total station electronic distance meter. The surveying was performed under contract by Horrocks and Associates, consulting engineers, of Richfield, Utah on August 12, 1977 (Mr. T. Jones, surveyor).

Figure 12 shows the location of three detailed gravity profiles in the Monroe Hot Springs area labelled "RH" (Red Hill), "SC" (Sand Canyon), and "MC" (Monroe Canyon). Figure 13 shows the location of two detailed gravity profiles in the Joseph Hot Springs area labelled "J1" and "J2".

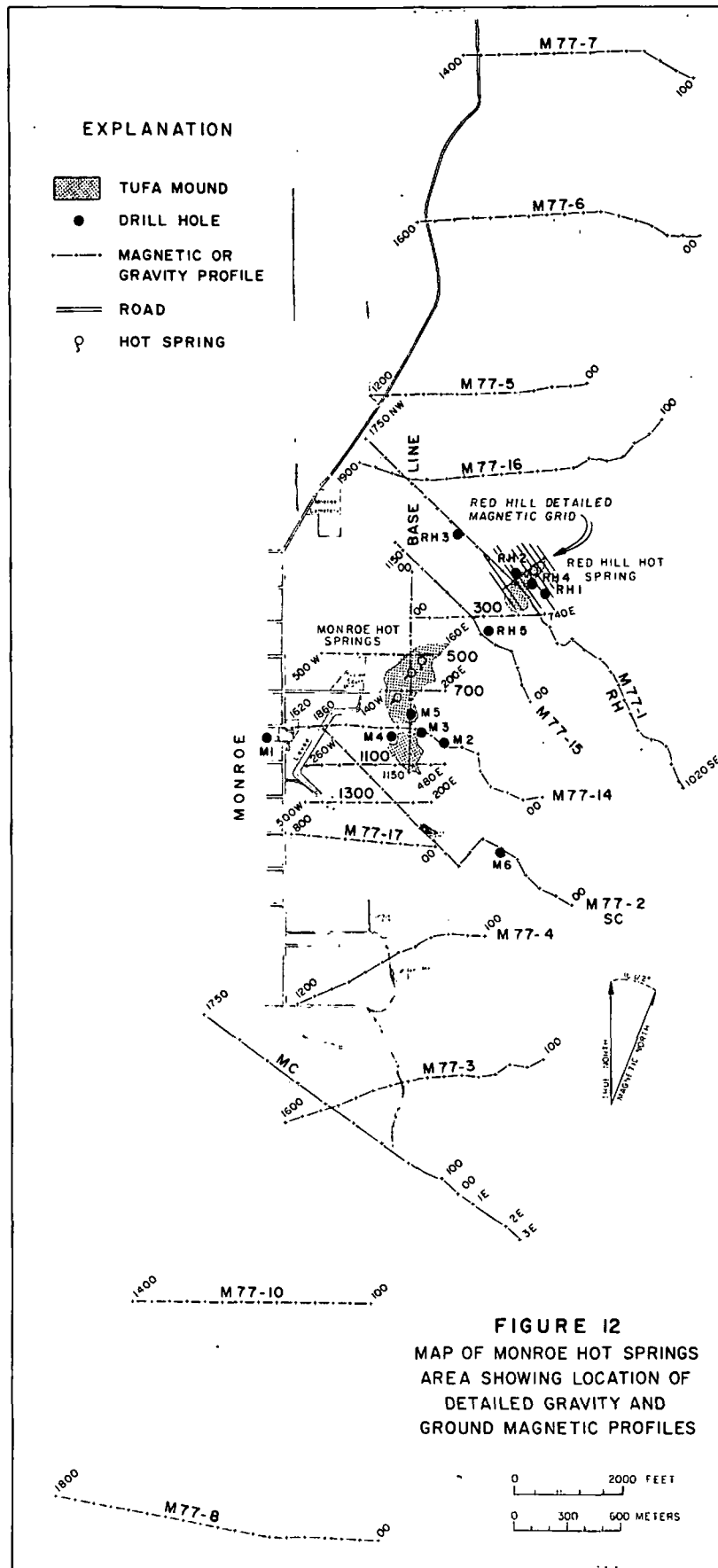
Detailed Ground Magnetic Data

A total of 840 ground magnetic stations were established along 19 profiles in the Monroe Hot Springs area, and a total of 105 stations were established along two profiles in the Joseph Hot Springs area. A standard looping technique was used to collect the magnetic data, with each day's work normally consisting of two closed loops taken back to Monroe magnetic base. A complete description of the magnetic base is given in Appendix 1.

Station spacing was 20 m in areas of special interest, i.e., near the hot springs, and 50 m elsewhere. Five readings were taken at each station and then averaged in an attempt to reduce the high-frequency magnetic noise associated with the volcanic environment. One reading was taken at the station itself, and four others were taken at points about 3 m from the station toward the principal compass directions.

Figures 12 and 13 show the location of detailed magnetic profiles within the Monroe and Joseph Hot Springs areas, respectively. Also shown on these figures are locations of the detailed magnetic grids (Figs. 4 and 5) surveyed in 1976 by the Gravity and Magnetics class at the University of Utah under the supervision of Dr. K. L. Cook.

A large power transmission line extends directly through the



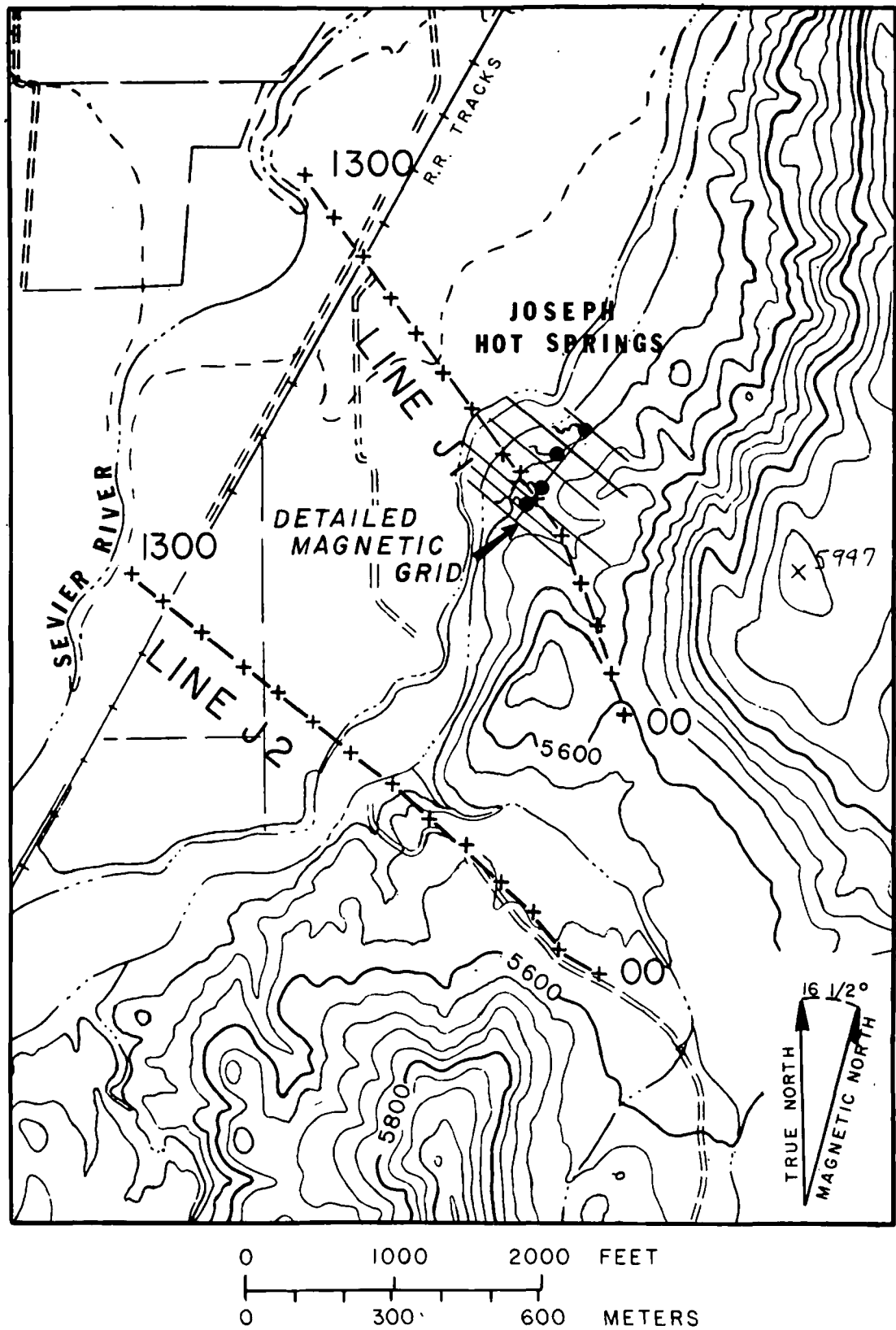


Figure 13. Map of Joseph Hot Springs area showing location of detailed gravity and ground magnetic profiles.

Monroe Hot Springs area and caused a great deal of magnetic noise. However, this noise was easily recognized by erratic magnetometer readings and no reading was attempted in areas immediately under or adjacent to the power line.

DATA REDUCTION

Gravity Data Reduction

Both regional and detailed gravity data were reduced on the University of Utah UNIVAC 1108 computer using FORTRAN software available in the Department of Geology and Geophysics. The reduction program converted instrument readings to relative gravity values using the appropriate gravimeter scale constants. Drift corrections were made assuming linear drift between the initial and final base station readings of a loop. Observed gravity values were computed as the difference between the drift-corrected station value and the observed gravity at the base station. Theoretical gravity values at sea level were calculated using the International Gravity Formula of 1934 (Swick, 1942). A free-air correction factor of 0.30861 mgal/m and a Bouguer correction density of 2.67 gm/cc were used, resulting in a total elevation correction of 0.19683 mgal/m applied above the chosen datum of sea level.

Although the chosen Bouguer correction density does not reflect the average density of surficial volcanic rocks found throughout the survey area (Table 1), the choice is considered reasonable. This value does represent the average density for crustal rocks above sea level (Nettleton, 1976, p. 157) and is a reasonable density for sedimentary rocks believed to underlie the extensive volcanic cover. Furthermore, since gravity surveys surrounding this survey have all

used a 2.67 gm/cc reduction density, it will be possible to tie the surveys together for future regional studies.

Simple Bouguer gravity anomaly values were determined by subtracting the theoretical gravity values from the observed gravity values. Complete Bouguer gravity anomaly values were computed by adding terrain corrections (determined by techniques described in the next section) to the simple Bouguer gravity anomaly values.

A total of 953 station locations and their respective complete Bouguer gravity anomaly values were then machine plotted on a map at a scale of 1:62500. Fifteen additional stations were incorporated into the map from the work of Fishman (1976). These data were then hand-contoured at a 1-mgal interval. Twenty station values were found to be inconsistent with surrounding data probably due to elevation errors and were omitted, leaving a total of 948 stations used to construct the map. Figure 14 shows the final complete Bouguer gravity anomaly map contoured at a 2-mgal interval.

A total of 88 gravity stations established along detailed profiles were reduced in the same manner as the regional data except that the reduction program was modified to accept elevation data to the nearest 0.1 ft (0.03'm). Principal facts for both the regional and detailed gravity stations are given in Appendix 5.

Gravity Terrain Corrections

Extreme topographic relief within the survey area required that terrain corrections be taken out to a radial distance of 167 km (100 miles) from each station. After examining possible techniques and

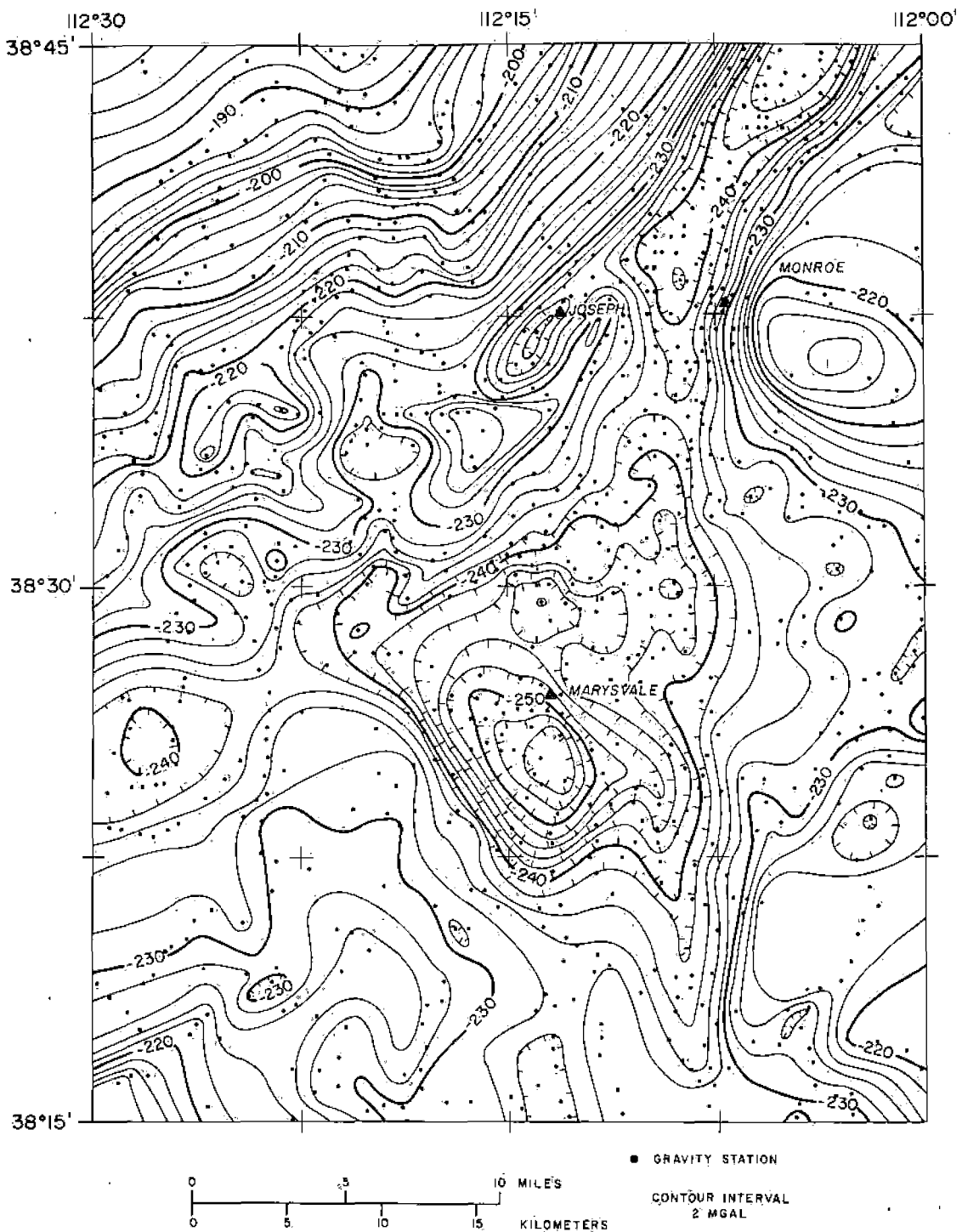


Figure 14. Complete Bouguer gravity anomaly map of the survey area.

available software, a three-part procedure was chosen to compute the terrain corrections. The three parts cover adjacent areas referred to as the inner, intermediate, and outer zones. For all three zones, the terrain corrections were computed assuming a density of 2.67 gm/cc.

The inner-zone terrain correction covers the area through zone E of the Hayford-Bowie (U.S.C. & G.S.) terrain correction charts (Swick, 1942), i.e., out to a radial distance of 1.28 km from the station. Standard U.S.C. & G.S. templates were used to estimate visually the compartment elevations. For those cases in which the corrections in zone C, D, or E exceed 1 mgal, the zone was divided into two parts and re-corrected. Plouff (1977, oral communication) has found that failure to follow this procedure will cause consistently positive errors of 1 mgal or more in the correction. An inclined plane approximation to the topography was used to estimate the correction for zones B and C where possible. Sandberg's (1958) tables were used for this purpose. Inner-zone terrain corrections were computed from compartment elevation estimates using a Hewlett-Packard HP9100B programmable calculator.

The intermediate-zone terrain corrections were computed using a FORTRAN program written by Hardman (1964) as modified by Carter (1978). The program used a "digital terrain model", available from Fishman (1976), which was prepared by digitizing topographic maps on a 1-km grid. The correction is computed for the area between inner and outer squares centered on the station and measuring 2 km and 40 km on a side, respectively. There is some mismatch in going from the circular pattern of the inner zone to the square pattern of the

intermediate zone. The error introduced thereby is largely a function of the nature of the terrain at the transition between the zones. This method has been used in many previous gravity surveys (Hardman, 1964; Fishman, 1976; Brumbaugh, 1977; Case, 1977; and Carter, 1978); and apparently the error introduced is minimal.

The outer-zone terrain corrections were computed using a FORTRAN program written by Plouff (1977). The program uses topographic data on a geographic grid of arbitrary spacing, and calculates the correction by approximating the gravity effect of a rectangular compartment with a vertical line mass at the center of the compartment. Correction is made for the effect of the earth's curvature. For this survey, digitized topography on a 3-minute grid was obtained from the U.S. Geological Survey in Denver and used to compute terrain corrections for the circular area from 22.6 km to 167 km radial distance from the station. The inner radius of 22.6 km was chosen so that it contained the same amount of surface area as the 40-km outer square of the intermediate zone. Although some error is again introduced in changing from a square to a circular pattern, the above procedure should minimize the error.

The total terrain correction for each station was taken as the sum of the inner, intermediate, and outer-zone corrections for that station. The largest correction was 51.14 mgal for the station located on Mount Baldy (elevation 3680 m) in the Tushar Mountains. The smallest correction was 1.83 mgal for a station in gently rolling terrain near the Pavant Ranger Station. The average terrain correction throughout the survey area was 6.41 mgal.

Table 2. Comparison of Terrain-Correction Values

Station Name (This Survey)	Terrain Correction "A" (mga1)	Station Name (Previous Survey)	Terrain Correction "B" (mga1)	Difference A-B (mga1)
MH140	2.99	RS5	2.39	+0.60
MH140	2.99	76-146	2.89	+0.10
MH149	2.13	RS45	2.84	-0.71
MH493	4.03	RS94	3.24	+0.79
MH498	3.62	RS96	2.87	+0.75
MH511	3.78	RS103	2.95	+0.83
MH548	3.76	RS82	3.11	+0.65
MH606	3.77	RS126	3.42	+0.35
MH719	6.98	RS123	6.26	+0.72
MH875	3.73	76-133	5.36	-1.63
MH933	6.44	RS65	5.24	+1.20

R.M.S. Difference = 0.85 mga1

Sources of previous data:

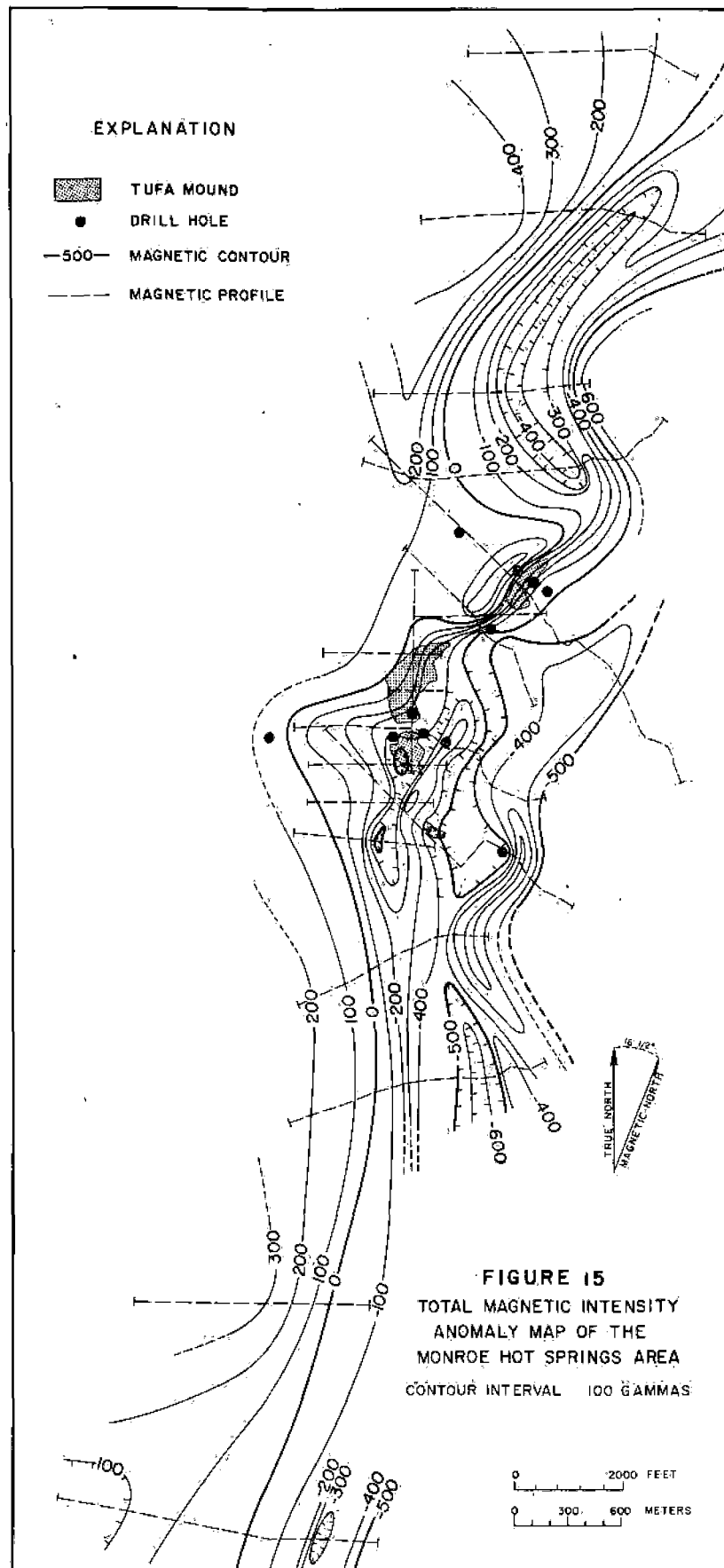
"RS" stations - Sontag (1965)

"76" stations - Gravity and Magnetics class, Univ. of Utah,
Fall, 1976, under supervision of K. L. Cook.

Comparison was made between 11 corrections of this survey with terrain corrections determined at the same locations by previous investigators. The results of this comparison are shown in Table 2. Close agreement between values cannot be expected since the corrections from previous surveys were taken out to a distance of 58 km only, whereas in this survey the terrain corrections were taken out to 167 km. This difference is the apparent cause of generally higher values determined in the present survey. Also, terrain corrections in the previous surveys were made with 15-minute topographic quadrangles, whereas terrain corrections for the present study were made with 7-1/2 minute quadrangle maps. In view of the different techniques and maps used, the comparison does indicate that the terrain corrections determined herein are reasonable values, and apparently no gross errors were made.

Ground Magnetic Data Reduction

The first step in reducing the ground magnetic data was to average the five total magnetic field intensity readings taken at each station. Diurnal corrections were then made with a hand calculator by assuming linear change of the earth's magnetic field between successive readings at the base station. Diurnal corrections generally ranged between 10 and 40 gammas. Drift of the proton precession magnetometer was considered negligible. Because of the small areal extent of the magnetic surveys, corrections were not made to remove the earth's main magnetic field gradient. Diurnal-corrected values were then subtracted from the total magnetic field intensity



value at the Monroe magnetic base to obtain the drift-corrected total magnetic field intensity anomaly. A listing of magnetic anomaly values for all magnetic profiles is given in Appendix 6.

The reduced ground magnetic data collected in the Monroe Hot Springs area were plotted as profiles and hand-smoothed to reduce the effects of both cultural noise and noise due to surficial volcanic rocks. Smoothed values were plotted on a map at a scale of 1:4800 at 50-m intervals along the profiles and contoured at an interval of 100 gammas. The resultant total magnetic intensity anomaly map is shown in Figure 15.

Error Analysis

Errors associated with the ground magnetic data are difficult to estimate quantitatively. Re-occupied magnetic stations were generally repeatable to within 10 gammas, which is a reasonable estimate of the error therein. However, the magnetic data are subject to terrain effects, cultural noise, and near-surface volcanic rocks within the survey area. These effects must be considered when interpreting the magnetic data.

Errors associated with gravity data can be attributed to uncertainties in horizontal and vertical control, tidal effects, instrument drift, terrain corrections, and the Bouguer reduction density. These errors will be analyzed for both the detailed and regional gravity data considering an "average" case for a station in moderate terrain, and a "worst-possible" case for a station at extreme elevation in rough terrain.

Consider first the detailed gravity data collected along the precisely surveyed profiles. Vertical control was guaranteed to ± 0.1 ft (0.03 m) which corresponds to 0.006 mgal error. Horizontal control error is negligible. Since the data were not corrected for tidal effects, errors therein shall be included in the estimate for instrument drift. Considering that loops to base station were closed about every hour, the average error is estimated to be 0.05 mgal but could be as high as 0.15 mgal in the worst case. Terrain correction errors are estimated using the "rule-of-thumb" suggested by Plouff (1977, oral communication) of 10 percent of the total terrain correction. Following this guideline an average terrain correction error of 0.5 mgal should be expected, and possibly up to 1.0 mgal in the worst case. Errors associated with the Bouguer reduction density are thought to be small due to relatively low relief encountered along the detailed gravity profiles. In summary, the detailed gravity data are subject to an average error of about 0.6 mgal and possibly 1.2 mgal error in the worst case.

The regional gravity data are subject to the same errors as the detailed data, but the magnitude of the errors is greater due to less accurate vertical control and extreme topographic relief. Horizontal and vertical control were obtained from U.S.G.S. preliminary 7-1/2 minute topographic quadrangles. Horizontal control error is again estimated as negligible. Vertical control error is dependent on the type of station occupied. U.S.G.S. bench mark elevations are subject to negligible error, whereas spot elevations are subject to errors of one tenth the map contour interval, in this case 4 ft (J. Zuck, 1978,

oral communication). Since most gravity stations were established at spot elevations, an average vertical control error of 0.2 mgal is estimated, but could be as high as 0.4 mgal. Errors due to tidal effect and instrument drift are significant since regional gravity loops were often closed only once per day. An average error of 0.1 mgal is estimated, with a worst case estimate of 0.4 mgal. These estimates are based on comparisons of simple Bouguer values at 11 stations which were occupied twice during the collection of data. Observed changes ranged from 0.02 mgal up to 0.28 mgal, with an average change of 0.12 mgal.

Of all the possible errors in the regional gravity data, the greatest is believed due to the terrain corrections. Applying the "rule-of-thumb" of 10 percent terrain correction error mentioned above, an average estimate would be 0.6 mgal and could be greater than 5 mgal for some stations in the Tushar Mountains. Even this estimate does not take into account the error due to the choice of 2.67 gm/cc for the terrain correction density. This error cannot be estimated quantitatively without additional information regarding subsurface densities, but the geologic control data would suggest real densities somewhat lower than 2.67 gm/cc. Such errors expressed in the regional gravity data will appear as isolated complete Bouguer gravity anomaly highs correlated with extreme topographic features.

Error associated with the Bouguer reduction density of 2.67 gm/cc is also difficult to estimate without subsurface density information. Qualitatively, the errors will represent the cumulative effect of densities other than 2.67 gm/cc from the datum plane of sea level up

to the station elevation. These effects are expected to be significant over the broad high plateaus in the survey area which stand about 1500 m above the valleys. If the density of the plateaus is less than 2.67 gm/cc as expected, the error is such that the complete Bouguer gravity anomaly values will be more negative than if the true density was used in the Bouguer reduction.

In summary, the uncertainty in the regional gravity data is expected to be about 0.9 mgal for the average case, and up to 6 mgal or greater in the worst case. Errors from improper choice of density in the terrain and Bouguer corrections are not included in these quantitative estimates, therefore the qualitative effects described above must be considered when interpreting the regional gravity data.

In an attempt to evaluate further in a qualitative manner the effects of different reduction densities, a small portion of the regional gravity data was reduced using 2.5 gm/cc for both the terrain and Bouguer correction densities. Figures 16 and 17 show the complete Bouguer gravity anomaly data reduced at 2.67 and 2.5 gm/cc, respectively. These figures cover the area containing the highest elevations and most rugged terrain of the survey region, and show a large gravity low believed due to low-density material in the Mount Belknap caldera. Mount Belknap and Mount Baldy are two peaks of abrupt topographic relief with gravity stations on top of them. It can be seen in both figures that the contours are disrupted in the vicinity of these peaks. Since these disruptions are gravity highs that are closely associated with extreme topography, they are believed to be the result of too high a reduction density assumed for the

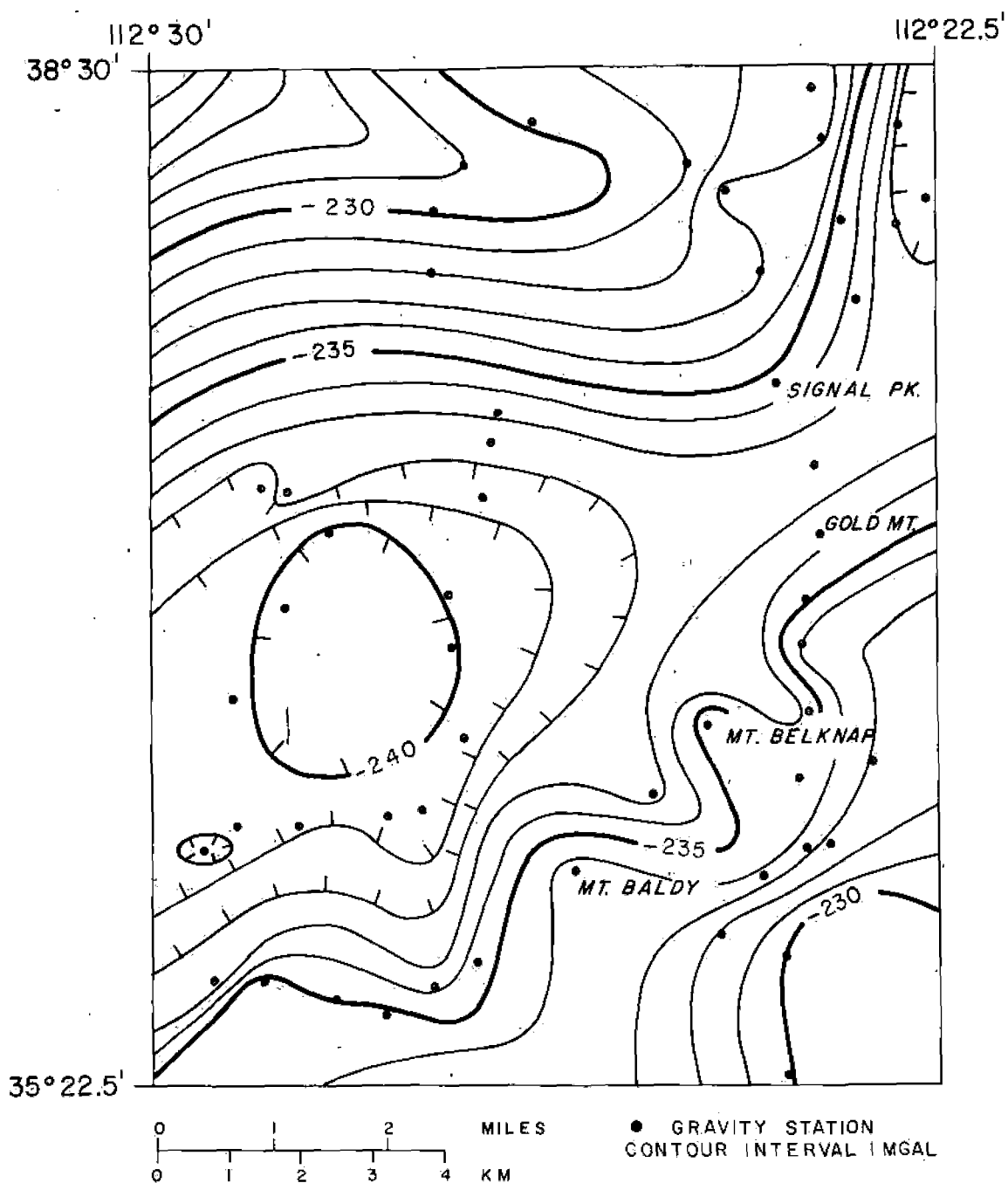


Figure 16. Complete Bouguer gravity anomaly map of the Mount Belknap caldera region. Density of 2.67 gm/cc was used for Bouguer and terrain corrections.

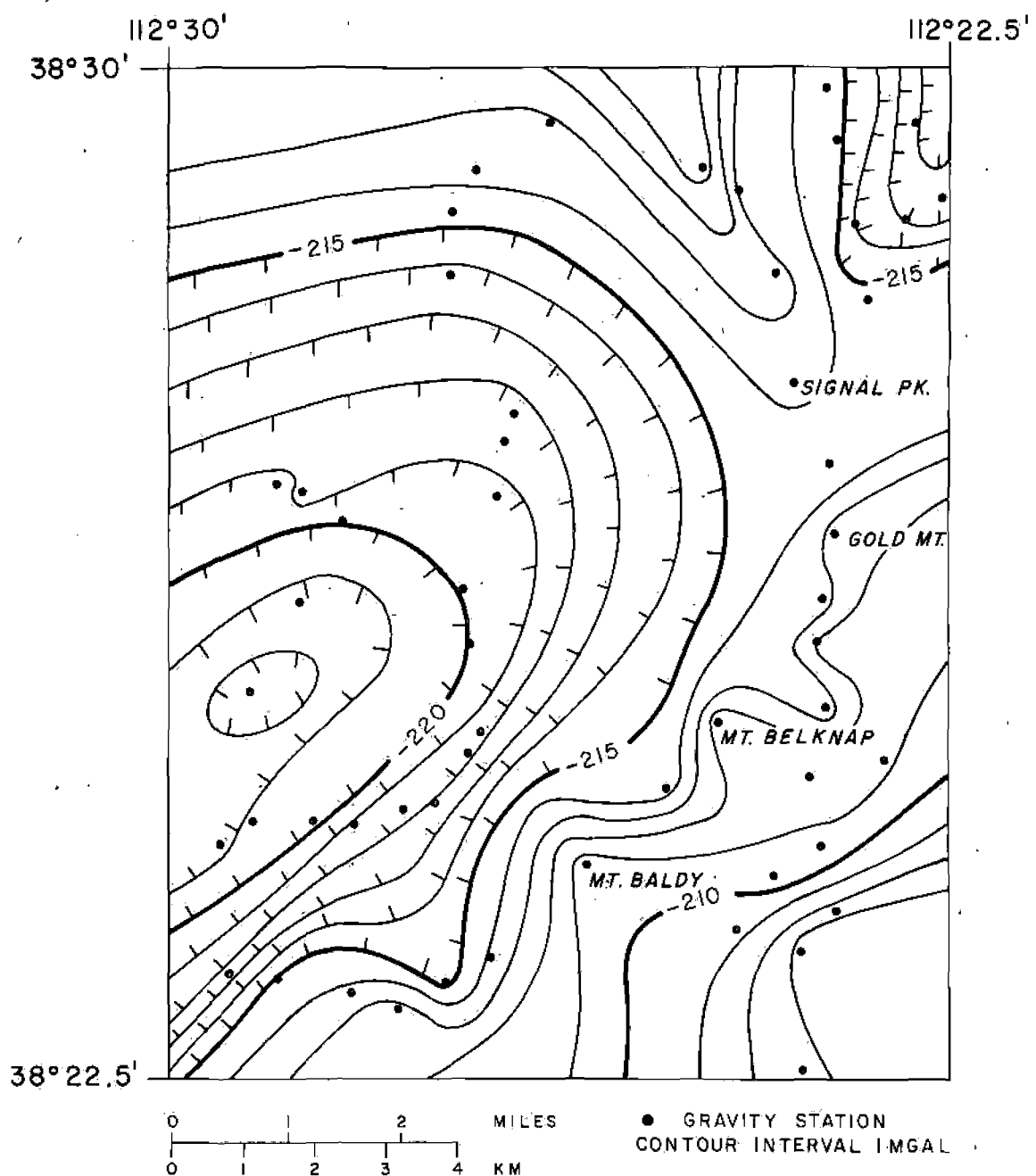


Figure 17. Complete Bouguer gravity anomaly map of the Mount Belknap caldera region. Density of 2.50 gm/cc was used for Bouguer and terrain corrections.

terrain correction. These effects were smoothed out in the complete Bouguer gravity anomaly map shown in Figure 14. Although the gravity low associated with the Mount Belknap caldera exists in both figures, the shape and magnitude of the anomaly are changed significantly. The values in the map reduced at 2.5 gm/cc are more positive, which is apparently the result of the lower Bouguer reduction density. The map reduced at 2.5 gm/cc is judged to present smoother and more "realistic" data than the 2.67 gm/cc reduction density map, even though the differences are not strongly pronounced. This is believed to be an indication that 2.5 gm/cc is a more accurate Bouguer reduction density than the 2.67 gm/cc used.

DATA PROCESSING

It was considered desirable to process the regional gravity data in order to study both the regional gravity trends and the residual gravity after removal of the regional gravity. The technique chosen to accomplish this was to fit polynomial surfaces of different orders to the gravity data as described by Montgomery (1973). Although this method is not as quantitative as wavelength filtering in terms of the actual wavelengths in the data that are filtered, it does have the advantage of being less troubled by edge effects. Since the gravity data show a steep gradient along the northern portion of the survey area, the minimization of edge effects was considered highly desirable. A number of recent gravity surveys (Crebs, 1976; Brumbaugh, 1977; Sawyer, 1977; and Case, 1977) have used both polynomial fitting and wavelength filtering to produce residual gravity maps. Although some differences between the two types of maps have been observed, they generally produce similar residual maps. For this reason, polynomial fitting alone was considered sufficient to accomplish the goal of removing the regional trends.

Preparation of Data

To enable machine-contouring of the polynomial surfaces and residual gravity maps, it was necessary to produce data on a regular grid from the randomly-located gravity station data. This was

accomplished by hand-digitization of the complete Bouguer gravity anomaly values which had been hand-contoured on a map at a 1-mgal interval. The Universal Transverse Mercator (UTM) grid system of 1-km grid spacing was used. An array of 47 by 58 data points was thus generated, covering the area from 368 km E to 414 km E, and from 4233 km N to 4290 km N, respectively, within zone 12 of the UTM grid system. This data grid was machine-contoured at a 2-mgal interval and the resulting complete Bouguer gravity anomaly map is shown in Figure 18.

It is important to consider the aliasing effect of the digitization process. The 1-km digitizing interval will cause aliasing of all frequencies in the data higher than the Nyquist frequency of 0.5 cycles/km. It must be noted that the original acquisition of the data also causes aliasing, although a specific Nyquist frequency cannot be calculated for the irregularly spaced station data. However, since 948 stations were used to construct a map covering about 2600 km², the average station density is about 0.36 station/km². A rough estimate, then, is that the data acquisition itself caused aliasing of frequencies higher than about 0.18 cycles/km. Since aliasing due to digitization removed only those frequencies higher than expected to be found in the original data, the digitization process should not noticeably change the original data. Indeed, a comparison between the two complete Bouguer gravity anomaly maps generated from random and gridded data (Figs. 14 and 18, respectively) shows them to be similar.

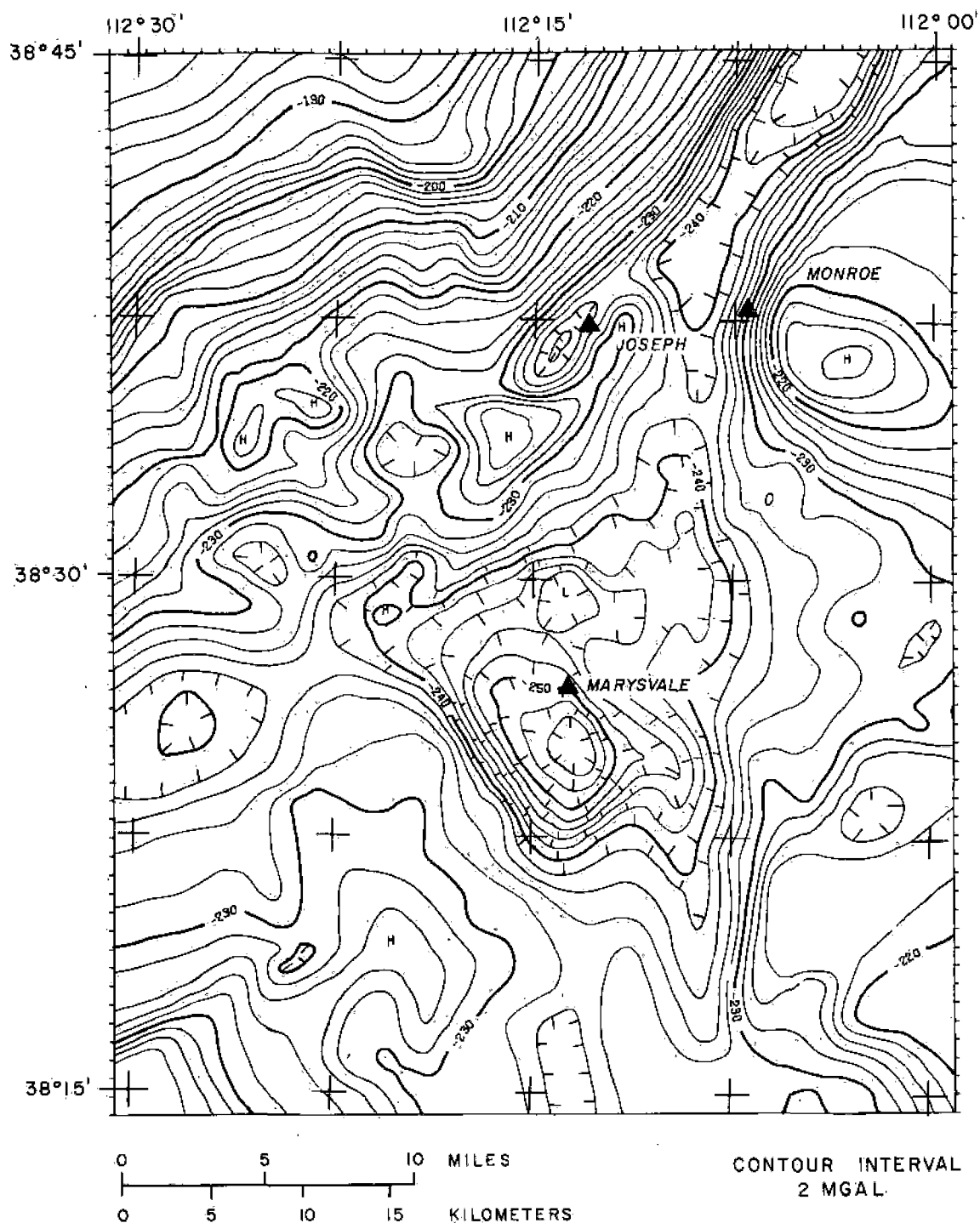


Figure 18. Complete Bouguer gravity anomaly map of the survey area.
Machine-contoured from 1-km digitized data.

Polynomial Surface Filtering

All polynomial surface calculations were made using FORTRAN computer programs originally written by Dr. Jerry R Montgomery. The gridded regional gravity data was used to compute polynomial surfaces of orders 1 through 10 which represent a best fit to the gravity data in a least-squares sense. The R.M.S. residual between the polynomial surface and the gridded gravity data was computed for each order polynomial, and is shown plotted in Figure 19. This curve was analyzed to help decide which order polynomials provide best fit to the data. The breaks on the curve shown at the third-, fifth-, and seventh-order polynomials indicate these to be the best choices. The polynomial surfaces and residual gravity maps for these orders were then machine-contoured at a 2-mgal interval. A tenth-order polynomial surface and residual map were also produced since this high-order surface closely approximates the original data and is similar to a low-pass gravity map. The third-, fifth-, seventh-, and tenth-order polynomial surfaces are shown in Figures 20, 21, 22, and 23, respectively. The corresponding residual complete Bouguer gravity anomaly maps are shown in Figures 24, 25, 26, and 27, respectively.

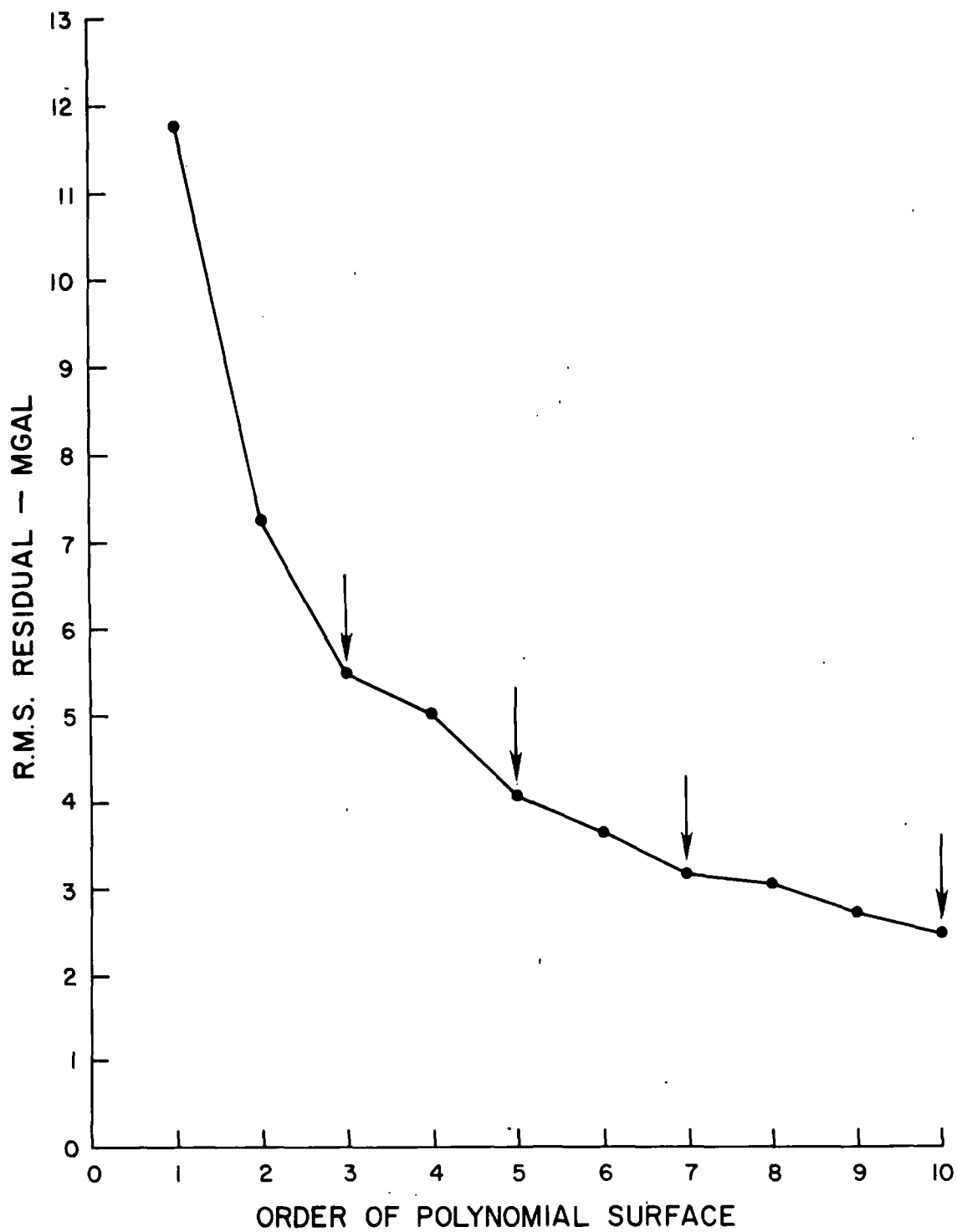


Figure 19. R.M.S. residual vs. order of polynomial surface determined for gridded gravity data. Arrows show order of surfaces and residual maps selected for analysis.

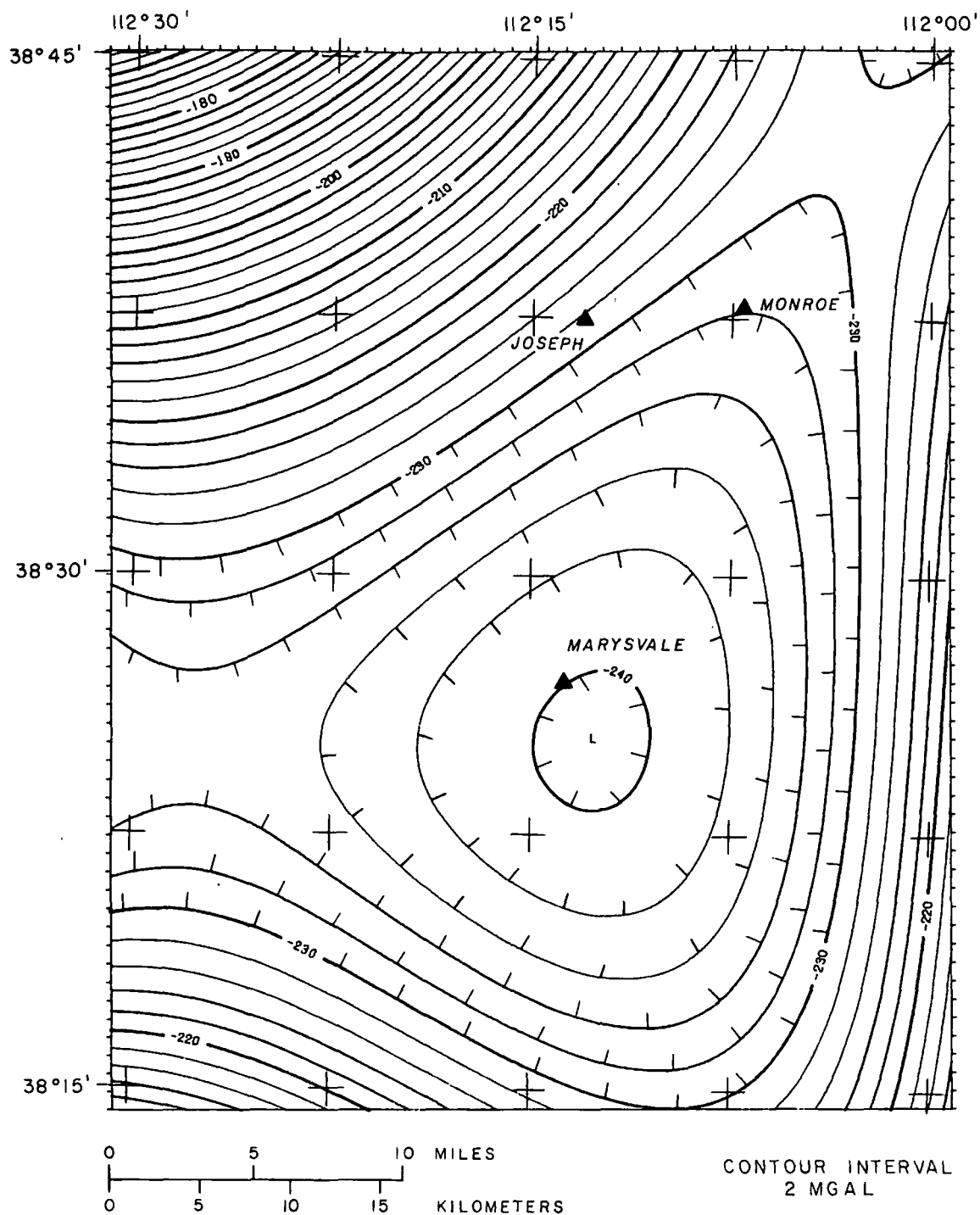


Figure 20. 3rd-order polynomial surface gravity anomaly map.

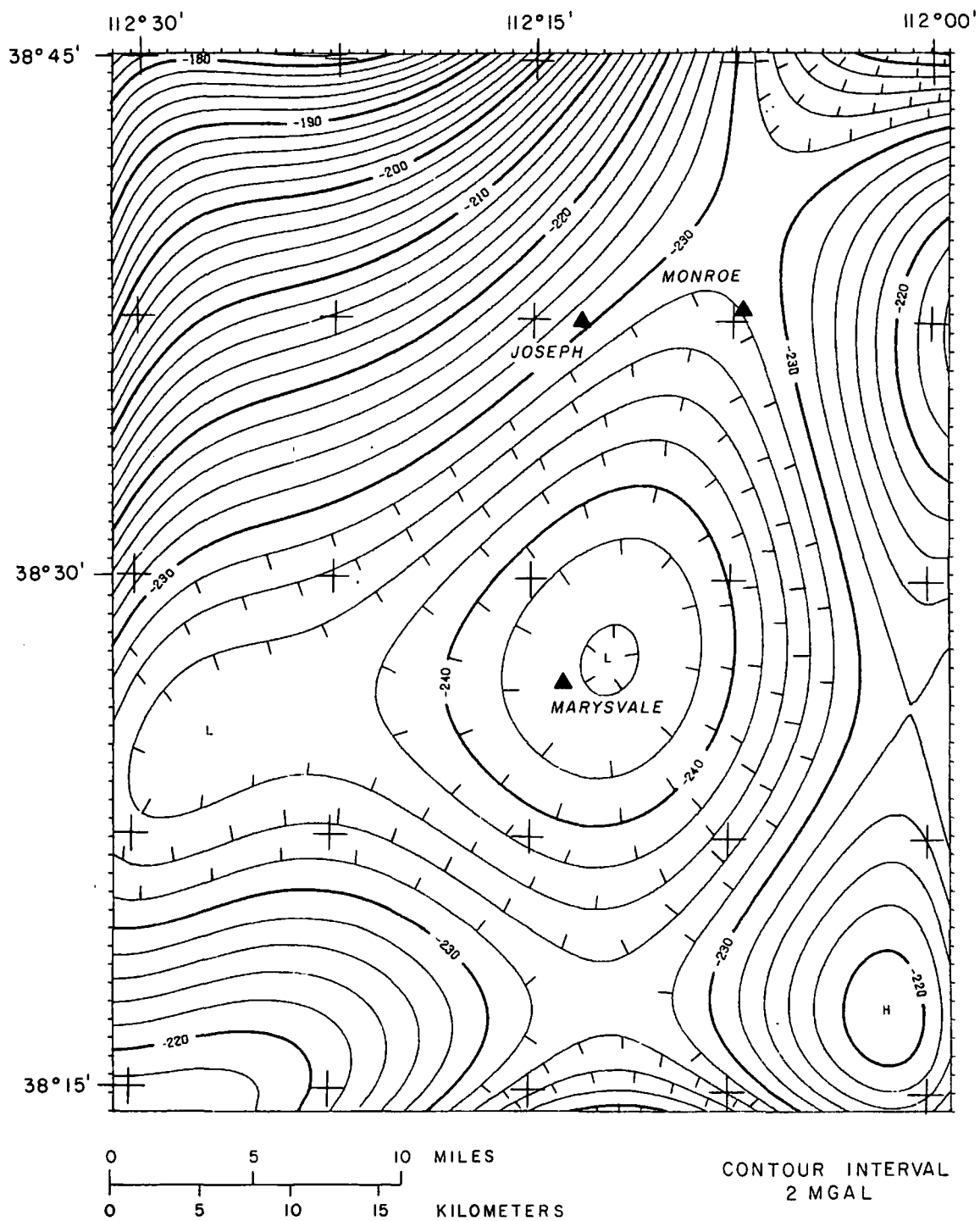


Figure 21. 5th-order polynomial surface gravity anomaly map.

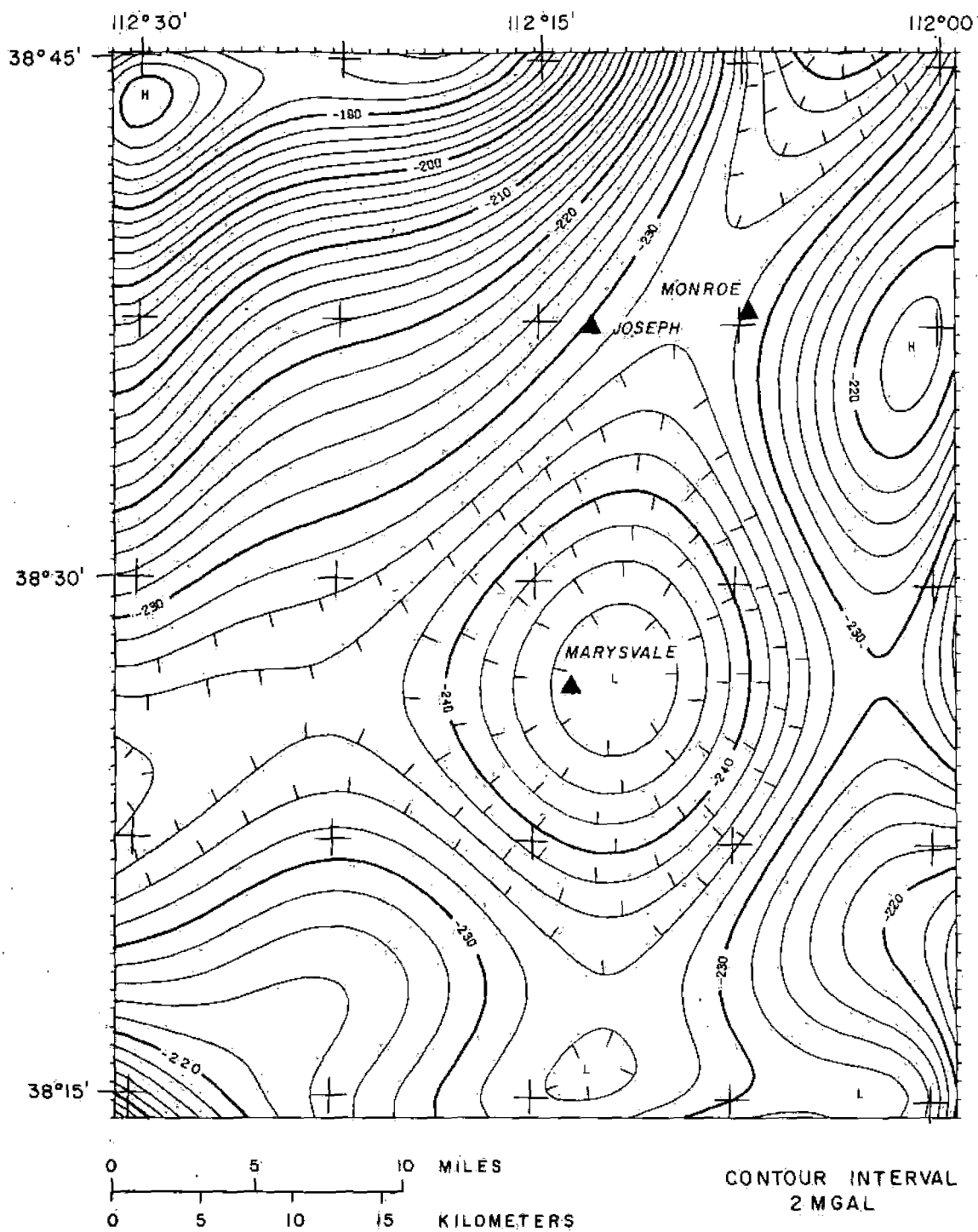


Figure 22. 7th-order polynomial surface gravity anomaly map.

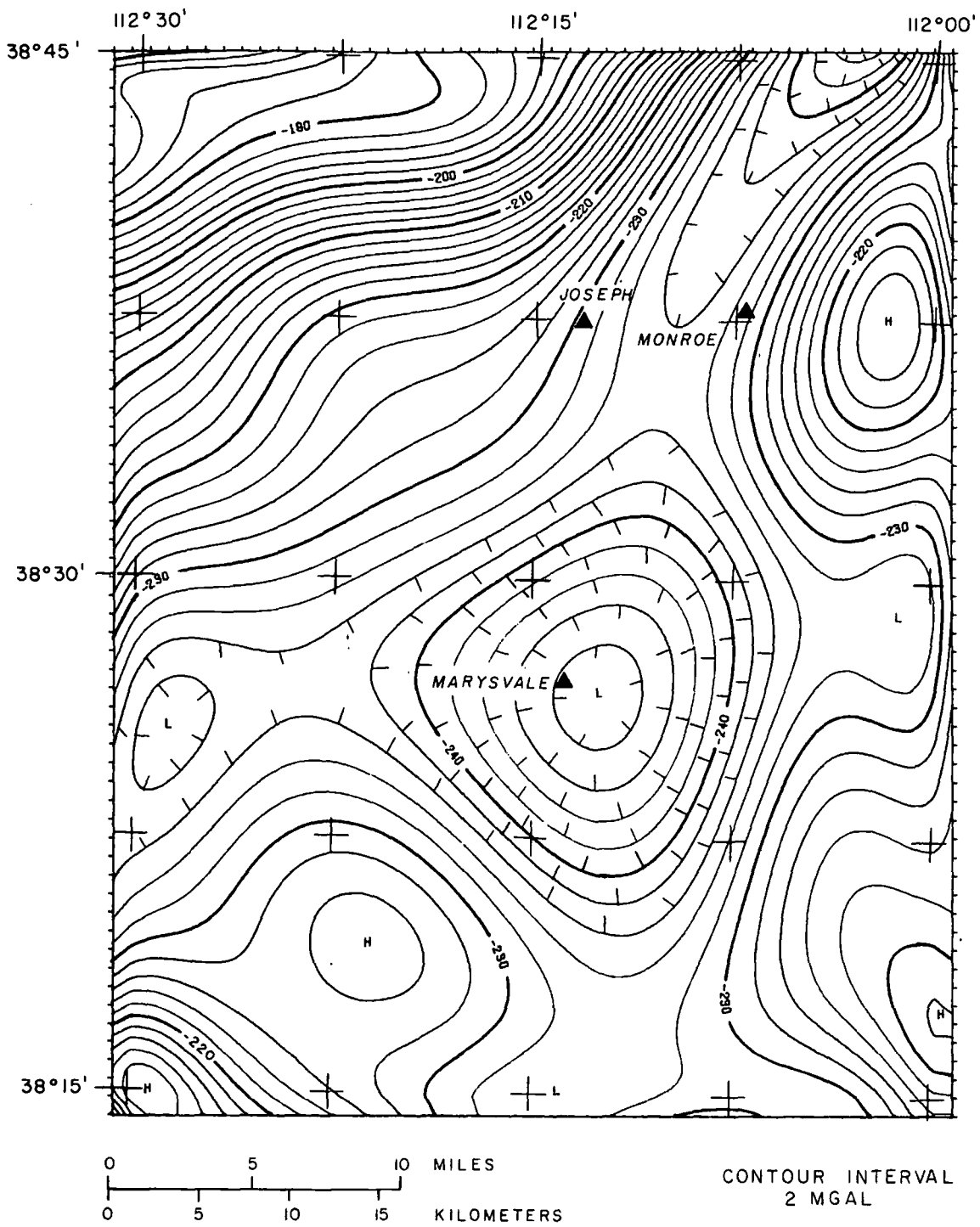


Figure 23. 10th-order polynomial surface gravity anomaly map.

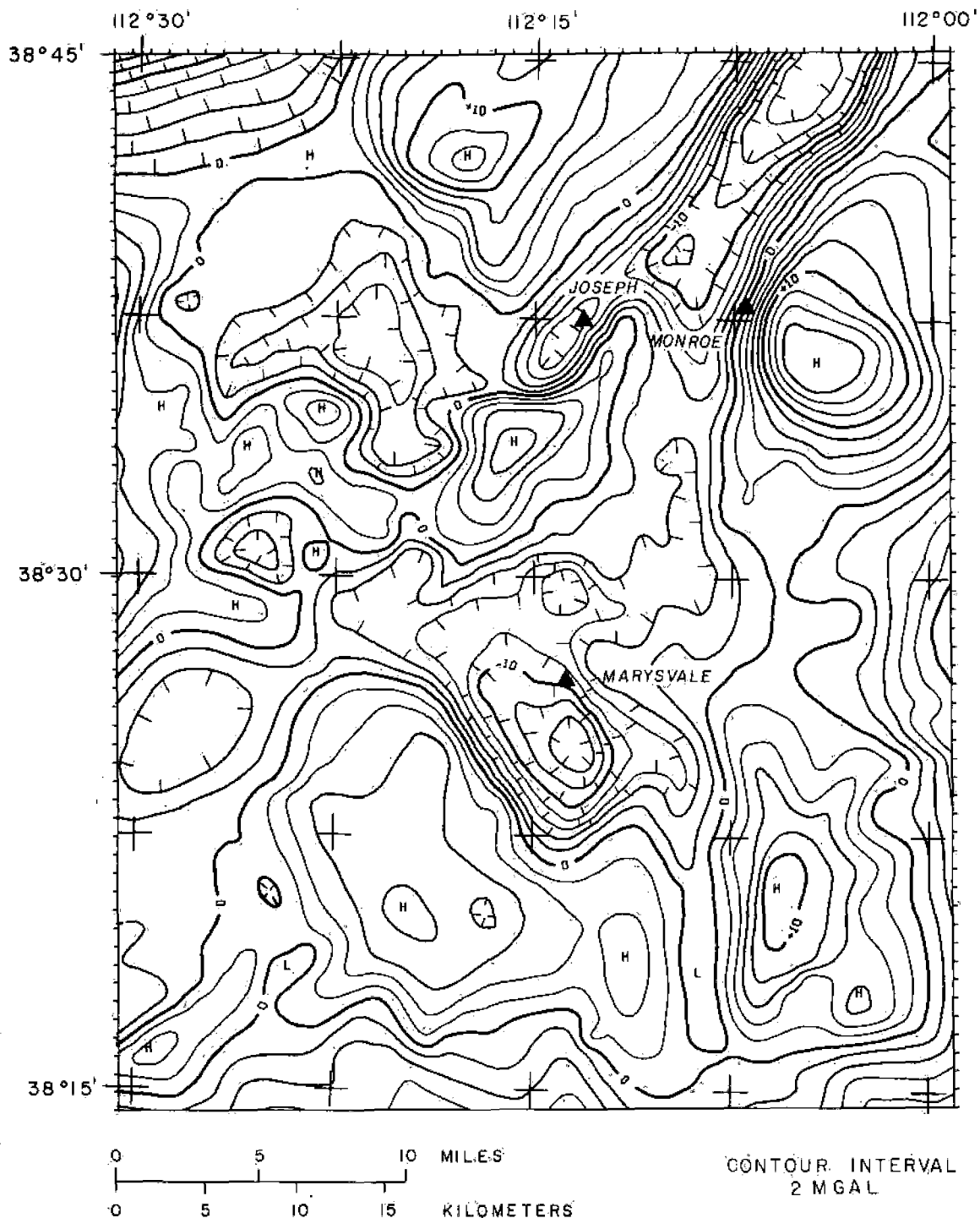


Figure 24. 3rd-order polynomial residual gravity anomaly map.

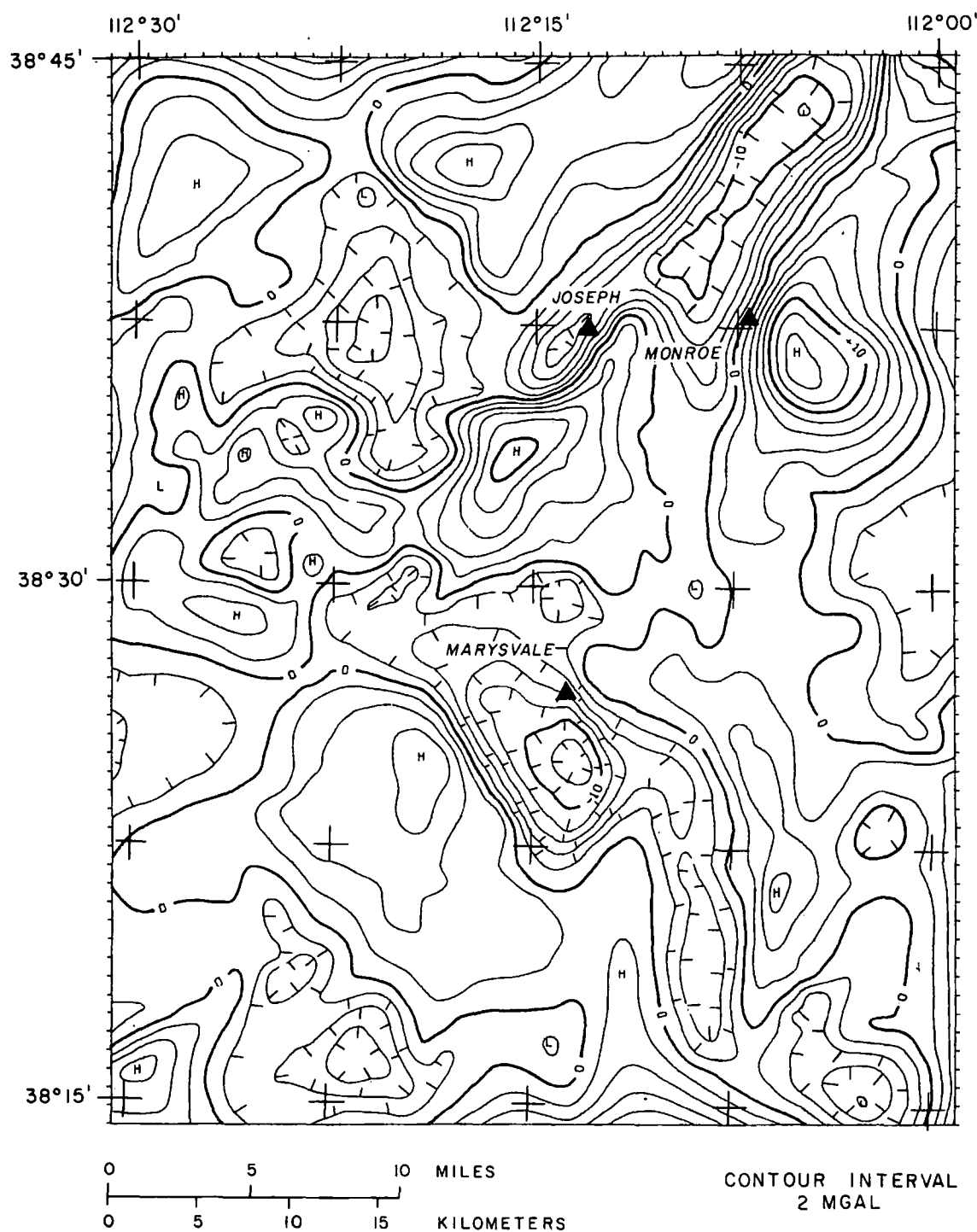


Figure 25. 5th-order polynomial residual gravity anomaly map.

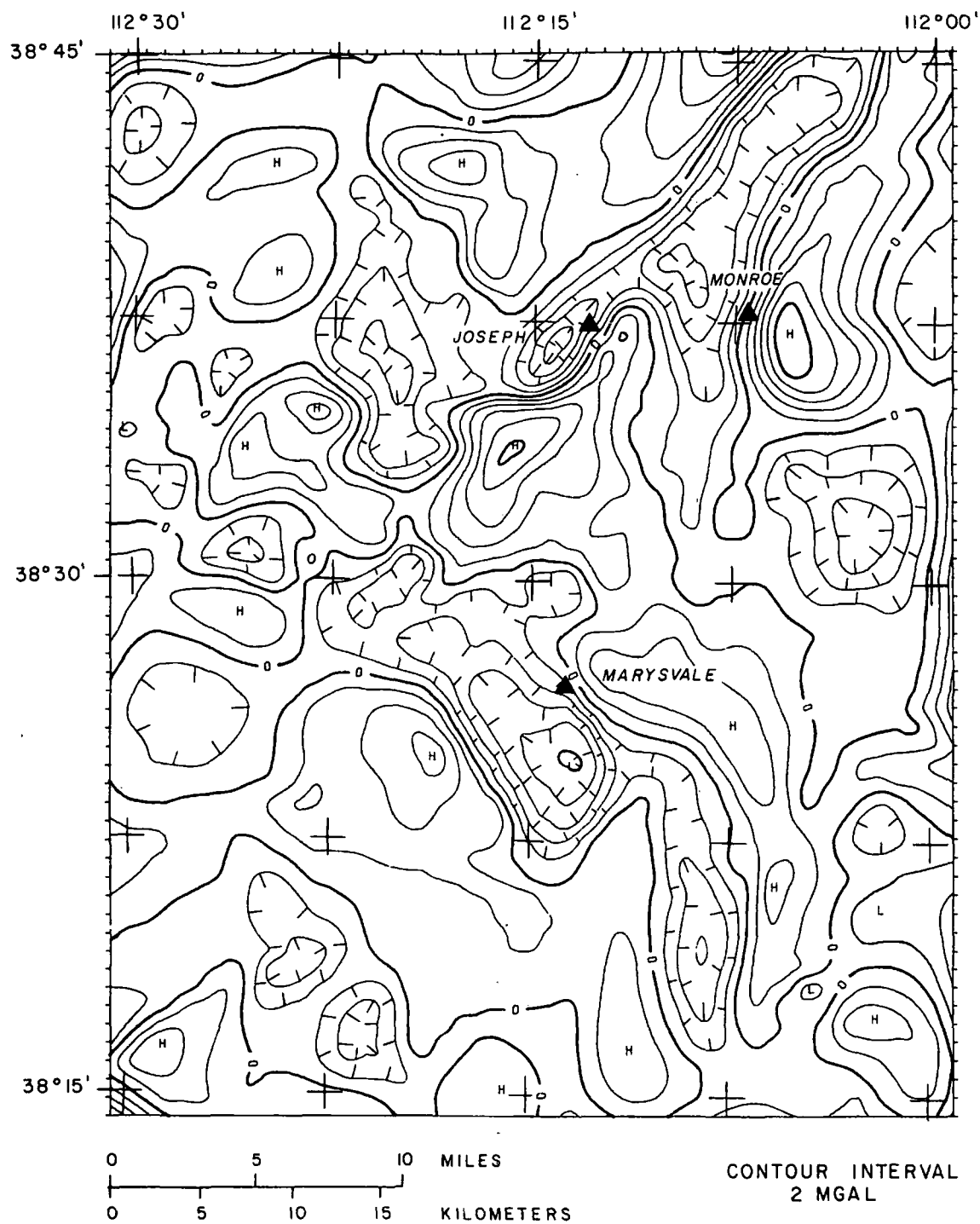


Figure 26. 7th-order polynomial residual gravity anomaly map.

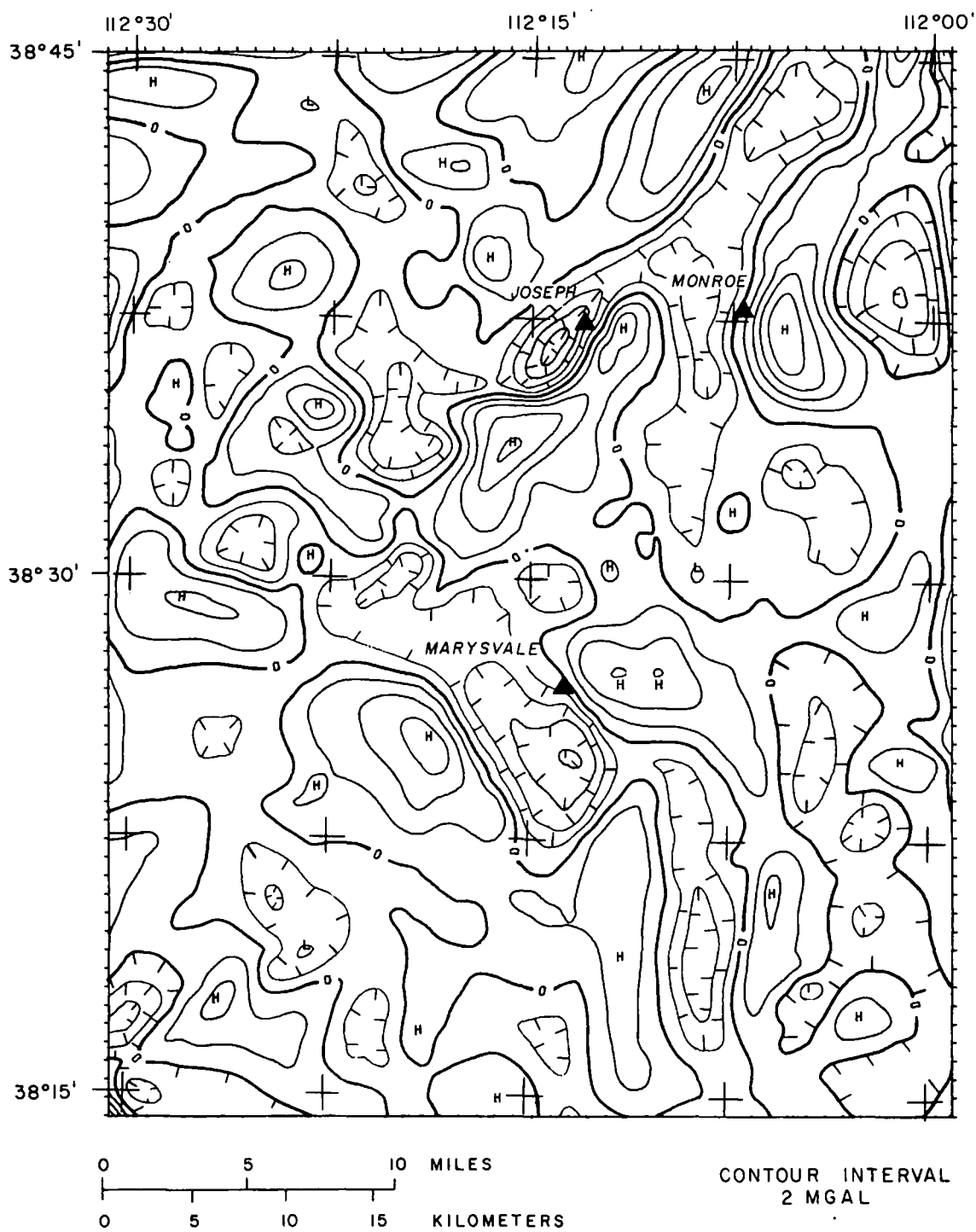


Figure 27. 10th-order polynomial residual gravity anomaly map.

INTERPRETATION

Methods of Interpretation

Both qualitative and quantitative techniques were used to interpret the gravity and ground magnetic data into a coherent geologic picture. The major features of the regional gravity data were first qualitatively correlated with known geologic features. Polynomial residual gravity maps were also studied to help clarify those features disguised by regional effects in the original data. Interpretive geologic cross sections were constructed along four regional gravity profiles. The detailed gravity and ground magnetic data were interpreted in a similar manner, and include four models in the Monroe Hot Springs area and two models for the Joseph Hot Springs area.

Interpretative geologic cross sections were constructed using both forward and inverse two-dimensional gravity and magnetic modeling techniques. The specific computer programs used to accomplish this are described by Snow (1978) and employ techniques developed by Talwani and others (1959) and Talwani (1965). Although the programs are capable of modeling finite strike-length ("2-1/2-D") bodies, this option was not used since in most cases the advantages are outweighed by the added complexity of the technique (John H. Snow, 1978, oral communication).

Modeling of the ground magnetic data was relatively simple since

the program calculates the magnetic effect of an arbitrarily-shaped two-dimensional body, i.e., it is possible to include the surface topography in the model itself. Modeling of gravity data in areas of extreme topographic relief presented a more complex problem since the complete Bouguer gravity anomaly values had been reduced to a datum of sea level using a Bouguer reduction density of 2.67 gm/cc. Modeling of the complete Bouguer gravity anomaly values directly would be inappropriate due to large masses of low density volcanics in the Pavant Range, northern Sevier Plateau, and Tushar Mountains. As mentioned previously, the complete Bouguer gravity anomaly values over these regions are more negative than if they had been reduced to a datum using a more appropriate density, i.e., 2.3 to 2.5 gm/cc. The quantitative estimates of depth, etc. in the geologic cross sections would be improperly biased unless some correction is made for this effect.

Initially it was thought that the problem could be solved by using the technique of Smith (1973), in which free-air gravity anomaly values are modeled and the surface topography is included in the model. This method essentially lets the modeling program perform the Bouguer reduction, and additionally corrects for the gross trend of the terrain, i.e. the trend perpendicular to the profile direction. Unfortunately, the technique does not correct for terrain effects due to surface irregularities near the station. A few tests on the data in this survey showed such effects to be significant in the free-air gravity anomaly values, thereby making it impractical to model such "noisy" data.

A technique better suited to the data of this survey, though still not ideal, is that used by Brown (1974). This method uses what is referred to as the "corrected" complete Bouguer gravity anomaly determined by the equation:

$$C' = C + 0.01276 (2.67 - D) H + ((D/2.67) - 1) TC$$

where:

C' = Corrected complete Bouguer gravity anomaly value in mgal, assuming material of density D gm/cc above datum.

C = Complete Bouguer gravity anomaly value in mgal, reduced using Bouguer density of 2.67 gm/cc.

D = Density of mass above datum in gm/cc.

H = Height of station above datum in feet.

TC = Terrain correction of station in mgal, calculated using assumed density of 2.67 gm/cc.

It should be noted that this equation differs from that given by Brown (1974) in that I have changed the sign of the second term from negative to positive. An examination of his profiles showed that apparently he used the equation as given herein, and the discrepancy is the result of a typographical error.

The concept of this corrected complete Bouguer gravity anomaly is simple. The datum is chosen as the lowest station elevation along a profile, and all gravity values along that profile are then reduced down to the datum using a more appropriate density for the surface material than 2.67 gm/cc. The terrain correction is also recalculated using the new density. The corrected complete Bouguer gravity anomaly values are now assumed to lie along the elevation of the datum, and the two-dimensional modeling program is used to simulate the effects

of bodies of various densities lying below the datum. By showing the flat-topped two dimensional model with the actual surface topography superimposed above it, a real-looking geologic cross section is produced and gross bias due to improper reduction density should have been eliminated. The primary disadvantage of this technique is that one must model all the mass above the datum elevation as one specified density, even though this might contradict the known geology.

The locations of gravity profiles are shown in Figure 28, and detailed ground magnetic profile locations are shown in Figures 12 and 13. Profiles were selected such that they cross perpendicular to the trend of the various anomalies as much as possible in order to satisfy the two-dimensional modeling assumption. Regional gravity profiles were located near to or through gravity stations whose corrected complete Bouguer gravity anomaly values were projected onto the profile along the trend of the gravity contours. All gravity values were corrected to a datum equal to the elevation of the lowest station along the profile, and assumed a density of 2.4 gm/cc for material above the datum. Profiles of the surface topography are included in each gravity model, but since they were plotted as straight lines between the elevation at each station the profiles may not accurately reflect topographic changes between stations.

All models were constructed by first compiling an initial model from the known structure, lithology, and geologic control data as described previously. Models were then adjusted as necessary to obtain a good fit to the geophysical data yet remain as consistent as possible with the known geology. Models were kept as simple as

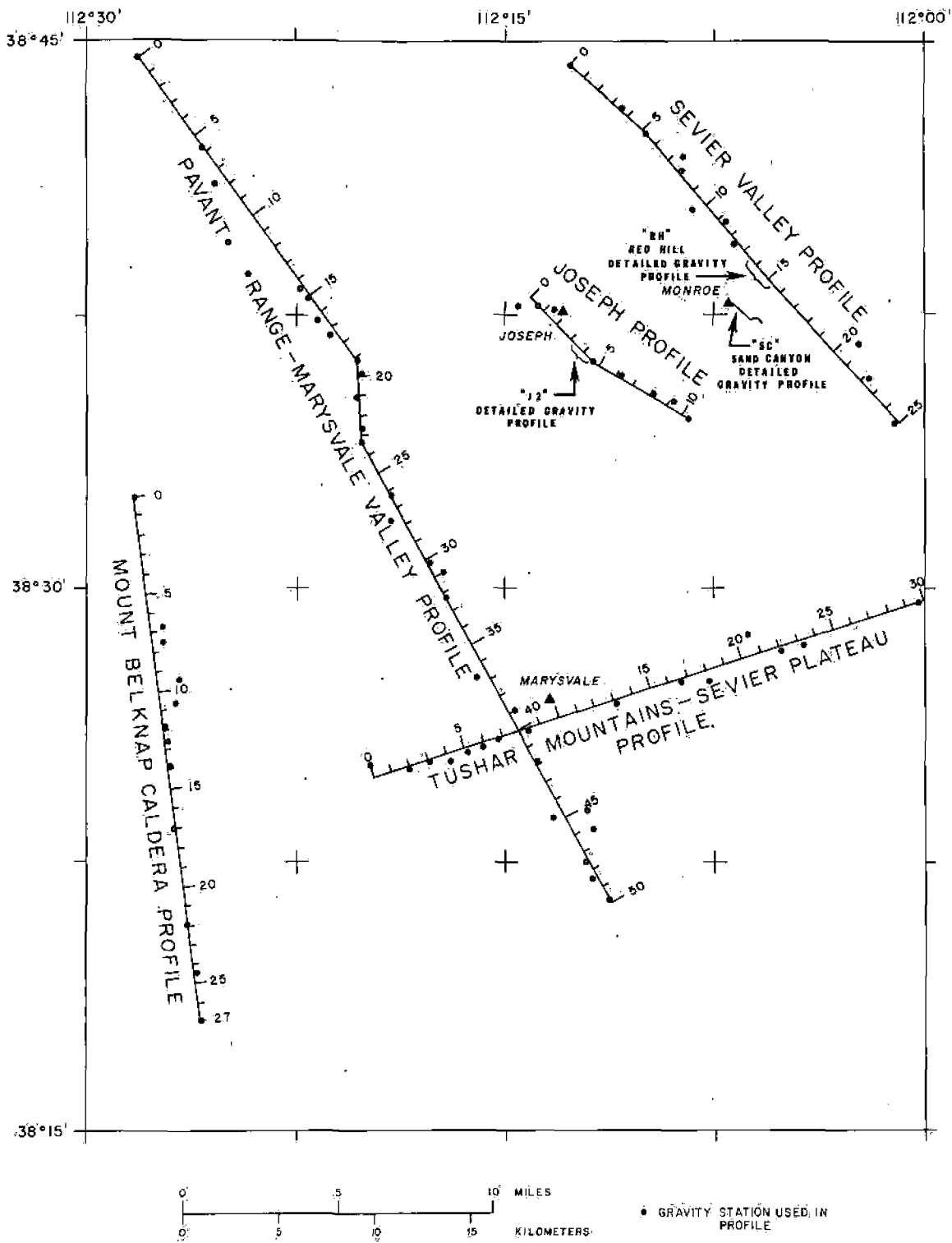


Figure 28. Map of survey area showing location of gravity profiles.

possible by adding subsurface bodies only when necessary. Regional profiles were modeled first, and then used as guidelines for modeling of the detailed profiles. Although the cross sections shown herein are not unique, they are believed to show reasonable interpretations of the subsurface geology.

Regional Gravity Survey

1) Complete Bouguer Gravity Anomaly Map

In general, gravity features on this map (Fig. 14) can be clearly correlated with the known geology. Major features of the map will be qualitatively discussed here, whereas quantitative interpretation of features along selected profiles is provided later.

One of the most striking features of the map is the steep regional gravity anomaly containing over 30 mgal relief which lies in the southern Pavant Range. The gradient follows closely the contact between sedimentary rocks and Bullion Canyon Volcanics, which is believed in part to be the cause of the gradient. Other subsurface changes which may contribute to this gradient are the deepening of the Moho eastward and the Cordilleran hingeline of Utah (Stokes, 1976) across which the carbonate Paleozoic section found to the west thins rapidly eastward as the Mesozoic sedimentary section thickens.

Distinct gravity lows are observed over alluvial-filled grabens throughout the survey area. Gravity contours in the Sevier Valley graben west of Monroe indicate that the graben either becomes shallower from north to south towards the Antelope Range, or alternatively, the downdropped block becomes more dense to the south

as would result from thinning of the low-density Arapien salt-shale formation known to underlie Sevier Valley near Richfield. A smaller graben is indicated by closed gravity contours in the vicinity of Joseph. The lowest gravity values in the survey area are found just south of Marysvale. The large somewhat circular gravity low here is interpreted as due to a deep graben. Although the circular shape might suggest a caldera as the source of this anomaly, this interpretation is not considered viable because of the absence of closely associated ash-flow tuffs that are a necessary component of caldera development. A smaller graben southeast of the Marysvale graben in the area known as the "elbow" is indicated by the extension of the Marysvale Valley gravity low into this region.

Gravity gradients are associated with most of the Basin and Range normal faults found throughout the survey area. The Sevier, Elsinore, Dry Wash, and Tushar faults are all clearly expressed in the gravity data due to the density contrast between the volcanics and alluvium. Two previously unmapped faults are indicated by gravity gradients on the southeast and northeast side of the Marysvale Valley graben. The fault on the southeast side has no apparent surface expression, and trends northeast crossing the valley just north of Piute Reservoir. The fault indicated by the gravity gradient on the northeast side of the Marysvale Valley graben trends northwest and is believed to lie between the Sevier River and the Bullion Canyon Volcanics mapped due west of Marysvale by Willard and Callaghan (1962). The East Branch Tushar fault, mapped by Willard and Callaghan (1962), is not manifested in the gravity data and therefore must be of very limited

throw or cause little density contrast.

The belt of igneous intrusions trending east-northeast across the survey area do not individually express themselves in the gravity data. A small deflection in the contours a few km northeast of the Red Hills caldera may be related to the central intrusive in the Antelope Range, but this is not certain. The Dry Creek Canyon intrusion is not manifested in the gravity data. A large circular gravity high in the northern Sevier Plateau east of Monroe may be due to a large intrusive body here, as suggested by the exposed Monroe Canyon intrusion which lies on the southern side of this anomaly.

In general, gravity lows are observed over known calderas in the survey area. These gravity lows are believed due to low-density volcanic fill providing a contrast with denser surrounding and underlying sedimentary and/or igneous rocks. The Mount Belknap caldera is expressed clearly as an oval-shaped gravity low of about 10 mgal relief. The Big John caldera corresponds with a small closed gravity low and a perturbation of the contours on the south side of the Mount Belknap caldera gravity low. The Red Hills caldera corresponds with a circular gravity low of about 3 mgal closure. The signature over the Three Creeks cauldron is not clear, if present at all. Although the gravity map does show disturbed contours in this area, without further geologic information no interpretation can be made.

A linear gravity anomaly of about 10 mgal relief lies across the west-central portion of the survey area, and trends east-northeast along the northern edge of the Mount Belknap and Red Hills caldera and

belt of intrusive rocks. Where this trend intersects the Sevier fault zone, the gravity gradient along the Sevier fault is clearly disrupted. This disruption may be due to thicker accumulations of low-density material in this portion of the northern Sevier Plateau, possibly indicative of another volcanic source area here.

Two small closed gravity lows in the Clear Creek downwarp are not believed related to a volcanic source area, but are interpreted as due to accumulations of low-density Joe Lott Tuff or Sevier River formation in small basins.

2) Polynomial Surface and Residual Gravity Anomaly Maps

Analysis of the polynomial surface gravity anomaly maps (Figs. 20 to 23) shows an interesting progression from the low-to-high-order surfaces. The third-order surface shows a large circular-shaped low centered near Marysvale with two arms extending outward, one west towards the Mount Belknap caldera and the other north along Sevier Valley. The fifth-order surface shows further development of this pattern as well as separation of the northern Sevier Plateau gravity high into two distinct highs. The seventh-order surface shows almost full development of the gravity low extending eastward into the northern Sevier Plateau from the Marysvale Valley low. The tenth-order surface (Fig. 23) is perhaps the most significant of all the polynomial surface maps generated in that it shows the strongest gravity features and filters out minor inflections associated with weaker features. The strongest gravity features observed are the Sevier Valley and Marysvale Valley grabens and associated lows, the

Pavant Range regional gravity gradient, the Mount Belknap caldera gravity low, the low extending eastward out of the Marysvale Valley graben into the generally high gravity values over the northern Sevier Plateau, and the gravity high over the Tushar Mountains. Anomalies correlated with the Big John and Red Hills calderas, Three Creeks cauldron, Clear Creek downwarp, and Joseph graben are not seen in the tenth-order surface and are minor features in terms of the regional geology in the survey area.

With some exceptions, the polynomial residual gravity anomaly maps (Figs. 24 to 27) do not reveal features correlatable with the known geology which were not obvious in the original data. The exceptions occur in those areas obscured by large regional gradients such as found in the Pavant Range and northern Sevier Plateau. The best example is the large closed gravity low in the Pavant Range seen most distinctly in the third- and fifth-order residual maps. Also, northeast of this low, northwest-trending gravity contours are observed in the third- through seventh-order residual maps. The closed gravity low may be related to a volcanic source area in this part of the Pavant Range, and perhaps related to the Three Creeks cauldron. The northwest-trending contours may be related to a major volcanic-sedimentary rock contact which was obscured in the original data by the regional gradient. A close examination of the geologic map of Callaghan and Parker (1962b) does suggest a lineation near the northwest-trending gravity gradient northeast of which sedimentary rocks extend farther southwest. This could be explained as a line northeast of which the Pavant thrust carried sedimentary rocks farther

southeastward. Another noteworthy feature in the residual maps is the closed gravity low in the northern Sevier Plateau shown on the seventh-order residual map. This could also indicate a volcanic source area here, although no specific geologic evidence for this is seen in the geologic map of Callaghan and Parker (1961a).

3) Interpretive Geologic Cross Sections

a) Sevier Valley Profile

The gravity changes along this profile (Fig. 29) are interpreted as due to combinations of effects from the Sevier Valley graben and changes in thicknesses of both sedimentary rocks and Bullion Canyon Volcanics. The gravity low is believed due to the alluvial-filled Sevier Valley graben lying between the Elsinore and Sevier faults. The depth estimate of 1300 m actually refers to the combined depth of alluvium, Joe Lott Tuff, and Arapien salt-shale, all of which are expected to have a density of about 2.0 gm/cc.

It was found impossible to fit the gravity data using a steeply dipping contact along the Sevier fault. Although this fault is shown as rather gently dipping, it is actually believed to consist of a complex zone of en echelon faulting. A more precise interpretation of the nature of the faulting here is shown later when the detailed gravity data across the Red Hill Hot Spring are interpreted. The Elsinore fault is shown as vertical since the low station density across this feature did not constrain the model otherwise.

An interesting aspect of the model is that the Sevier Valley graben is shown as asymmetrical. This asymmetry is apparent in the

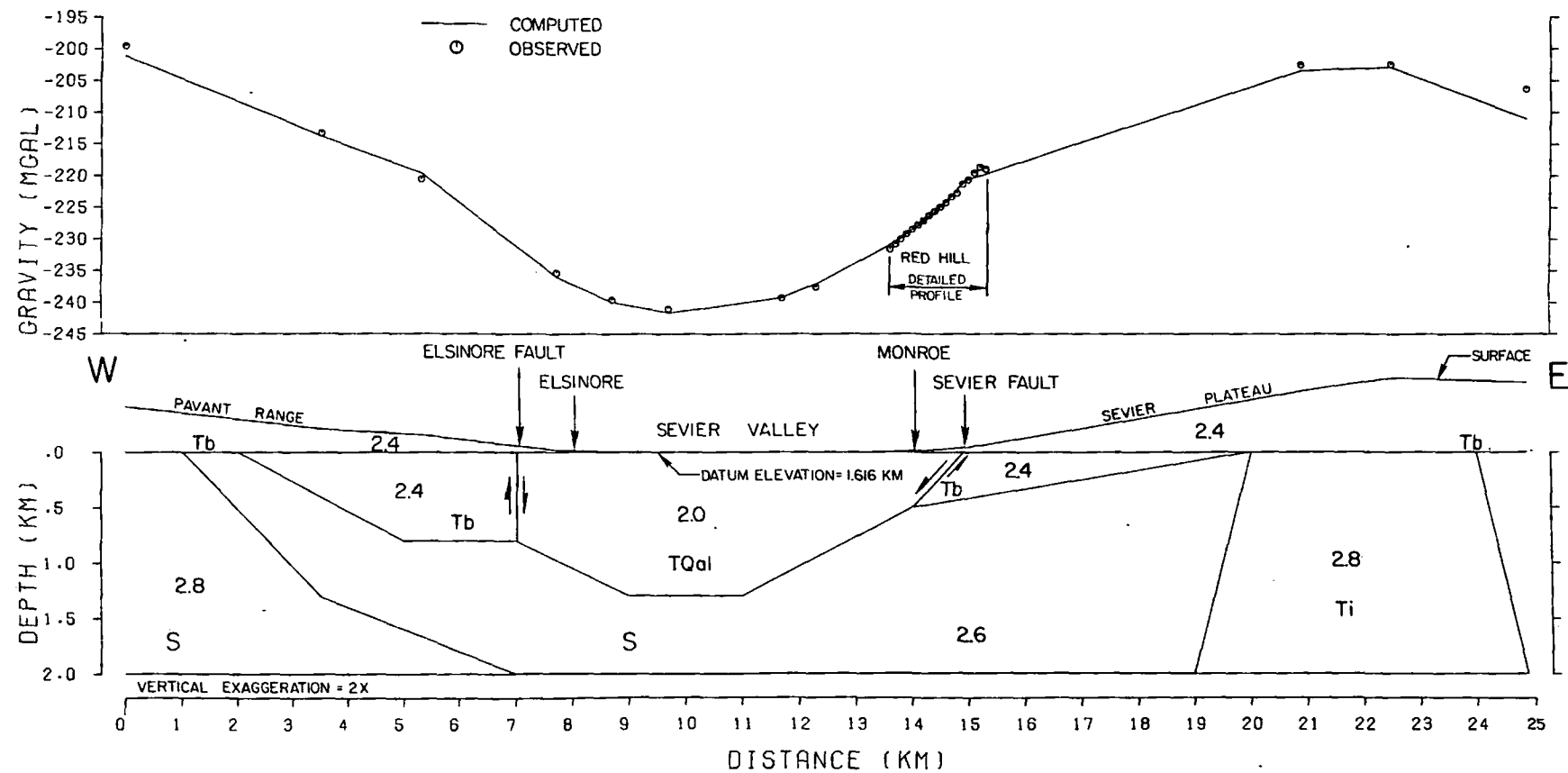


Figure 29. Interpretive geologic cross section along Sevier Valley gravity profile. Densities shown in gm/cc.

regional gravity map (fig. 14) as the main gravity low is centered closer to the west side of the valley. This may indicate that the bedrock-alluvium contact is steeper on the west side of Sevier Valley.

Deeper structures in the model are reasonable, but largely conjectural. Beneath the Bullion Canyon Volcanics on either side of the valley, a body of 2.6 gm/cc density is shown representing sedimentary rocks. This body thins westward while a denser sedimentary section of 2.8 gm/cc density thickens across the Cordilleran "hingeline" of Utah as described by Stokes (1976). A large intrusive body is shown underlying the northern Sevier Plateau at the east end of the profile. The probable existence of an intrusive body here is indicated by the exposure of quartz monzonite in Monroe Canyon just south of this profile. Although the density of 2.8 gm/cc shown for this intrusive body may be slightly higher than expected for this unit, 2.8 gm/cc is still a reasonable density and it was necessary to use this value to fit the observed gravity data.

b) Pavant Range - Marysvale Valley Profile

This profile (Fig. 30) shows a total gravity relief of about 70 mgal between the Pavant Range and Marysvale over a distance of less than 50 km. Although much of this steep gradient could be due to deepening of the Moho across the Basin and Range - Colorado Plateau transition zone, it has been suggested by Snow (1978) that much of this gravity relief might be explained by near-surface geologic changes. In order to test this hypothesis and its applicability here, the model shown in Figure 30 was constructed by fitting the gravity data using subsurface bodies of reasonable density and keeping them as

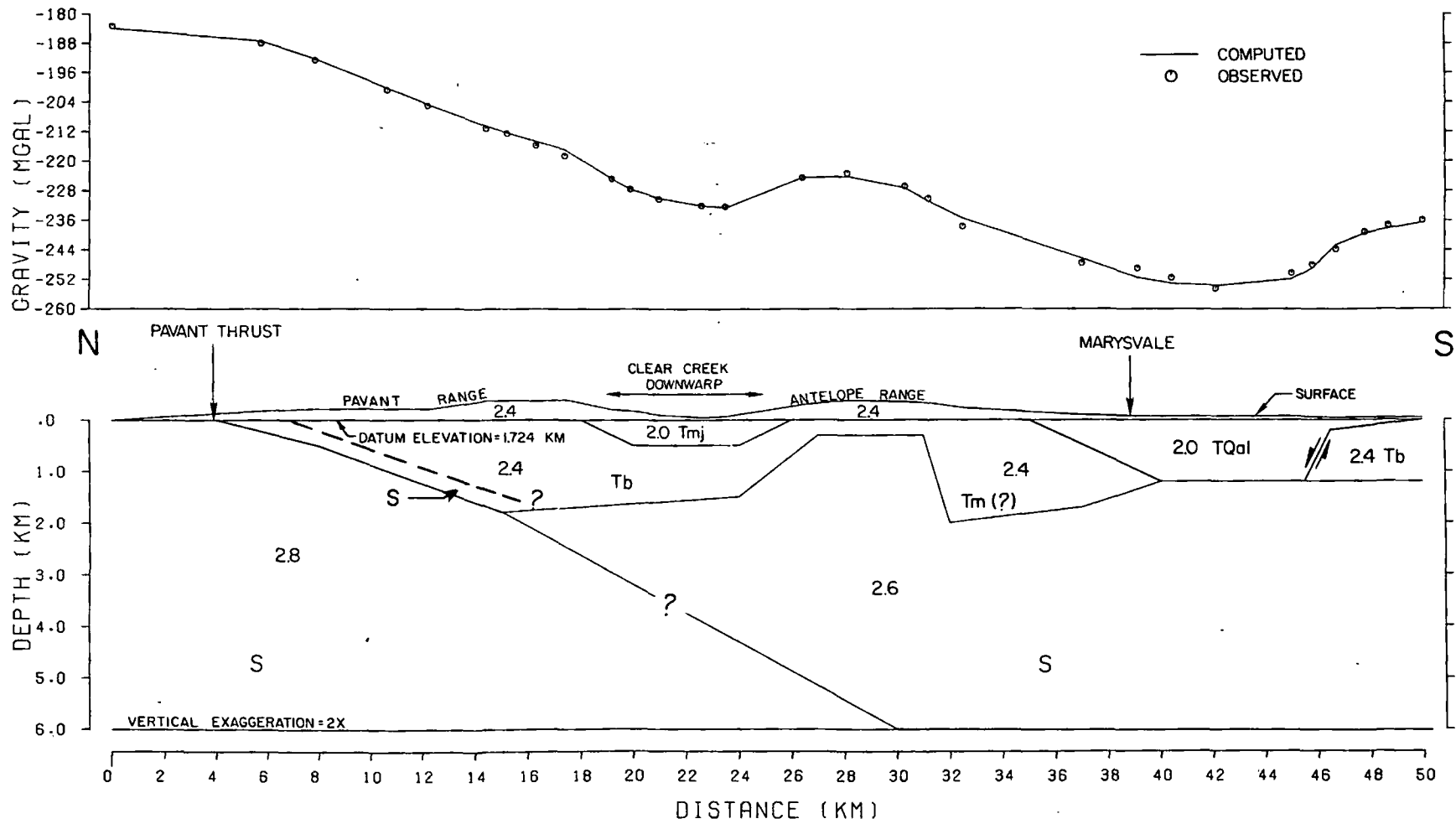


Figure 30. Interpretive geologic cross section along Pavant Range - Marysvale Valley gravity profile. Densities shown in gm/cc.

shallow as possible.

The gravity data were successfully modeled within the upper 6 km of the crust by assuming both lateral changes in the density of underlying sedimentary rocks and a large density contrast between Paleozoic carbonate rocks and Tertiary volcanics of the Marysvale Volcanic field. The sedimentary rocks are shown as changing density from 2.8 gm/cc on the north to 2.6 gm/cc on the south. If one considers these bodies to represent Paleozoic and Mesozoic sedimentary rocks, respectively, this picture is consistent with the changes in the sedimentary sequence across the Cordilleran "hingeline" as described by Stokes (1976). Additionally, the densities shown are reasonable since the Paleozoic section here is largely limestone and dolomites, and the Mesozoic section consists of less dense sandstones and shales. Although Mesozoic Navaho Sandstone is known to crop out south of the Pavant thrust, the extent of this unit at depth is not known and cannot be determined from the sparse gravity data in this area. One sample of Navaho Sandstone collected in this area (sample MH415, Appendix 3) gave a density of about 2.4 gm/cc. Therefore, since we cannot expect to differentiate the volcanics and Navaho sandstone here, both units were modeled at 2.4 gm/cc density. It should be emphasized that until additional geologic control (including rock densities) are obtained in this area, the exact proportion of the contribution to the gravity effect of the near-surface rocks versus the effect of deepening of the Moho must be considered uncertain.

A body of low-density material about 500 m thick is shown across

the Clear Creek downwarp. This body represents the Joe Lott Tuff Member of the Mount Belknap Volcanics which accumulated here during eruption of the Mount Belknap caldera.

The rise in gravity values across the Antelope Range has been modeled as an upwarp in the underlying sediments. An equally reasonable interpretation would show this high as due to intrusive material under the Antelope Range.

The alluvial-filled graben shown beneath Marysvale slopes gently on the north side to a depth of 1200 m. As with the Sevier Valley graben, the valley fill may in part consist of Joe Lott Tuff which presents no appreciable density contrast with alluvium. A steep gravity gradient on the south end of the Marysvale Valley graben is modeled as due to a Basin and Range fault of about 1 km displacement.

c) Mount Belknap Caldera Profile

The gravity low over the Mount Belknap caldera (Fig. 31) is interpreted as due to low-density volcanic material presenting a density contrast with denser sedimentary and intrusive rocks. Assuming a density contrast of 0.2 gm/cc between the volcanics and sedimentary rocks, the caldera fill is shown to extend to a depth of 2500 m below the surface.

An alternative interpretation of the gravity low is possible if a significant density contrast exists between the Mount Belknap Volcanics in the caldera and surrounding Bullion Canyon Volcanics. However, since the geologic control data do not support this possibility, the first interpretation is preferred.

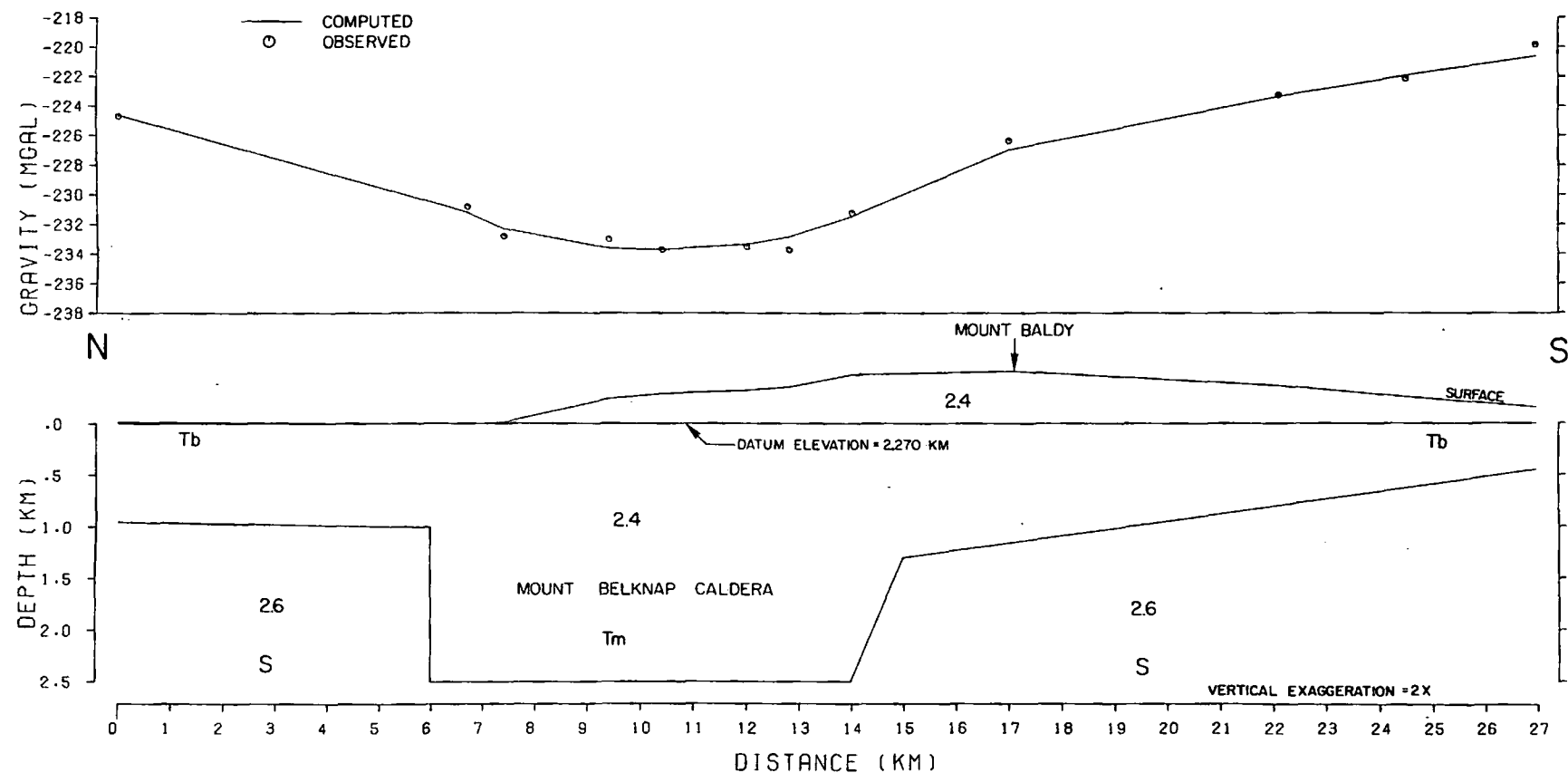


Figure 31. Interpretive geologic cross section along Mount Belknap caldera gravity profile. Densities shown in gm/cc.

The model of the Mount Belknap caldera shown here is similar to that shown by Karig (1965) over the Bonanza caldera in the San Juan volcanic field of southwestern Colorado. They are similar in terms of the size of the caldera, the magnitude of the gravity low observed, the density contrast used, and the interpreted depth of volcanic fill. Although the model shown in Figure 31 does not consider the region below the bottom of the volcanic fill, it is reasonable to expect a crystalline batholith, perhaps granitic in composition, beneath the caldera. Since 2.6 gm/cc is a reasonable density for both sedimentary and intrusive rocks, no attempt was made to differentiate these units in the model.

d) Tushar Mountains - Sevier Plateau Profile

The gravity low shown along this profile (Fig. 32) is interpreted as due to the Marysvale Valley graben. The model indicates about 1200 m of alluvial fill, which may include considerable thicknesses of the Joe Lott Tuff. The west side of the graben is marked by the Tushar fault, along which displacement has been great enough in the area of Deer Trail Mountain to expose sedimentary rocks lying beneath the Bullion Canyon Volcanics. The east side of the graben is marked by a vertical fault not shown on the geologic map of Willard and Callaghan (1962), but nevertheless supported by a distinctly linear contact between alluvium and Bullion Canyon Volcanics about 10 km in length located just east of the Sevier River.

A small alluvial-filled graben of about 200 m depth is shown a few kilometers east of the above unnamed fault, and coincides with

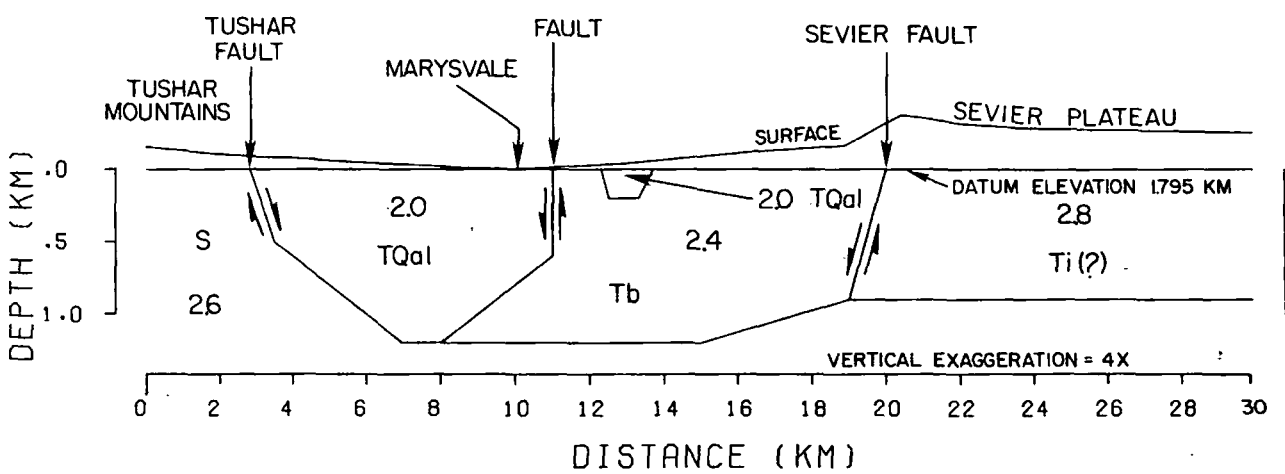
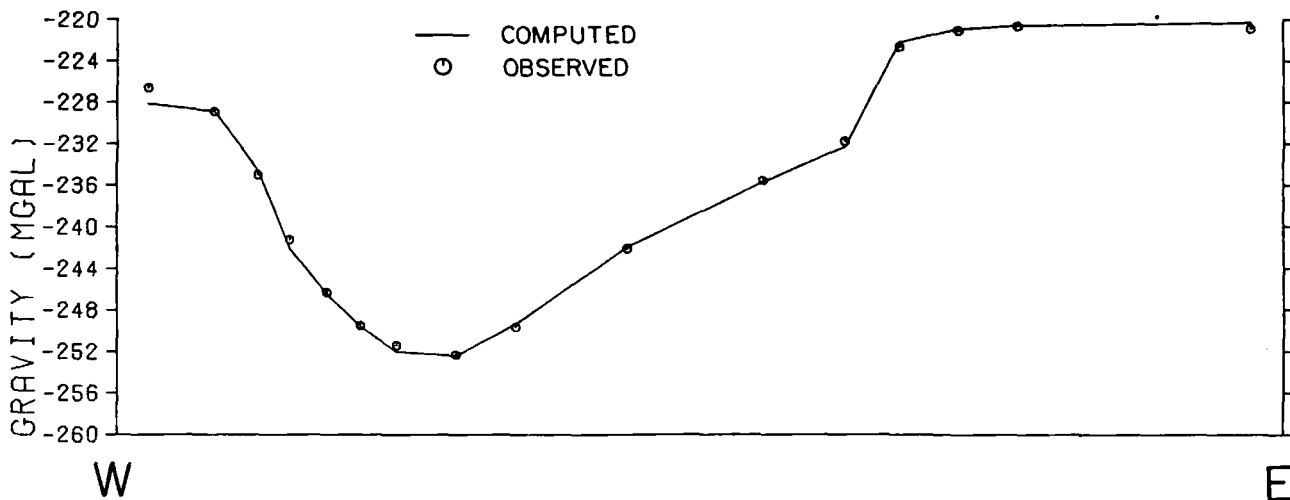


Figure 32. Interpretive geologic cross section along Tushar Mountains - Sevier Plateau gravity profile. Densities shown in gm/cc.

alluvium between volcanics mapped by Willard and Callaghan (1962).

This graben is typical of the zone between the Sevier Plateau and the Marysvale Valley graben which is believed to contain numerous en echelon faults of relatively small displacement.

It was necessary to model a large body of 2.8 gm/cc density beneath the Sevier Plateau to fit the gravity data, which possibly indicates the presence of a large intrusive mass at depth. Numerous occurrences of alunitic alteration in this portion of the Sevier Plateau (Willard and Callaghan, 1962) indicate past hydrothermal activity, thereby lending support to the suggestion of a volcanic source area with a large intrusive mass at depth.

Detailed Gravity and Ground Magnetic Surveys

1) Monroe Hot Springs Area

a) Total Magnetic Intensity Anomaly Map

This map (Fig. 15) shows a strong magnetic gradient with contours trending parallel to the Sevier fault along the entire length of the map. High magnetic values are observed over alluvium and low magnetic values are observed over Bullion Canyon Volcanics of the Sevier Plateau. This is interpreted as due to magnetite in the alluvium in contrast with essentially non-magnetic altered volcanics found east of Monroe. The details of the map are believed controlled by the action of both thermal and non-thermal waters changing the magnetic character of the alluvium by alteration of magnetite to a non-magnetic mineral.

The strong magnetic gradient across the Red Hill Hot Spring is apparently the result of thermal spring waters altering magnetic

alluvium around the Red Hill tufa mound. As the contours extend southwestward, they broaden and form a large "nose" swinging out into the valley. This nose is possibly the result of surface waters flowing out of Sand Canyon and altering the magnetic nature of the alluvium. Alternatively, alluvial material brought down Sand Canyon may be less magnetic than that from Order Canyon which drains into the Red Hill Hot Spring area. This second interpretation is plausible since basaltic andesite of the Bullion Canyon Volcanics is mapped in the drainage of Order Canyon but not in the drainage of Sand Canyon, and basaltic andesite is presumed to be the source of the magnetic alluvium.

Of particular interest is the linear magnetic low which extends southward almost 1 km from the central tufa mound of the Monroe Hot Springs. This low is aligned with the Sevier fault and is interpreted as due to alteration of magnetite in the alluvium by fluids rising along the Sevier fault zone.

b) Red Hill Magnetic Profile (M77-1)

In this model (Fig. 33), the 700-gamma magnetic anomaly across the Red Hill Hot Spring is shown due to a body of magnetic alluvium and/or volcanics in Sevier Valley. The magnetic susceptibility value of 0.003 c.g.s. units used for the body is reasonable as suggested by a measurement of 0.0042 c.g.s. units on outcropping basaltic andesite from the Sevier Plateau. It is difficult to imagine a body of magnetic alluvium extending to the depth indicated in the model, therefore a preferred interpretation is that beneath the alluvium

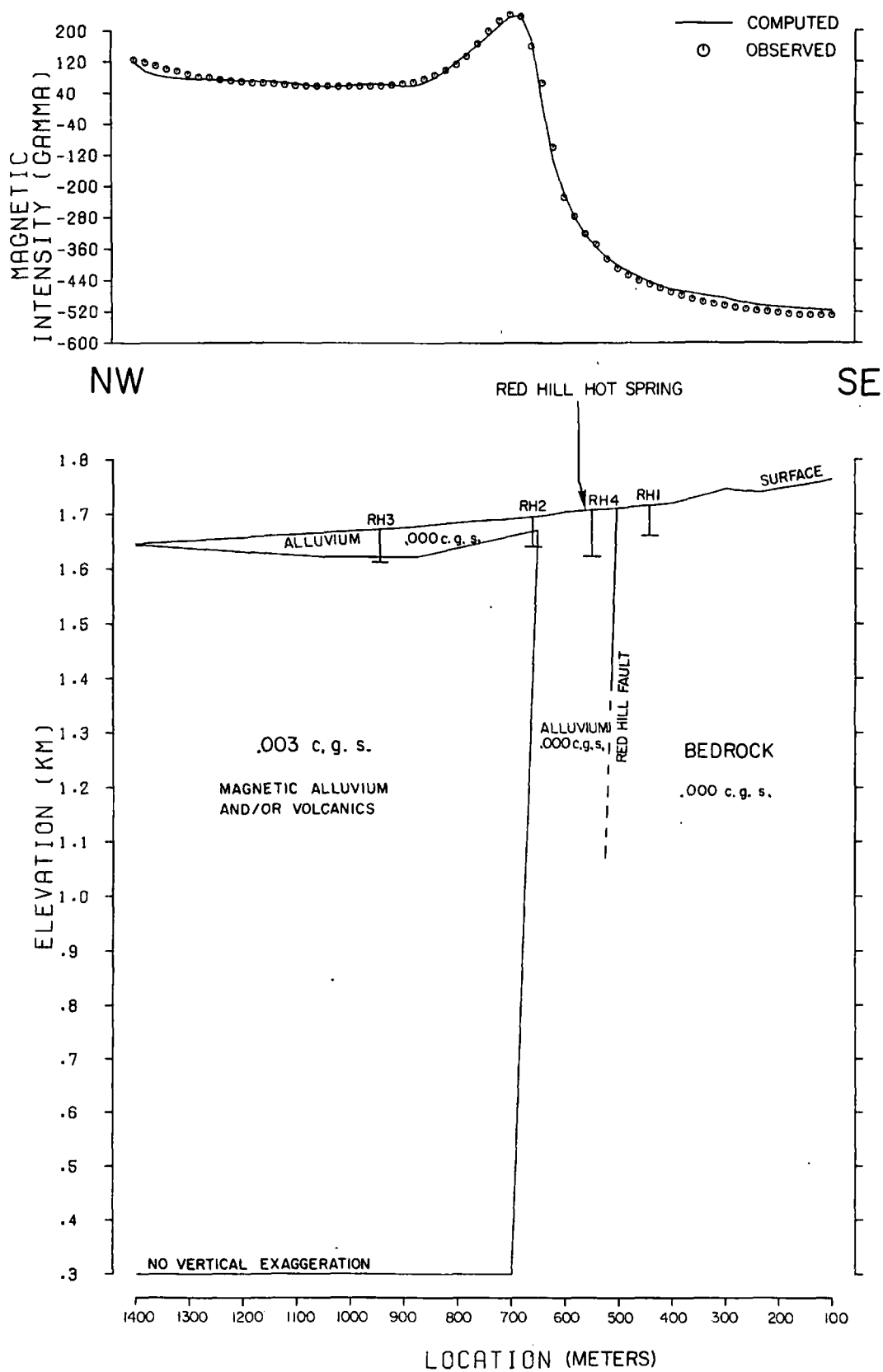


Figure 33. Interpretive geologic cross section along Red Hill ground magnetic profile (M77-1). Magnetic susceptibilities shown in c.g.s. units.

there lies a block of magnetic basaltic andesite downdropped to the west along the Sevier fault zone. The depth to the inferred volcanic layer under the alluvium cannot be interpreted from the magnetic data as there would be no significant susceptibility contrast across the magnetic alluvium-basaltic andesite interface.

The southeastern edge of the magnetic alluvium body shown in the model does not coincide with the near-surface bedrock-alluvium contact revealed by the thermal gradient drillholes. This is believed due to alteration of magnetite in the magnetic alluvium near the Red Hill Hot Spring by fluids rising along a fault. As later models substantiate, the fault related to the Red Hill Hot Spring is probably not the main branch of the Sevier Fault Zone, but rather a major en echelon fault. To distinguish between this important fault and the Sevier Fault zone in general, the name Red Hill fault is suggested and will be used herein.

c) Red Hill Gravity Profile ("RH")

The linear nature of the gravity observed along this profile (Fig. 34) eliminates any interpretation showing a large displacement of materials of different density along the Red Hill fault. The interpretation shown in this model is that the Sevier fault zone consists of a number of en echelon faults, of which the Red Hill fault is an important member. The gravity model suggests that a downdropped block of Bullion Canyon Volcanics lies between the main branch of the Sevier fault and the Red Hill fault about 300 m beneath the alluvium. This is consistent with the magnetic model previously discussed.

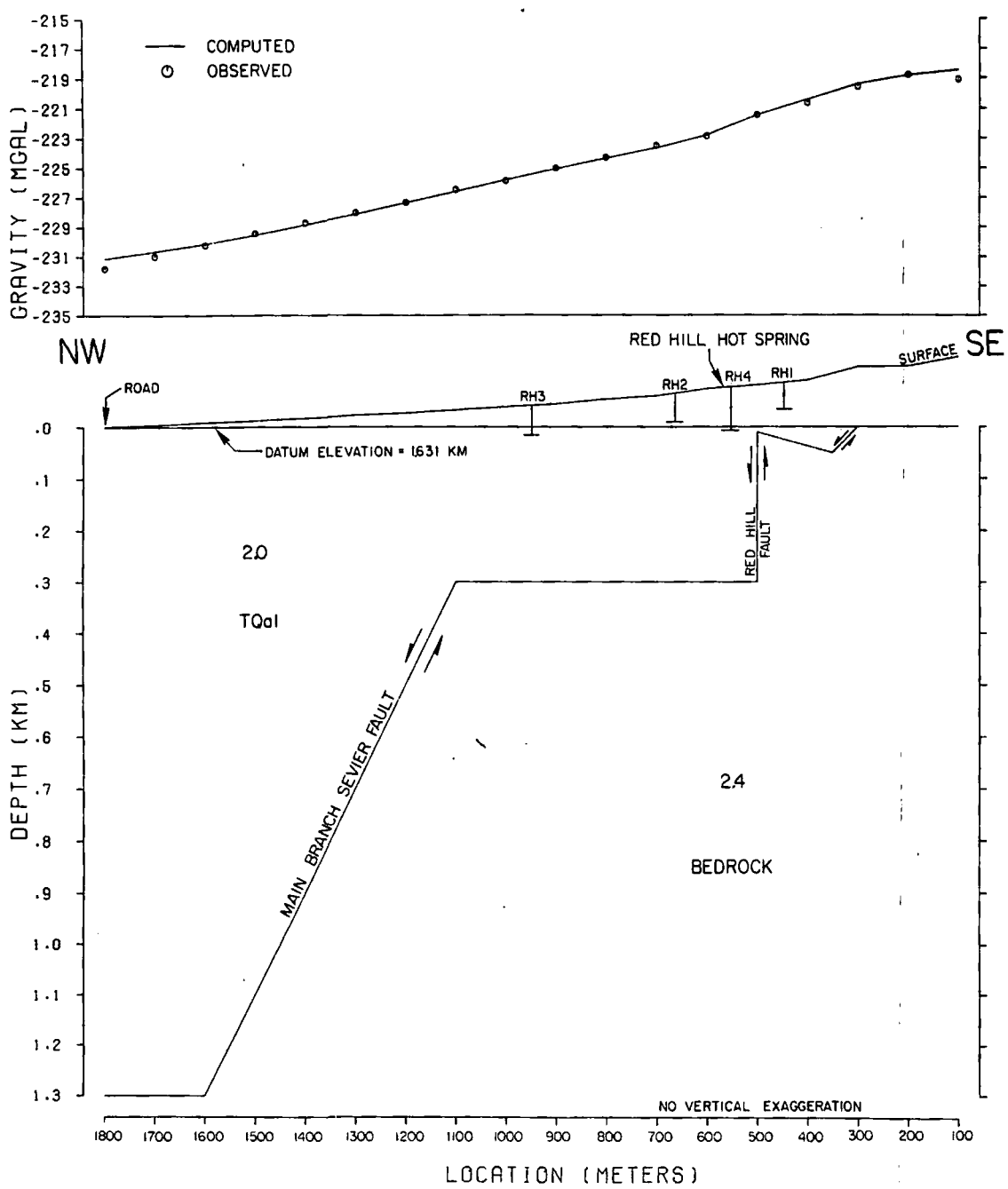


Figure 34. Interpretive geologic cross section along Red Hill gravity profile (RH). Densities shown in gm/cc.

A density of 2.4 gm/cc was used to model the Bullion Canyon Volcanics as suggested by the geologic control data. The dip on the Red Hill fault is shown as vertical as the gravity could not resolve the subsurface otherwise. West of the main branch of the Sevier fault, the alluvium is shown to extend to a depth of 1300 m as suggested by the regional gravity profile constructed across Sevier Valley.

d) SS Canyon Magnetic Profile (M77-14)

This profile (Fig. 35) crosses the linear magnetic low mentioned previously which extends southward from the Monroe Hot Springs tufa mound. This magnetic low is probably due to a zone of non-magnetic alluvium created by thermal fluids rising along the Sevier fault. The rise in magnetic values east of the Sevier fault was modeled as due to a thin layer of magnetic alluvium representing material being carried down SS Canyon. West of the Sevier fault the magnetic alluvium is shown as thickening at location 1200 along what may be an en echelon fault of the Sevier fault zone, or alternatively a zone of alluvium which has not been affected by the thermal waters rising along the Sevier fault.

A magnetic susceptibility value of 0.001 c.g.s. units was used to model the magnetic alluvium washed down SS Canyon, as suggested by the geologic control data. As mentioned previously, the lower susceptibility of the alluvium here as compared with the alluvium being washed down Order Canyon may be due to less magnetic basaltic andesite present in the drainage of SS Canyon.

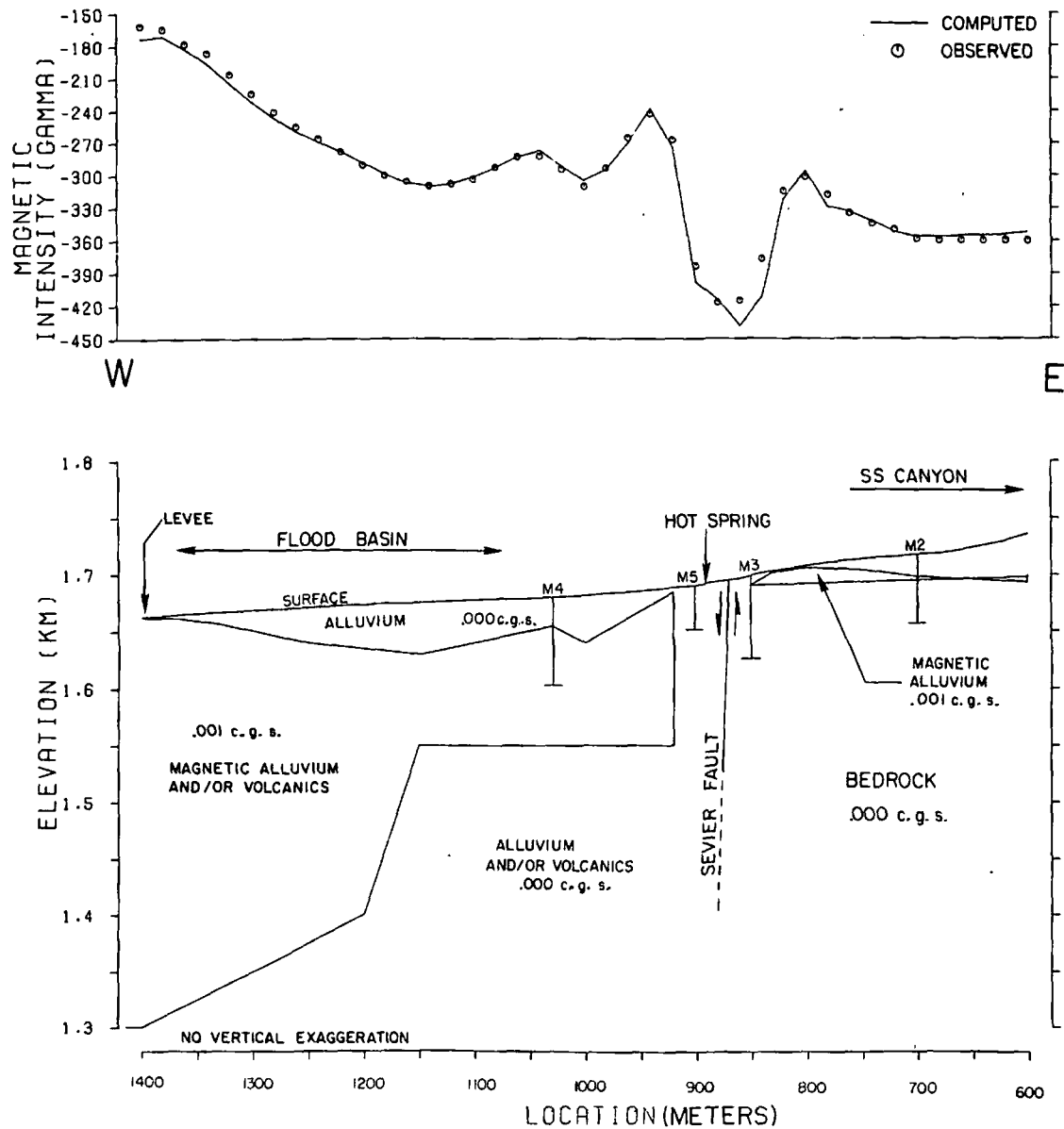


Figure 35. Interpretive geologic cross section along SS Canyon ground magnetic profile (M77-14). Magnetic susceptibilities shown in c.g.s. units.

e) Sand Canyon Gravity Profile ("SC")

Similar to the Red Hill gravity profile, the linear nature of the gravity profile along Sand Canyon (Fig. 36) suggests a zone of en echelon faulting rather than one fault of large displacement. A small fault of about 150 m displacement is shown at the mouth of Sand Canyon near the alluvium-Bullion Canyon Volcanics ("bedrock") contact. The bedrock is shown as level at that depth out to location 1400 where the main branch of the Sevier fault cuts the bedrock and extends to a depth of 1300 m to the west in Sevier Valley. A density of 2.4 gm/cc was used for the Bullion Canyon Volcanics as suggested by the geologic control data.

It should be mentioned that the detailed gravity could have been modeled using one low angle alluvium-bedrock contact instead of a series of en echelon faults. However, the interpretation of en echelon faulting is preferred since drill holes across faults elsewhere in the Monroe KGRA do indicate vertical or steeply dipping faults near the surface.

Unfortunately, this gravity profile is not located coincident with the magnetic profile in SS Canyon, and the two cannot be compared directly. However, they are similar in that they both suggest two major en echelon faults, with a downdropped block of bedrock between the faults at a depth of 100 m to 200 m.

2) Joseph Hot Springs Area

a) Joseph Magnetic Profile (J2)

The magnetic data along this profile (Fig. 37) are interpreted as

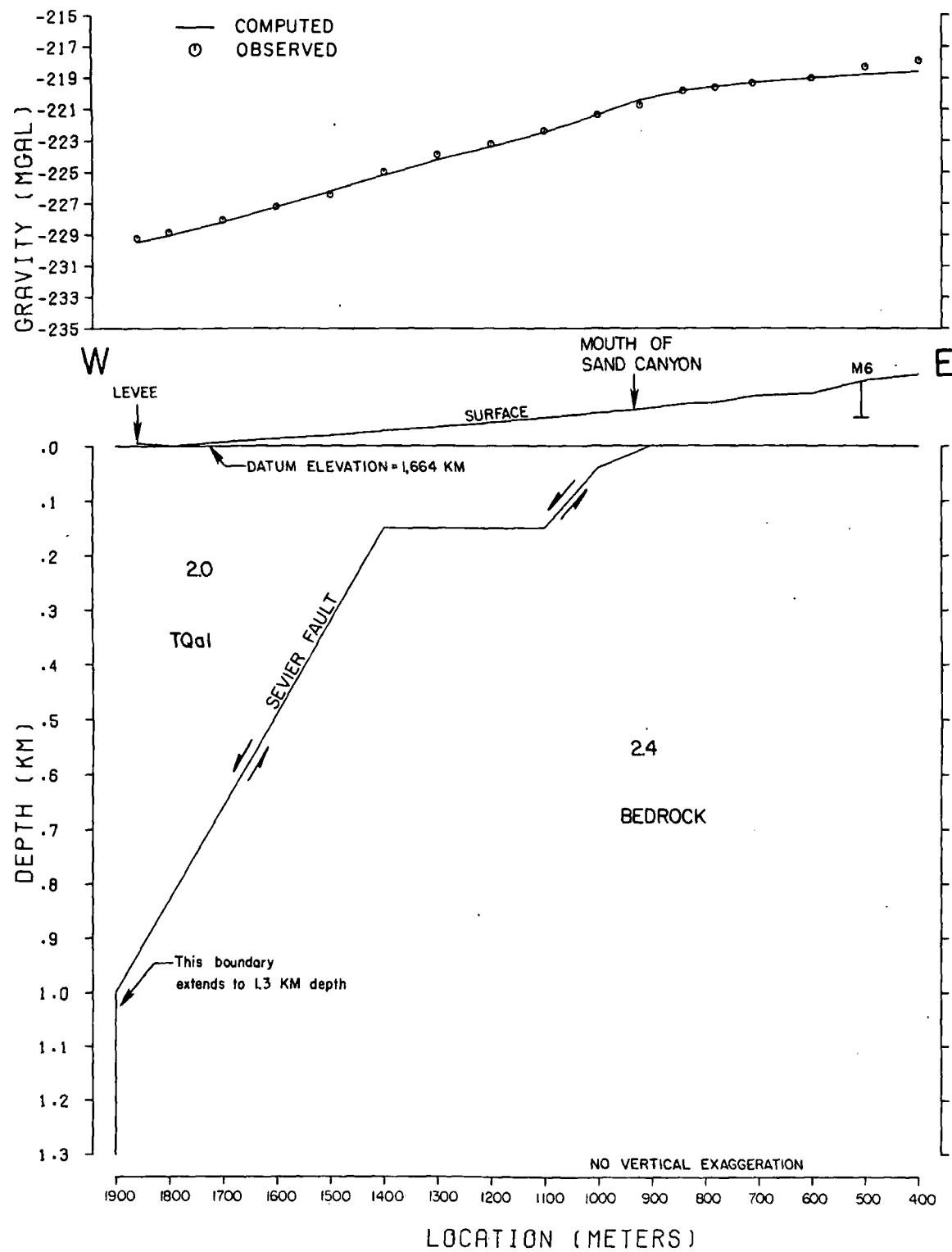


Figure 36. Interpretive geologic cross section along Sand Canyon gravity profile (SC). Densities shown in gm/cc.

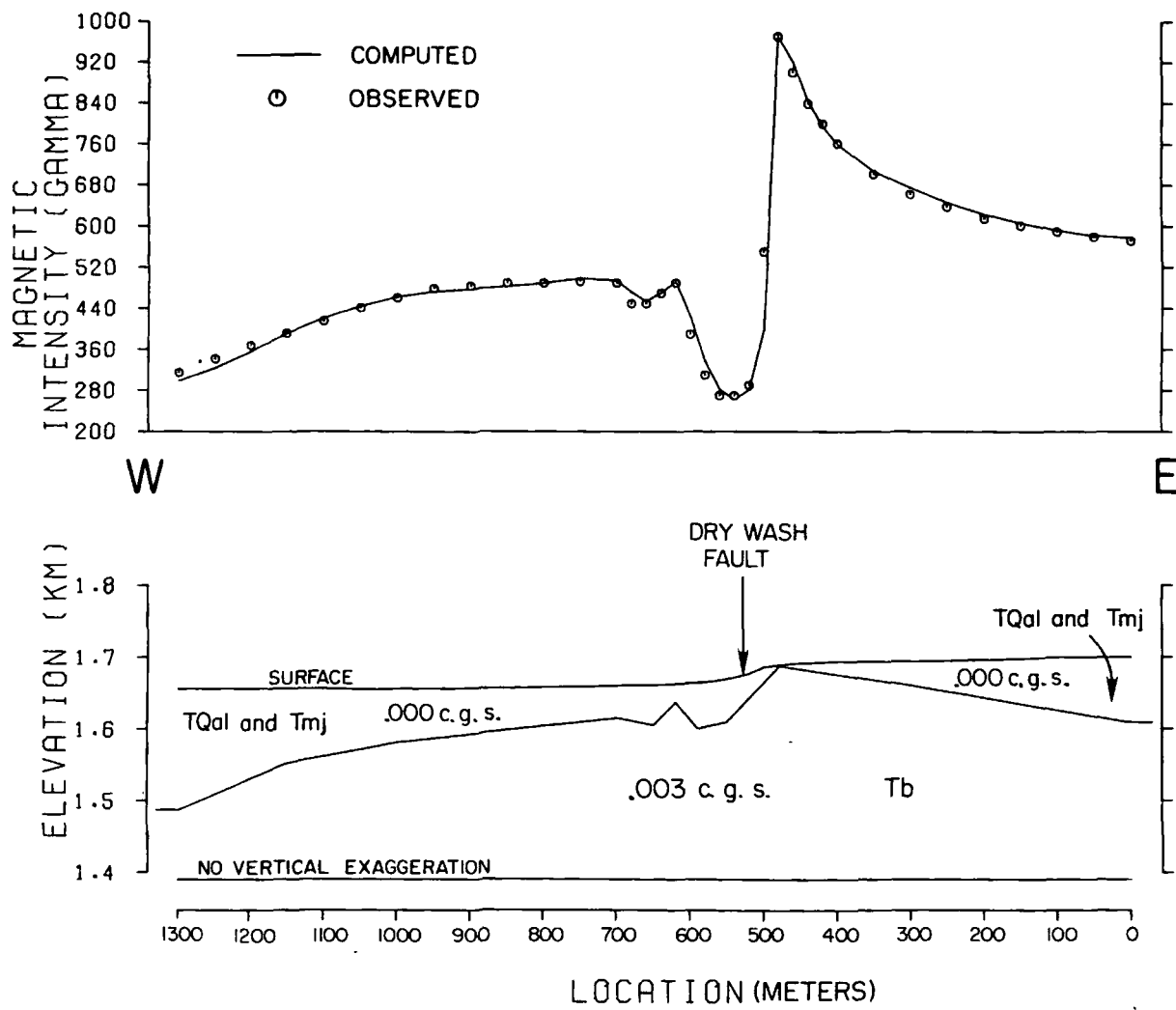


Figure 37. Interpretive geologic cross section along Joseph ground magnetic profile (J2). Magnetic susceptibilities shown in c.g.s. units.

reflecting changes in depth to the basaltic andesite unit of the Bullion Canyon Volcanics which comprises most of the outcrop in hills east of the Dry Wash fault. The large magnetic peak occurs coincident with the location of basaltic andesite outcrop exposed at the top of a 20 m cliff. The magnetic low west of the Dry Wash fault is largely a topographic effect from this cliff, although may in part be due to a low susceptibility zone along the Dry Wash fault as indicated by the downwarp in the magnetic body here. Both west and east of the Dry Wash fault the magnetic values decrease slowly; this is believed due to deepening of the basaltic andesite beneath alluvium and/or Joe Lott Tuff.

The magnetic susceptibility value of 0.003 c.g.s. units assumed for the basaltic andesite is based on a measurement of 0.0026 c.g.s. units made on outcrop from a peak about 500 m east of Line J1. An important feature of this model is that there has been relatively little displacement of volcanics by the Dry Wash fault, and consequently the volcanics should lie at a relatively shallow depth on the downthrown (west) side of the fault.

b) Joseph Gravity Profile (J2)

This profile (Fig. 38) was extended beyond the limits of the detailed gravity coverage in order to examine the full extent of the gravity anomaly. Gravity stations from the regional gravity survey were incorporated from west of the town of Joseph southeastward to Poverty Flat.

The gravity values are surprisingly similar across the Dry Wash

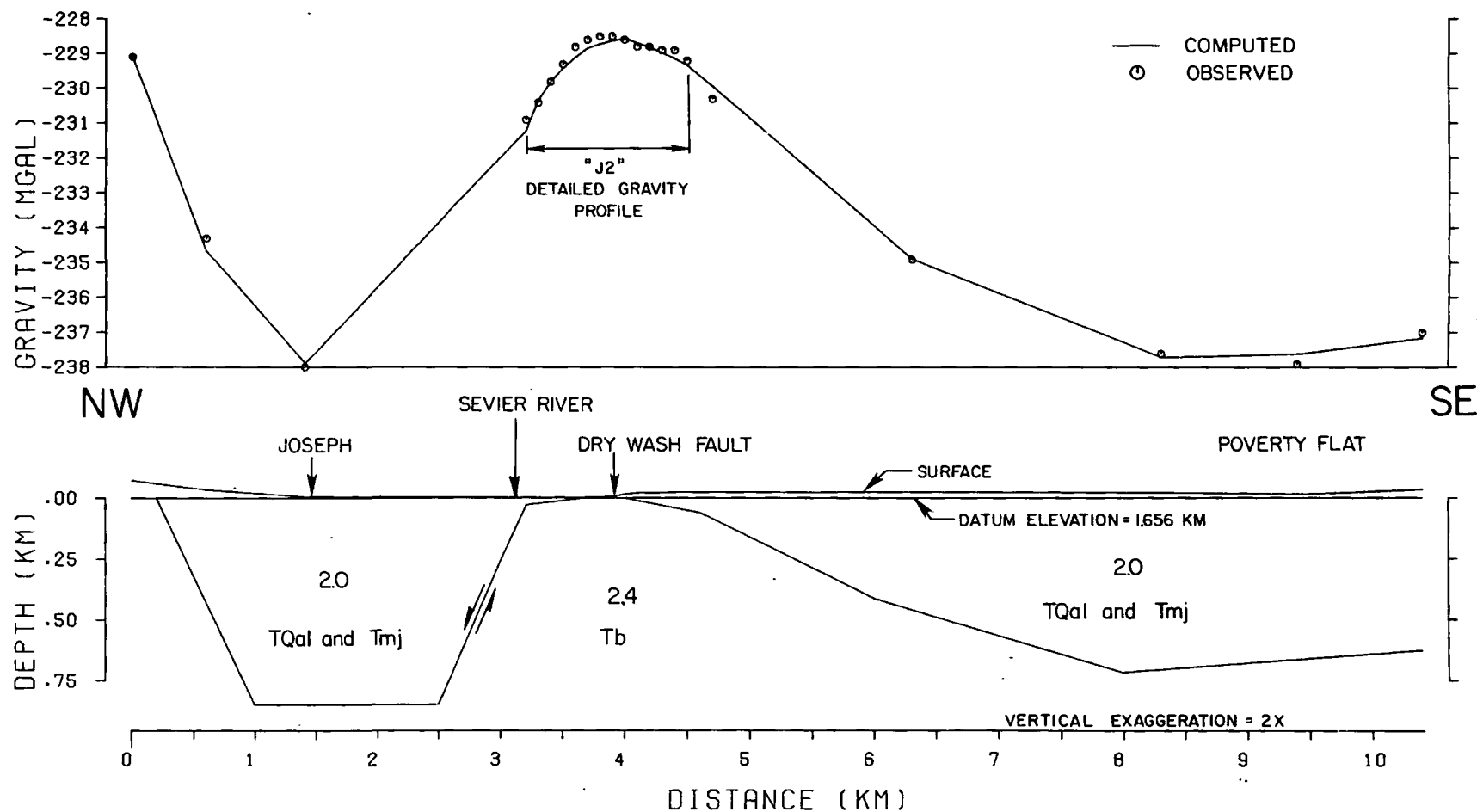


Figure 38. Interpretive geologic cross section along Joseph gravity profile (J2). Densities shown in gm/cc.

fault, and do not decrease until some distance northwestward of its mapped location. This is interpreted to indicate shallow alluvium directly northwest of the Dry Wash fault. However, a major fault of about 800 m throw is postulated near the location of the Sevier River about 500 m northwest of the Dry Wash fault.

Southeast of the Dry Wash fault the Bullion Canyon Volcanics are shown to dip gently reaching a depth of about 700 m beneath Poverty Flat. Alluvium above the Bullion Canyon Volcanics probably includes significant thicknesses of Joe Lott Tuff, but the alluvium and tuff are modeled as one since no density contrast between them is expected.

It should be noted that the lack of an anomaly corresponding with the Dry Wash fault is explained as due to relatively little displacement along the fault. However, the fault may extend to considerable depths and be a major feature of importance to geothermal exploration despite the fact that it creates no appreciable density contrast.

SUMMARY AND CONCLUSIONS

Regional gravity data were collected throughout a portion of south-central Utah in the vicinity of Monroe and Marysvale. These gravity data were reduced to a datum of sea level using a Bouguer reduction density of 2.67 gm/cc. Terrain corrections were computed out to a radial distance of 167 km from the station also assuming a density of 2.67 gm/cc. A complete Bouguer gravity anomaly map was compiled from this data incorporating a total of 948 gravity stations.

Analysis of the complete Bouguer gravity anomaly map reveals a strong correlation with most structural features mapped in the survey area. A large regional gravity gradient in the northwest portion of the survey area may be due to the contrast of dense sedimentary rocks with less dense Tertiary volcanics of the Marysvale volcanic field, as well as a lateral change in the density of the sedimentary rocks across the Cordilleran hingeline, and only partly the result of changes in depths to the Moho across the Basin and Range-Colorado Plateau transition". Gravity lows are seen over the alluvial-filled grabens of Sevier and Marysvale Valleys. Strong gravity gradients are associated with most normal faults in the survey area, especially the Elsinore, Dry Wash, Sevier, and Tushar faults. Gravity lows correspond with the Mount Belknap, Big John, and Red Hills calderas. The gravity data appear to be disrupted near the Three Creeks cauldron but the exact signature is not clear. A belt of east-northeast-

trending gravity contours is aligned with the northern edge of the calderas and igneous intrusions and appears related to the Wah Wah-Tushar mineral belt of southern Utah. The gradient along the Sevier fault is disrupted where this trend intersects the northern Sevier Plateau. This disruption may indicate the presence of a volcanic source area in this portion of the Sevier plateau.

Polynomial residual gravity anomaly maps were produced and analyzed. Generally the residual maps show features similar to the original gravity data, except in those areas of strong regional gradients. A residual gravity low in the Pavant Range was revealed when the regional gradient was removed by a fifth-order polynomial surface, and the gravity low may indicate a major volcanic source area.

Four regional gravity profiles were modeled using two-dimensional forward and inverse algorithms. Subsurface models were constrained by both geologic control data and surface geology. A profile across Sevier Valley shows this feature to be an alluvial-filled graben of about 1300 m average depth, flanked on either side by major Basin and Range normal faults. A profile from the Pavant thrust southward to Marysvale Valley shows that the large regional gradient in the southern Pavant Range can be modeled by reasonable density changes in the upper crust, and is not necessarily related to changes in the depth to the Moho across the Basin and Range-Colorado Plateau transition. A profile across the Mount Belknap caldera shows that the gravity low may be due to low-density volcanic fill about 2500 m deep assuming a density contrast of 0.2 gm/cc between the surround and

underlying rocks. A profile across Marysvale Valley extends from the Tushar Mountains to the northern Sevier plateau, and shows Marysvale Valley to be an alluvial-filled graben of about 1200 m average depth, also flanked on either side by large normal faults. Although all depth estimates shown in these models are believed reasonable, it must be remembered that they are very dependent on the chosen density contrast. Since the density contrast is poorly determined by available data the models shown must not be considered unique.

Detailed gravity and ground magnetic data were collected in the vicinity of hot springs in both the Monroe and Joseph KGRA's. The detailed gravity data employed precision levelling and were reduced in the same manner as the regional gravity data. Total magnetic intensity data collected along 19 profiles in the Monroe KGRA were corrected for diurnal drift and compiled into a total magnetic intensity anomaly map. This map shows a strong magnetic high over the alluvium in Sevier Valley grading into a region of magnetic lows over altered Bullion Canyon Volcanics east of the Sevier fault. This is believed due to alluvium in Sevier Valley containing up to one percent magnetite derived from a basaltic andesite unit of the Bullion Canyon Volcanics. A strong magnetic gradient across the Red Hill Hot Spring is believed due to thermal waters rising along the Red Hill fault, a branch of the Sevier fault zone. A linear magnetic low observed in the vicinity of the Monroe Hot Springs is believed due to alteration of magnetite in the alluvium by thermal fluids rising along the main branch of the Sevier fault zone.

Subsurface geologic models were constructed along six gravity and

magnetic profiles in the Monroe and Joseph KGRA's using two-dimensional modeling techniques. A magnetic profile across the Red Hill Hot Spring in the Monroe KGRA shows that the large magnetic gradient can be modeled as due to a body of magnetic alluvium and/or volcanics in Sevier Valley just west of the Red Hill fault. A model of gravity data along the same profile suggests that the major throw along the Sevier fault zone does not occur in the vicinity of the Red Hill Hot Spring, but consists of a zone of en echelon faulting, as evidenced by the linear nature of the gravity data. These data were modeled with the main branch of the Sevier fault zone located about 500 m west of the Red Hill Hot Spring, and about 300 m displacement is shown along the Red Hill fault. A gravity and magnetic profile were also modeled across the Monroe Hot Spring area. The magnetic profile along SS canyon shows that a magnetic low observed near a hot spring can be modeled as due to a zone of non-magnetic alluvium, presumably due to alteration of magnetite in the alluvium by thermal fluids rising along the Sevier fault. A gravity profile along Sand Canyon was modeled showing one fault at the mouth of the canyon with 150 m throw, and the main branch of the Sevier fault zone located about 500 m to the west.

A magnetic and gravity profile were also modeled across the Dry Wash fault in the Joseph KGRA a short distance south of the Joseph Hot Springs. The magnetic data suggest relatively little displacement of a basaltic andesite unit of the Bullion Canyon Volcanics across the Dry Wash fault. The gravity data were modeled showing no significant depth of alluvium on the downthrown side of the Dry Wash fault, but a

major fault located about 500 m to the west near the Sevier River is postulated to extend to a depth of about 800 m beneath the town of Joseph.

In conclusion, the regional gravity survey yielded information regarding both the location and nature of large-scale faulting throughout the survey area. This information may be valuable to future geothermal prospecting for resources which are not associated with surface hot springs. Also, the depths of the major grabens have been estimated and additional knowledge of the major volcanic features throughout the area has been gained.

Information which should prove useful to the development of known geothermal resources in the Monroe and Joseph KGRA's has been interpreted from detailed gravity and ground magnetic data. In particular, faults near the hot springs are interpreted to be zones of en echelon faulting as indicated by the gravity data. Zones of low magnetic intensity are believed related to thermal waters rising along faults and altering magnetite in the alluvium to a non-magnetic mineral. It is believed that the results of this study will aid the development of the geothermal resources by helping to locate both test and production drill holes in the most favorable positions. The faults and depths indicated the gravity models can be used to predict the locations of faults until such time as more specific data is available. The magnetic lows in the Monroe Hot Springs area can be considered preliminary target sites for drilling as they are probably indicative of zones of fracturing and fluid flow.

APPENDIX 1
DESCRIPTION OF FIELD BASE STATIONS

MONROE GRAVITY FIELD BASE STATION

Designation: MH001
Elevation: 5357 ft (1633 m)
Latitude: 38° 38.24' N
Longitude: 112° 7.24' W
Observed Gravity: 979499.18 mgal¹
Description: U.S.G.S. benchmark stamped "3E", located at the top of two steps on the concrete front porch of a private residence, northwest corner of intersection of Third North and Main Streets, Monroe, Utah.

MARYSVALE GRAVITY FIELD BASE STATION

Designation: MH477
Elevation: 5866 ft (1788 m)
Latitude: 38° 26.96' N
Longitude: 112° 13.80' W
Observed Gravity: 979437.80 mgal¹
Description: U.S.G.S. benchmark stamped "H83", located 1 m inside white picket fence, approximately 50 m south of the Chevron station on west side of Main Street just north of flashing yellow signal, Marysvale, Utah.

MONROE MAGNETIC BASE STATION

Designation: MB
Magnetic Field: Arbitrarily assigned a value of zero.
Location: Reading point is on top of flood control levee, halfway between the two large drains in the flood basin, about 100 m east of South Sevier High School, Monroe, Utah.

¹For documentation regarding observed gravity values and gravity base station ties, refer to Appendix 2.

APPENDIX 2
GRAVITY BASE STATION TIES

Observed Ties¹

Tie (A to B)	Looping Technique	Observed Difference (B-A, mgal)
University of Utah to Richfield	ABABA	-276.91
Monroe to Loa	ABA	- 94.94
Monroe to Beaver	ABA	- 49.09
Monroe to Richfield	ABABABA	+ 9.90
Monroe to Marysvale	ABABABA	- 61.38

Computed Ties¹

Tie	A Computed Difference (mgal)	B Published Difference (mgal)	A-B Error (mgal)
Univ. Utah to Beaver via Richfield and Monroe	-335.90	-336.05	+ 0.15
Univ. Utah to Loa via Richfield and Monroe	-381.75	-382.00	+ 0.25
Univ. Utah to Richfield	-276.91	-277.05	+ 0.14
Richfield to Loa via Monroe	-104.84	-104.95	+ 0.11
Richfield to Beaver via Monroe	- 58.99	- 59.00	+ 0.01
Loa to Beaver via Monroe	+ 45.85	+ 45.95	+ 0.10

¹All base stations and observed gravity values taken from Cook and others, 1971, except Monroe and Marysvale field bases which have been described in Appendix 1. Ties made by M. Halliday using LaCoste and Romberg gravimeter No. 264.

APPENDIX 3

GEOLOGIC CONTROL DATA RELEVANT TO THE REGIONAL GRAVITY SURVEY

Sample	Density (gm/cc)	Rock Unit ¹	Description
MH002	2.25	Tbc	Latite, brownish red
MH053	2.31	Tbc	Latite, light brown
MH066	2.23	Tbc	Chert breccia
MH068	2.53	Tbc	Basaltic andesite, black, vesicular
MH076	2.22	Tbc	Basaltic andesite, black, vesicular
MH077	2.29	Tbc	Basaltic andesite, black, vesicular
MH087	2.58	Tbc	Latite, light reddish brown
MH091	2.34	Tbc	Latite, light brown
MH125	2.55	Tbc	Latite porphyry, purple
MH127	2.53	S	Quartzite, white
MH164	2.04	Tmj	Welded tuff, white
MH166	2.41	Tbc	Basaltic andesite, black, vesicular
MH202	1.59	Tmj	Welded tuff, white
MH235	2.20	Tbc	Tuff, white, altered
MH242	2.63	Tbc	Latite, gray
MH254	2.65	Ti	Quartz monzonite, white, pink tint
MH255	2.47	Tbc	Quartz latite, gray
MH265	2.40	Tm	Rhyolite, light gray
MH312	2.27	Tbc	Crystal tuff, light brownish gray
MH329	1.90	Tmj	Welded tuff, white
MH332	2.06	Tmj	Welded tuff, white
MH358	2.01	Tmj	Welded tuff, white
MH392	2.36	Tbc	Crystal tuff, light brown
MH399	2.18	Tbc	Latite, light reddish purple
MH409	1.98	S	Silty sandstone, yellow (Moenkopi)
MH415	2.37	S	Sandstone, red, cross-bedded (Navajo)
MH420	1.93	Tmj	Welded tuff, grayish white
MH460	2.41	Tm	Tuffaceous rhyolite, reddish brown
MH528	2.46	Tm	Tuffaceous rhyolite, reddish purple
MH533	2.44	TQb	Basalt, black, vesicular
MH614	2.31	Tbc	Basaltic andesite, black, vesicular
MH648	2.39	Tbc	Alunite, red and white
MH692	2.31	Tm	Rhyolite, gray, flow-banded
MH712	2.55	Tbc	Latite porphyry, grayish purple
MH749	2.57	S	Quartzite, reddish white
MH763	2.49	Tm	Rhyolite, white (Mt. Baldy)
MH799	2.55	Tbc	Latite porphyry, red
MH800	2.46	Tbc	Latite porphyry, gray
MH838	2.56	Ti	Quartz monzonite, pinkish white

¹Rock samples classified according to the generalized stratigraphic column shown in Figure 7.

Sample	Density (gm/cc)	Rock Unit ¹	Description
MH860	2.67	Tbc	Welded tuff, grayish purple (Delano Pk.)
MH897	2.26	Tm	Rhyolite, white (Gold Mtn.)
MH903	2.45	Tm	Rhyolite, red and white
MH904	2.39	Tm	Rhyolite, white, flow-banded
MH915	2.39	Tm	Rhyolite, white
MH931	2.64	Tbc	Latite porphyry, reddish purple
MH941	2.51	Tm	Rhyolite, white
MH942	2.51	Tm	Rhyolite, gray
MH945	2.43	Tm	Rhyolite, white
MH946	2.47	Tm	Rhyolite, white

APPENDIX 4

GEOLOGIC CONTROL DATA RELEVANT TO THE
DETAILED GRAVITY AND GROUND MAGNETIC SURVEYSDensities of Drill Hole Core Samples

Sample	Depth below surface (ft)	Rock Unit ¹	Density (gm/cc)
M2	30	Tbc	2.29
M2	100	Tbc	2.19
M2	200	Tbc	2.29
M3	45	Tbc	2.43
M3	160	Tbc	2.29
M3	250	Tbc	2.51
M6	65	Tbc	2.43
M6	215	Tbc	2.52
RH1	45	Tbc	2.46
RH1	60	Tbc	2.49
RH1	197	Tbc	2.50

Magnetic Susceptibility Measurements

Sample	Depth below surface (ft)	Sample type	Magnetic Susceptibility (c.g.s. units)
M2	30	Core	0.0001
M2	100	Core	0.0006
M2	200	Core	0.0002
M3	45	Core	0.0001
M3	160	Core	0.0005
M3	250	Core	0.0003
M4	20	Alluvium	0.0006
M4	120	Alluvium	0.0005
M4	240	Alluvium	0.0003
M5	N.D.	Alluvium	0.0001
M6	65	Core	0.0001
M6	215	Core	0.0000
RH1	10-20	Alluvium	0.0000
RH1	40-50	Alluvium	0.0001
RH1	45	Core	0.0001
RH1	60	Core	0.0000
RH1	95-105	Alluvium	0.0000

¹Rock samples classified according to the generalized stratigraphic column shown in Figure 7.

Sample	Depth below surface (ft)	Sample type	Magnetic Susceptibility (c.g.s. units)
RH1	145-155	Alluvium	0.0000
RH1	190-200	Alluvium	0.0000
RH1	197	Core	0.0001
RH2	0-20	Alluvium	0.0011
RH2	40-60	Alluvium	0.0013
RH2	80-100	Alluvium	0.0012
RH2	140-160	Alluvium	0.0009
RH2	200-210	Alluvium	0.0010
RH3	0-20	Alluvium	0.0011
RH3	100-120	Alluvium	0.0016
RH3	180-200	Alluvium	0.0017
RH4	0-20	Alluvium	0.0000
RH4	100-120	Alluvium	0.0003
RH4	180-200	Alluvium	0.0001
RH4	280-300	Alluvium	0.0002
RH5	0-20	Alluvium	0.0012
RH5	100-120	Alluvium	0.0024
RH5	240-260	Alluvium	0.0004
MH166	Outcrop	Basaltic Andesite	0.0026
MH614	Outcrop	Basaltic Andesite	0.0042

Drill Hole Descriptions

Drill Hole	Ground Level Elevation (ft)	Total Depth (ft)
M1	5420	302
M2	5635	205
M3	5580	241
M4	5515	253
M5	5570	126
M6	5750	248
RH1	5670	197
RH2	5550	211
RH3	5500	201
RH4	5620	297
RH5	5660	281

APPENDIX 5

PRINCIPAL FACTS OF GRAVITY DATA

NOTES: 1) Units are as follows:

Latitude degrees, minutes
Longitude degrees, minutes
Elevation feet
Free-air gravity anomaly value. . . . mgal
Simple Bouguer gravity anomaly
value¹. mgal
Terrain-correction value¹ mgal
Complete Bouguer gravity anomaly
value mgal

2) Station coding is as follows:

"MH" -- Regional gravity station established
by M. Halliday during summer of 1977.
"HF" -- Regional gravity station established
by Fishman (1976).
"RH" -- Red Hill profile detailed gravity station.
"SC" -- Sand Canyon profile detailed gravity station.
"MC" -- Monroe Canyon profile detailed gravity station.
"J1" -- Joseph J1 profile detailed gravity station.
"J2" -- Joseph J2 profile detailed gravity station.

¹A density of 2.67 gm/cc was used for both the Bouguer
and terrain corrections.

STATION NUMBER	LATITUDE DEG MIN	LONGITUDE DEG MIN	ELEVATION IN FEET	FREE-AIR ANOMALY	SIMPLE BOUGUER	TERRAIN CORRECTION	COMPLETE BOUGUER
MH001	38. 33.24	112. 7.24	5357.	-56.94	-239.40	4.09	-235.31
MH002	38. 32.51	112. 4.34	11192.	117.10	-264.10	32.33	-231.77
MH003	38. 32.17	112. 4.36	11230.	118.54	-263.96	32.55	-231.41
MH004	38. 37.92	112. 7.23	5381.	-54.08	-237.36	4.34	-233.02
MH005	38. 37.61	112. 7.23	5395.	-52.62	-236.37	4.39	-231.98
MH006	38. 38.03	112. 6.84	5404.	-51.57	-235.64	4.87	-230.77
MH007	38. 37.99	112. 6.34	5572.	-40.76	-230.55	6.27	-224.28
MH008	38. 39.32	112. 7.08	5304.	-60.53	-241.18	3.97	-237.21
MH009	38. 38.89	112. 7.08	5318.	-59.21	-240.34	4.31	-236.03
MH010	38. 39.95	112. 7.21	5302.	-61.95	-242.54	3.58	-238.96
MH011	38. 41.24	112. 7.35	5340.	-61.98	-243.86	2.82	-241.04
MH012	38. 41.71	112. 6.95	5347.	-61.88	-244.00	2.85	-241.15
MH013	38. 42.14	112. 6.99	5365.	-62.03	-244.76	2.71	-242.05
MH014	38. 42.91	112. 6.99	5367.	-62.76	-245.56	2.67	-242.89
MH015	38. 43.24	112. 6.44	5327.	-64.71	-246.15	2.66	-243.49
MH016	38. 43.21	112. 5.92	5297.	-66.40	-246.81	2.66	-244.15
MH017	38. 42.98	112. 5.91	5299.	-65.97	-246.45	2.64	-243.81
MH018	38. 39.20	112. 6.23	5325.	-53.51	-234.87	5.45	-229.42
MH019	38. 39.72	112. 6.11	5332.	-53.76	-235.37	4.71	-230.66
MH020	38. 40.39	112. 5.81	5364.	-54.38	-237.08	4.70	-232.38
MH021	38. 40.30	112. 6.43	5296.	-59.91	-240.29	3.85	-236.44
MH022	38. 40.60	112. 6.44	5291.	-59.56	-239.77	3.79	-235.98
MH023	38. 41.00	112. 6.91	5322.	-61.90	-243.16	3.07	-240.09
MH024	38. 41.00	112. 6.41	5302.	-61.36	-241.94	3.40	-238.54
MH025	38. 42.44	112. 5.91	5298.	-63.73	-244.18	2.74	-241.44
MH026	38. 42.69	112. 5.91	5298.	-65.43	-245.88	2.73	-243.15
MH027	38. 42.70	112. 6.29	5320.	-64.87	-246.07	2.70	-243.37
MH028	38. 42.60	112. 5.04	5278.	-64.92	-244.69	3.02	-241.67
MH029	38. 42.69	112. 5.62	5289.	-65.32	-245.46	2.84	-242.62
MH030	38. 42.97	112. 5.62	5286.	-66.29	-246.33	2.68	-243.65

STATION NUMBER	LATITUDE DEG MIN	LONGITUDE DEG MIN	ELEVATION IN FEET	FREE-AIR ANOMALY	SIMPLE BOUGUER	TERRAIN CORRECTION	COMPLETE BOUGUER
MH031	30. 43.40	112. 5.63	5281.	-67.39	-247.27	2.59	-244.68
MH032	30. 43.85	112. 5.64	5274.	-67.94	-247.58	2.63	-244.95
MH033	30. 41.49	112. 5.88	5296.	-61.13	-241.51	3.44	-238.07
MH034	30. 41.48	112. 5.27	5341.	-56.66	-238.58	3.56	-235.02
MH035	30. 41.56	112. 4.78	5375.	-53.60	-236.67	4.06	-232.61
MH036	30. 41.75	112. 4.32	5339.	-52.61	-234.46	4.54	-229.92
MH037	30. 42.01	112. 4.06	5329.	-53.90	-235.41	4.04	-231.37
MH038	30. 42.16	112. 3.83	5331.	-53.91	-235.48	3.96	-231.52
MH039	30. 42.37	112. 4.16	5295.	-57.62	-237.97	3.40	-234.57
MH040	30. 42.83	112. 3.62	5269.	-61.23	-240.69	3.65	-237.04
MH041	30. 43.01	112. 4.41	5270.	-64.76	-244.46	2.94	-241.52
MH042	30. 43.46	112. 4.93	5267.	-67.59	-246.99	2.63	-244.36
MH043	30. 44.85	112. 5.11	5265.	-68.59	-247.91	2.50	-245.41
MH044	30. 44.38	112. 5.50	5268.	-68.00	-247.43	2.60	-244.83
MH045	30. 44.23	112. 4.93	5260.	-69.27	-248.42	2.53	-245.89
MH046	30. 43.86	112. 5.06	5262.	-68.74	-247.96	2.63	-245.33
MH047	30. 43.86	112. 5.93	5281.	-67.32	-247.19	2.70	-244.49
MH048	30. 44.54	112. 5.91	5276.	-66.26	-245.96	2.74	-243.22
MH049	30. 44.54	112. 6.53	5318.	-60.79	-241.92	3.51	-238.41
MH050	30. 44.87	112. 6.46	5410.	-55.93	-240.20	3.42	-236.78
MH051	30. 44.61	112. 6.71	5410.	-55.69	-239.95	4.14	-235.81
MH052	30. 44.34	112. 6.98	5410.	-56.06	-240.32	4.46	-235.86
MH053	30. 43.84	112. 7.48	5410.	-55.58	-239.85	5.11	-234.74
MH054	30. 44.12	112. 3.63	5258.	-68.06	-247.15	2.59	-244.56
MH055	30. 44.12	112. 4.22	5256.	-68.77	-247.79	2.52	-245.27
MH056	30. 44.50	112. 3.64	5256.	-68.74	-247.76	2.41	-245.35
MH057	30. 44.78	112. 3.65	5256.	-69.10	-248.12	2.41	-245.71
MH058	30. 44.57	112. 3.09	5258.	-66.96	-246.05	2.48	-243.57
MH059	30. 44.12	112. 3.06	5255.	-66.21	-245.20	2.75	-242.45
MH060	30. 44.56	112. 2.52	5252.	-64.47	-243.36	2.61	-240.75

STATION NUMBER	LATITUDE DEG MIN	LONGITUDE DEG MIN	ELEVATION IN FEET	FREE-AIR ANOMALY	SIMPLE BOUGUER	TERRAIN CORRECTION	COMPLETE BOUGUER
MH061	38. 43.68	112. 3.63	5258.	-66.75	-245.83	2.85	-242.98
MH062	38. 43.24	112. 3.62	5263.	-64.54	-243.80	3.20	-240.60
MH063	38. 42.81	112. 3.00	5272.	-57.80	-237.37	4.15	-233.22
MH064	38. 42.37	112. 3.05	5352.	-51.77	-234.06	4.79	-229.27
MH065	38. 42.82	112. 2.21	5331.	-51.74	-233.31	4.71	-228.60
MH066	38. 43.68	112. .70	6152.	-23.98	-233.51	5.66	-227.85
MH067	38. 44.15	112. .53	6378.	-19.91	-237.14	9.34	-227.80
MH068	38. 44.21	112. .82	6572.	-19.19	-243.03	12.45	-230.58
MH069	38. 43.81	112. 1.56	5677.	-42.03	-235.39	4.56	-230.83
MH070	38. 42.09	112. .91	6109.	-23.32	-231.40	6.85	-224.55
MH071	38. 42.52	112. .42	6090.	-25.89	-233.32	5.15	-228.17
MH072	38. 41.51	112. 1.91	5925.	-29.28	-231.09	7.81	-223.28
MH073	38. 41.94	112. 2.21	5631.	-40.30	-232.10	5.83	-226.27
MH074	38. 41.51	112. 3.04	5697.	-37.30	-231.34	5.57	-225.77
MH075	38. 38.09	112. 3.57	8757.	57.02	-241.24	22.13	-219.11
MH076	38. 37.83	112. 3.33	9150.	67.38	-244.27	24.48	-219.79
MH077	38. 37.89	112. 3.13	9022.	70.57	-236.72	18.52	-218.20
MH079	38. 38.08	112. 4.14	7716.	31.40	-231.41	12.18	-219.23
MH080	38. 40.04	112. 4.15	6294.	-14.28	-228.66	5.68	-222.98
MH081	38. 37.11	112. 6.84	5477.	-46.39	-232.93	5.55	-227.38
MH082	38. 37.11	112. 6.33	5591.	-39.35	-229.78	7.40	-222.38
MH083	38. 37.11	112. 7.49	5416.	-52.49	-236.96	4.51	-232.45
MH084	38. 36.22	112. 6.88	5490.	-48.77	-235.76	7.76	-228.00
MH085	38. 36.68	112. 6.88	5517.	-45.84	-233.75	5.99	-227.76
MH086	38. 35.80	112. 4.72	6248.	-16.88	-229.68	15.02	-214.66
MH087	38. 34.81	112. 5.19	7521.	22.87	-233.29	8.51	-224.78
MH088	38. 34.25	112. 5.35	7841.	29.44	-237.63	10.99	-226.64
MH089	38. 33.76	112. 4.78	8660.	54.82	-240.14	11.25	-228.89
MH090	38. 33.47	112. 4.07	9136.	71.44	-239.73	13.21	-226.52
MH091	38. 33.43	112. 5.52	9323.	69.41	-248.14	15.59	-232.55

STATION NUMBER	LATITUDE DEG MIN	LONGITUDE DEG MIN	ELEVATION IN FEET	FREE-AIR ANOMALY	SIMPLE BOUGUER	TERRAIN CORRECTION	COMPLETE BOUGUER
MH092	30. 32.69	112. 5.53	9414.	74.04	-246.61	13.03	-233.58
MH093	30. 31.88	112. 4.87	10350.	103.59	-248.93	17.22	-231.71
MH094	30. 31.82	112. 4.33	10268.	103.21	-246.51	14.06	-232.45
MH095	30. 32.03	112. 2.99	10320.	109.59	-241.91	10.10	-231.81
MH096	30. 32.05	112. 2.25	10134.	107.45	-237.71	7.91	-229.80
MH097	30. 31.61	112. 1.96	10080.	104.18	-239.15	7.51	-231.64
MH098	30. 31.61	112. 1.42	10033.	103.52	-238.20	7.34	-230.86
MH099	30. 31.83	112. .02	9481.	89.87	-233.05	5.31	-227.74
MH100	30. 31.21	112. .19	9607.	92.17	-235.04	5.67	-229.37
MH101	30. 30.45	112. .21	9186.	77.93	-234.95	5.63	-229.32
MH102	30. 29.64	112. .09	9147.	75.44	-236.10	4.37	-231.73
MH103	30. 29.90	112. .61	9333.	81.82	-236.07	5.04	-231.03
MH104	30. 30.39	112. 1.80	9439.	83.03	-238.46	6.53	-231.93
MH105	30. 30.44	112. 5.10	9906.	96.12	-241.28	6.81	-234.47
MH106	30. 31.11	112. 5.23	10254.	107.04	-242.21	9.27	-232.94
MH107	30. 31.33	112. 2.91	10340.	110.12	-242.26	9.41	-232.85
MH108	30. 30.60	112. 7.86	5415.	-55.57	-240.01	4.80	-235.21
MH109	30. 30.48	112. 8.00	5415.	-56.87	-241.30	4.30	-237.00
MH110	30. 36.21	112. 8.23	5408.	-59.03	-243.22	4.66	-238.56
MH111	30. 36.21	112. 8.54	5412.	-59.13	-243.46	4.52	-238.94
MH112	30. 35.99	112. 8.41	5421.	-58.90	-243.54	4.64	-238.90
MH113	30. 35.73	112. 8.62	5449.	-57.90	-243.49	4.44	-239.05
MH114	30. 35.32	112. 8.96	5490.	-55.98	-242.97	4.38	-238.59
MH115	30. 35.11	112. 8.96	5521.	-54.95	-243.00	5.23	-237.77
MH116	30. 35.13	112. 8.21	5517.	-55.53	-243.44	6.04	-237.40
MH117	30. 35.04	112. 7.90	5571.	-53.09	-242.75	6.61	-236.14
MH118	30. 34.76	112. 7.98	5640.	-50.62	-242.92	7.37	-235.55
MH119	30. 34.47	112. 7.97	5819.	-45.26	-243.45	7.51	-235.94
MH120	30. 34.30	112. 7.69	6230.	-32.00	-244.19	10.70	-233.49
MH121	30. 33.78	112. 8.37	6121.	-36.90	-245.36	6.97	-238.41

STATION NUMBER	LATITUDE DEG MIN	LONGITUDE DEG MIN	ELEVATION IN FEET	FREE-AIR ANOMALY	SIMPLE BOUGUER	TERRAIN CORRECTION	COMPLETE BOUGUER
MH122	38. 34.01	112. 8.40	5989.	-40.24	-244.23	7.08	-237.15
MH123	38. 33.46	112. 8.52	6221.	-34.29	-246.18	6.78	-239.40
MH124	38. 33.60	112. 8.00	6410.	-25.61	-243.94	8.05	-235.89
MH125	38. 33.62	112. 7.71	6875.	-9.95	-244.12	9.72	-234.40
MH126	38. 33.45	112. 6.67	8047.	32.37	-241.71	10.39	-231.32
MH127	38. 33.49	112. 7.20	7681.	15.21	-246.41	13.89	-232.52
MH128	38. 33.59	112. 8.80	6821.	-39.52	-244.60	6.09	-238.51
MH129	38. 34.22	112. 9.36	5747.	-47.44	-243.19	4.39	-238.80
MH130	38. 34.67	112. 9.37	5620.	-50.94	-242.35	4.36	-237.99
MH131	38. 32.56	112. 3.58	10890.	120.02	-250.89	19.96	-230.93
MH132	38. 43.23	112. 7.55	5392.	-58.38	-242.03	3.20	-238.83
MH133	38. 42.76	112. 7.57	5420.	-58.21	-242.82	2.80	-240.02
MH134	38. 42.77	112. 7.93	5460.	-54.21	-240.17	3.00	-237.17
MH135	38. 42.45	112. 6.26	5486.	-52.59	-239.44	3.22	-236.22
MH136	38. 41.85	112. 8.64	5428.	-54.93	-239.80	4.52	-235.28
MH137	38. 41.47	112. 6.64	5378.	-58.58	-241.76	3.60	-238.16
MH138	38. 41.47	112. 7.95	5376.	-60.26	-243.36	2.93	-240.43
MH139	38. 40.96	112. 8.63	5340.	-60.65	-242.73	3.27	-239.46
MH140	38. 40.99	112. 7.93	5344.	-61.49	-243.51	2.99	-240.52
MH141	38. 40.50	112. 8.86	5324.	-61.85	-243.19	3.19	-240.00
MH142	38. 40.60	112. 8.63	5320.	-62.19	-243.39	3.18	-240.21
MH143	38. 40.35	112. 9.16	5327.	-61.67	-243.11	3.25	-239.86
MH144	38. 40.45	112. 8.30	5315.	-62.84	-243.87	3.07	-240.80
MH145	38. 39.94	112. 8.63	5323.	-62.77	-244.07	2.96	-241.11
MH146	38. 39.71	112. 8.62	5324.	-62.93	-244.26	2.92	-241.34
MH147	38. 39.71	112. 9.09	5334.	-62.59	-244.26	3.49	-240.77
MH148	38. 39.27	112. 8.86	5334.	-62.78	-244.45	2.95	-241.50
MH149	38. 38.44	112. 8.87	5338.	-62.74	-244.56	2.13	-242.43
MH150	38. 38.44	112. 8.49	5337.	-62.80	-244.58	3.44	-241.14
MH151	38. 38.88	112. 8.21	5326.	-62.47	-243.87	3.27	-240.60

STATION NUMBER	LATITUDE DEG MIN	LONGITUDE DEG MIN	ELEVATION IN FEET	FREE-AIR ANOMALY	SIMPLE BOUGUER	TERRAIN CORRECTION	COMPLETE BOUGUER
MH152	30. 39.21	112. 7.92	5317.	-62.44	-243.53	3.17	-240.36
MH153	30. 39.32	112. 7.64	5312.	-62.11	-243.04	3.46	-239.58
MH154	30. 38.89	112. 7.64	5323.	-61.24	-242.54	3.67	-238.87
MH155	30. 38.23	112. 7.63	5347.	-59.31	-241.43	3.92	-237.51
MH156	30. 38.00	112. 7.55	5359.	-58.08	-240.61	3.91	-236.70
MH157	30. 37.82	112. 7.65	5371.	-56.85	-239.79	4.13	-235.66
MH158	30. 37.75	112. 8.20	5362.	-60.53	-243.16	3.62	-239.54
MH159	30. 37.73	112. 9.54	5443.	-57.53	-242.92	2.83	-240.09
MH160	30. 36.17	112. 9.97	5471.	-54.91	-241.26	2.78	-238.48
MH161	30. 36.58	112. 10.45	5566.	-51.30	-240.86	2.64	-238.24
MH162	30. 37.54	112. 10.84	5885.	-35.19	-235.63	3.14	-232.49
MH163	30. 37.51	112. 10.06	5820.	-59.02	-237.25	2.67	-234.58
MH164	30. 37.19	112. 10.86	5725.	-40.51	-235.56	2.36	-233.14
MH165	30. 36.70	112. 10.76	5652.	-43.26	-235.76	2.83	-232.93
MH166	30. 30.70	112. 11.71	5947.	-32.40	-234.95	3.01	-231.94
MH167	30. 30.94	112. 11.39	6050.	-29.84	-235.90	4.29	-231.61
MH168	30. 37.52	112. 9.11	5400.	-60.05	-243.98	3.16	-240.82
MH169	30. 38.17	112. 9.73	5416.	-58.31	-242.78	2.85	-239.93
MH170	30. 39.27	112. 9.43	5348.	-62.23	-244.39	2.87	-241.52
MH171	30. 39.27	112. 9.70	5352.	-62.05	-244.34	2.89	-241.45
MH172	30. 38.85	112. 9.70	5358.	-61.25	-243.75	2.89	-240.86
MH173	30. 38.85	112. 9.98	5381.	-60.00	-243.27	2.91	-240.36
MH174	30. 38.46	112. 10.94	5424.	-53.42	-238.16	2.95	-235.21
MH175	30. 37.90	112. 11.36	5452.	-48.29	-233.98	2.90	-231.08
MH176	30. 37.52	112. 12.21	5418.	-50.91	-235.44	2.94	-232.50
MH177	30. 37.60	112. 13.24	5456.	-54.34	-240.17	2.26	-237.91
MH178	30. 37.70	112. 13.80	5643.	-45.93	-238.13	3.45	-234.68
MH179	30. 37.71	112. 14.57	5897.	-33.26	-234.11	3.69	-230.42
MH180	30. 37.93	112. 13.03	5437.	-54.32	-239.51	3.26	-236.25
MH181	30. 38.09	112. 12.74	5411.	-54.99	-239.29	3.38	-235.91

STATION NUMBER	LATITUDE DEG MIN	LONGITUDE DEG MIN	ELEVATION IN FEET	FREE-AIR ANOMALY	SIMPLE BOUGUER	TERRAIN CORRECTION	COMPLETE BOUGUER
MH182	38. 38.13	112. 12.19	5403.	-53.84	-237.87	3.06	-234.81
MH183	38. 38.60	112. 11.97	5392.	-54.94	-238.59	3.09	-235.50
MH184	38. 38.32	112. 12.94	5439.	-52.63	-237.88	3.53	-234.35
MH185	38. 38.60	112. 12.73	5432.	-51.86	-236.88	3.55	-233.33
MH186	38. 39.03	112. 12.48	5427.	-50.67	-235.51	3.65	-231.86
MH187	38. 39.21	112. 11.93	5409.	-53.25	-237.48	3.45	-234.03
MH188	38. 39.72	112. 10.11	5350.	-60.97	-243.20	3.25	-239.95
MH189	38. 39.70	112. 9.71	5350.	-61.25	-243.47	3.02	-240.45
MH190	38. 39.07	112. 10.69	5369.	-59.35	-242.22	3.05	-239.17
MH191	38. 40.29	112. 9.87	5365.	-58.70	-241.44	4.01	-237.43
MH192	38. 37.54	112. 9.97	5552.	-50.92	-240.02	2.57	-237.45
MH193	38. 37.00	112. 9.73	5508.	-53.43	-241.04	2.89	-238.15
MH194	38. 36.64	112. 9.67	5509.	-53.29	-240.93	3.06	-237.87
MH195	38. 36.26	112. 9.67	5502.	-53.27	-240.67	3.31	-237.36
MH196	38. 36.21	112. 9.11	5450.	-56.76	-242.38	3.83	-238.55
MH197	38. 36.64	112. 8.84	5421.	-58.54	-243.18	3.60	-239.58
MH198	38. 37.10	112. 8.00	5397.	-56.69	-240.51	3.89	-236.62
MH199	38. 35.22	112. 7.72	5429.	-55.87	-240.76	5.48	-235.30
MH200	38. 35.69	112. 7.70	5429.	-57.31	-242.22	6.59	-235.63
MH201	38. 34.68	112. 8.49	5645.	-51.09	-243.36	6.20	-237.16
MH202	38. 34.86	112. 10.06	5749.	-45.29	-241.10	3.32	-237.78
MH203	38. 35.33	112. 9.66	5561.	-51.90	-241.31	3.55	-237.76
MH204	38. 35.70	112. 9.68	5519.	-52.55	-240.52	3.58	-236.94
MH205	38. 30.11	112. 10.26	5512.	-50.57	-238.31	3.11	-235.20
MH206	38. 35.84	112. 10.82	5585.	-47.77	-237.99	2.77	-235.22
MH207	38. 35.20	112. 10.73	5601.	-48.05	-238.82	2.96	-235.86
MH208	38. 34.88	112. 11.20	5624.	-47.99	-239.54	2.98	-236.56
MH209	38. 34.42	112. 11.50	5662.	-47.27	-240.12	3.04	-237.08
MH210	38. 34.01	112. 10.64	5773.	-45.27	-241.90	3.30	-238.60
MH211	38. 33.79	112. 10.24	5839.	-43.85	-242.72	3.66	-239.06

STATION NUMBER	LATITUDE DEG MIN	LONGITUDE DEG MIN	ELEVATION IN FEET	FREE-AIR ANOMALY	SIMPLE BOUGUER	TERRAIN CORRECTION	COMPLETE BOUGUER
MH212	38. 34.19	112. 10.07	5722.	-47.73	-242.62	4.07	-238.55
MH213	38. 33.18	112. 10.58	5958.	-40.85	-243.78	3.42	-240.36
MH214	38. 32.57	112. 10.78	6235.	-30.90	-243.27	3.37	-239.90
MH215	38. 32.50	112. 11.44	6125.	-33.16	-241.78	2.98	-238.80
MH216	38. 32.90	112. 11.91	6077.	-32.51	-239.50	3.05	-236.45
MH217	38. 33.11	112. 12.43	6023.	-33.20	-238.34	3.18	-235.16
MH218	38. 34.40	112. 12.87	5751.	-38.44	-234.32	2.82	-231.50
MH219	38. 37.38	112. 11.76	5442.	-46.43	-231.78	4.16	-227.62
MH220	38. 37.07	112. 13.86	5579.	-51.78	-241.80	3.10	-238.70
MH221	38. 36.19	112. 13.57	5487.	-50.42	-237.31	3.02	-234.29
MH222	38. 36.20	112. 14.08	5498.	-53.37	-240.64	3.61	-237.03
MH223	38. 36.10	112. 14.68	5565.	-51.49	-241.03	3.37	-237.66
MH224	38. 37.09	112. 14.39	5721.	-45.95	-240.81	3.43	-237.38
MH225	38. 35.44	112. 14.12	5528.	-46.01	-234.29	4.26	-230.03
MH226	38. 35.31	112. 13.59	5580.	-42.30	-232.36	3.27	-229.09
MH227	38. 34.42	112. 13.46	5877.	-32.64	-232.81	2.84	-229.97
MH228	38. 34.86	112. 13.51	5705.	-35.10	-229.41	3.05	-226.36
MH229	38. 35.87	112. 11.98	5786.	-37.71	-234.78	2.71	-232.07
MH230	38. 36.22	112. 11.88	5581.	-43.21	-233.30	2.76	-230.54
MH231	38. 35.73	112. 12.39	5658.	-40.94	-233.65	3.01	-230.64
MH232	38. 33.57	112. 12.86	5968.	-32.28	-235.55	3.06	-232.49
MH233	38. 34.00	112. 12.96	5811.	-37.36	-235.29	3.27	-232.02
MH234	38. 32.72	112. 12.40	6189.	-29.82	-240.62	3.45	-237.17
MH235	38. 32.33	112. 12.40	6399.	-24.59	-242.54	3.90	-238.64
MH236	38. 32.00	112. 12.60	6738.	-12.86	-242.35	3.46	-238.89
MH237	38. 31.77	112. 12.71	6837.	-10.79	-243.66	2.91	-240.75
MH238	38. 31.99	112. 13.51	6679.	-12.31	-239.80	2.38	-237.42
MH239	38. 32.27	112. 14.12	6821.	-5.64	-237.96	2.27	-235.69
MH240	38. 31.97	112. 14.82	6919.	-3.67	-239.33	3.41	-235.92
MH241	38. 32.84	112. 14.86	7033.	2.45	-237.09	4.20	-232.89

STATION NUMBER	LATITUDE DEG MIN	LONGITUDE DEG MIN	ELEVATION IN FEET	FREE-AIR ANOMALY	SIMPLE BOUGUER	TERRAIN CORRECTION	COMPLETE BOUGUER
MH242	38. 33.12	112. 14.07	7053.	2.51	-237.71	5.89	-231.82
MH243	38. 31.52	112. 13.63	6536.	-17.55	-240.17	2.48	-237.69
MH244	38. 31.33	112. 14.35	6400.	-23.73	-241.71	3.00	-238.71
MH245	38. 31.21	112. 14.97	6222.	-31.88	-243.80	6.75	-237.05
MH246	38. 31.74	112. 11.13	6408.	-25.08	-243.33	3.60	-239.73
MH247	38. 31.64	112. 11.62	6610.	-18.81	-243.95	3.28	-240.67
MH248	38. 31.19	112. 11.76	6715.	-14.86	-243.58	3.02	-240.56
MH249	38. 32.30	112. 11.82	6228.	-30.10	-242.23	3.20	-239.03
MH250	38. 32.60	112. 13.17	6530.	-14.22	-238.33	3.83	-234.50
MH251	38. 31.09	112. 13.74	6428.	-23.87	-242.81	2.89	-239.92
MH252	38. 31.09	112. 13.29	6525.	-21.36	-243.60	2.76	-240.84
MH253	38. 30.84	112. 14.64	6768.	-13.28	-243.80	3.04	-240.76
MH254	38. 30.86	112. 15.06	7082.	-7.82	-249.03	10.07	-238.96
MH255	38. 30.34	112. 14.75	7051.	-11.95	-252.10	7.14	-244.96
MH256	38. 30.57	112. 14.16	6379.	-27.67	-244.94	3.00	-241.94
MH257	38. 30.03	112. 13.90	6150.	-41.34	-250.80	3.82	-246.98
MH258	38. 30.00	112. 13.51	6335.	-34.47	-250.24	3.29	-246.95
MH259	38. 30.68	112. 12.87	6892.	-9.23	-243.97	3.12	-240.85
MH260	38. 30.48	112. 12.63	7079.	-2.93	-244.04	3.46	-240.58
MH261	38. 30.00	112. 12.72	7295.	-5.09	-253.56	10.79	-242.77
MH262	38. 30.60	112. 12.23	6925.	-8.12	-243.98	2.77	-241.21
MH263	38. 30.19	112. 12.01	7139.	-2.24	-245.39	3.68	-241.71
MH264	38. 30.04	112. 10.83	6689.	-19.04	-246.86	3.51	-243.35
MH265	38. 30.42	112. 10.28	6915.	-11.80	-247.33	3.52	-243.81
MH266	38. 30.49	112. 10.78	7103.	-5.62	-247.55	4.15	-243.40
MH267	38. 30.51	112. 11.32	7129.	-2.41	-245.22	3.26	-241.96
MH268	38. 30.96	112. 11.39	6850.	-11.21	-244.52	3.02	-241.50
MH269	38. 31.12	112. 10.89	7021.	-7.14	-246.26	4.02	-242.26
MH270	38. 31.36	112. 10.02	6453.	-26.27	-246.05	4.88	-241.17
MH271	38. 30.93	112. 9.67	6711.	-18.58	-247.15	6.05	-241.10

STATION NUMBER	LATITUDE DEG MIN	LONGITUDE DEG MIN	ELEVATION IN FEET	FREE-AIR ANOMALY	SIMPLE BOUGUER	TERRAIN CORRECTION	COMPLETE BOUGUER
MH272	30. 31.04	112. 9.23	6889.	-14.41	-249.05	6.49	-242.56
MH273	30. 30.20	112. 6.24	7885.	19.08	-249.49	7.53	-241.96
MH274	30. 30.79	112. 8.30	8120.	24.56	-252.01	11.50	-240.51
MH275	30. 42.52	112. 9.94	6339.	-12.64	-228.54	4.82	-223.72
MH276	30. 43.00	112. 9.96	6410.	-7.89	-226.21	3.73	-222.48
MH277	30. 43.24	112. 9.31	6131.	-19.01	-227.83	4.21	-223.62
MH278	30. 43.19	112. 10.82	6696.	7.06	-221.01	3.23	-217.78
MH279	30. 43.12	112. 13.25	7691.	47.81	-214.15	4.47	-209.68
MH280	30. 43.40	112. 13.91	7939.	60.09	-210.32	4.57	-205.75
MH281	30. 44.43	112. 12.71	8004.	58.46	-214.16	5.79	-208.37
MH282	30. 44.38	112. 13.44	7942.	62.03	-208.47	4.14	-204.33
MH283	30. 44.74	112. 13.78	7600.	55.04	-203.81	2.55	-201.26
MH284	30. 43.93	112. 14.68	7718.	58.74	-204.13	2.79	-201.34
MH285	30. 44.16	112. 15.85	7734.	59.92	-203.50	4.70	-198.80
MH286	30. 43.40	112. 16.02	7547.	56.46	-200.59	2.83	-197.76
MH287	30. 42.79	112. 16.97	7804.	66.43	-199.37	3.29	-196.08
MH288	30. 43.40	112. 17.15	7887.	68.96	-199.67	4.18	-195.49
MH289	30. 42.35	112. 17.43	7757.	65.89	-198.31	4.67	-193.64
MH290	30. 41.32	112. 16.91	8402.	77.99	-208.18	5.39	-202.79
MH291	30. 42.38	112. 15.98	8443.	78.21	-209.36	8.03	-201.33
MH292	30. 42.70	112. 15.41	7954.	64.48	-206.43	4.30	-202.13
MH293	30. 38.45	112. 16.27	7028.	14.89	-224.48	6.28	-218.20
MH294	30. 38.87	112. 16.39	7292.	24.32	-220.98	5.62	-215.36
MH295	30. 39.63	112. 16.41	7764.	46.80	-217.64	5.59	-212.05
MH296	30. 40.12	112. 16.28	7795.	48.97	-216.53	5.47	-211.06
MH297	30. 40.41	112. 15.81	7596.	43.24	-215.48	4.70	-210.78
MH298	30. 41.05	112. 15.23	7528.	42.06	-214.34	4.29	-210.05
MH299	30. 41.45	112. 14.18	7532.	38.33	-218.21	3.45	-214.76
MH300	30. 42.23	112. 13.79	7464.	38.74	-215.46	3.84	-211.64
MH301	30. 38.98	112. 17.36	7839.	47.40	-219.60	5.99	-213.61

STATION NUMBER	LATITUDE DEG MIN	LONGITUDE DEG MIN	ELEVATION IN FEET	FREE-AIR ANOMALY	SIMPLE BOUGUER	TERRAIN CORRECTION	COMPLETE BOUGUER
MH302	38. 38.70	112. 18.08	8559.	65.25	-226.26	7.35	-218.91
MH303	38. 38.00	112. 17.81	8418.	55.84	-230.88	8.53	-222.35
MH304	38. 38.00	112. 19.05	8041.	48.79	-225.09	4.89	-220.20
MH305	38. 38.44	112. 19.23	7957.	49.37	-221.64	4.11	-217.53
MH306	38. 38.81	112. 19.66	8082.	54.97	-220.30	4.05	-216.25
MH308	38. 40.11	112. 19.65	8536.	75.55	-215.18	5.18	-210.00
MH309	38. 40.16	112. 19.10	8777.	81.49	-217.46	6.58	-210.88
MH310	38. 39.71	112. 19.10	8751.	78.42	-219.64	6.30	-213.34
MH311	38. 39.13	112. 18.73	8729.	73.64	-223.67	7.36	-216.31
MH312	38. 40.65	112. 18.27	9325.	93.69	-223.92	15.33	-208.59
MH313	38. 40.96	112. 17.58	8692.	82.76	-213.29	7.48	-205.81
MH314	38. 40.93	112. 16.89	8538.	77.72	-213.09	6.83	-206.26
MH315	38. 41.50	112. 15.89	8115.	65.20	-211.20	4.82	-206.38
MH316	38. 40.45	112. 16.39	7938.	56.51	-213.86	5.01	-208.85
MH317	38. 40.43	112. 16.83	8352.	70.91	-213.56	6.16	-207.40
MH318	38. 39.71	112. 17.99	8882.	79.44	-223.08	8.86	-214.22
MH319	38. 35.20	112. 15.24	5583.	-44.61	-234.77	3.41	-231.36
MH320	38. 35.74	112. 15.84	5744.	-39.37	-235.01	3.30	-231.71
MH321	38. 35.73	112. 15.24	5603.	-47.22	-238.06	3.31	-234.75
MH322	38. 35.30	112. 16.25	5647.	-40.82	-233.16	3.88	-229.28
MH323	38. 34.82	112. 16.80	5670.	-37.36	-230.46	7.04	-223.44
MH324	38. 34.79	112. 17.40	5699.	-38.84	-232.95	8.89	-224.06
MH325	38. 34.80	112. 17.94	5731.	-37.95	-233.15	6.93	-226.22
MH326	38. 34.76	112. 18.51	5752.	-38.72	-234.64	7.37	-227.27
MH327	38. 34.77	112. 19.03	5784.	-37.46	-234.46	6.10	-228.36
MH328	38. 34.79	112. 19.50	5805.	-37.51	-235.23	6.47	-228.76
MH329	38. 34.83	112. 21.80	5966.	-28.77	-231.97	8.37	-223.60
MH330	38. 34.89	112. 22.31	6004.	-22.65	-227.15	7.58	-219.57
MH331	38. 34.79	112. 22.65	6028.	-22.96	-228.27	11.04	-217.23
MH332	38. 34.93	112. 23.27	6112.	-16.22	-224.40	7.66	-216.74

STATION NUMBER	LATITUDE DEG MIN	LONGITUDE DEG MIN	ELEVATION IN FEET	FREE-AIR ANOMALY	SIMPLE BOUGUER	TERRAIN CORRECTION	COMPLETE BOUGUER
MH353	36. 35.04	112. 24.06	6158.	-14.62	-224.36	7.29	-217.07
MH354	36. 35.13	112. 25.16	6330.	-8.38	-223.98	6.78	-217.20
MH355	36. 34.97	112. 25.86	6410.	-4.93	-223.25	4.79	-218.46
MH356	36. 36.15	112. 27.04	7291.	27.09	-221.24	2.39	-218.85
MH357	36. 35.95	112. 26.61	7164.	21.49	-222.51	2.33	-220.18
MH358	36. 36.05	112. 26.14	7056.	18.61	-221.72	2.11	-219.61
MH359	36. 36.15	112. 25.75	7011.	17.34	-221.46	1.88	-219.58
MH360	36. 36.58	112. 25.31	7278.	26.00	-221.89	1.97	-219.92
MH361	36. 35.76	112. 25.54	7022.	16.67	-222.50	1.95	-220.55
MH362	36. 36.76	112. 27.15	7167.	28.57	-215.53	2.24	-213.29
MH363	36. 36.98	112. 27.26	7166.	26.58	-215.49	1.95	-213.54
MH364	36. 37.03	112. 27.82	7309.	34.30	-214.64	1.94	-212.70
MH365	36. 37.85	112. 26.86	6888.	22.83	-211.77	2.30	-209.47
MH366	36. 38.47	112. 26.85	6898.	24.97	-209.98	3.11	-206.87
MH367	36. 38.69	112. 26.61	6904.	26.21	-208.94	2.28	-206.66
MH368	36. 38.88	112. 25.91	6892.	25.43	-209.31	2.04	-207.27
MH369	36. 39.67	112. 25.91	7194.	38.80	-206.23	1.83	-204.40
MH370	36. 40.00	112. 25.99	7134.	38.29	-204.69	2.01	-202.68
MH371	36. 40.74	112. 25.51	7221.	44.29	-201.65	2.29	-199.36
MH372	36. 41.07	112. 25.36	7058.	40.23	-200.16	3.15	-197.01
MH373	36. 41.93	112. 25.03	6734.	33.28	-196.09	3.45	-192.64
MH374	36. 42.34	112. 24.47	6623.	30.77	-194.81	3.29	-191.52
MH375	36. 42.40	112. 24.13	6572.	29.57	-194.27	3.06	-191.21
MH376	36. 42.52	112. 23.66	6500.	26.87	-194.52	3.63	-190.89
MH377	36. 42.93	112. 23.33	6425.	24.37	-194.46	2.80	-191.66
MH378	36. 35.69	112. 19.04	6573.	-7.95	-231.82	3.19	-228.63
MH379	36. 36.18	112. 19.13	6996.	6.36	-231.93	3.71	-228.22
MH380	36. 36.57	112. 18.98	7218.	15.25	-230.60	4.21	-226.39
MH381	36. 37.04	112. 19.33	7674.	31.14	-230.24	5.73	-224.51
MH382	36. 37.38	112. 19.46	7972.	39.84	-231.69	7.29	-224.40

STATION NUMBER	LATITUDE DEG MIN	LONGITUDE DEG MIN	ELEVATION IN FEET	FREE-AIR ANOMALY	SIMPLE BOUGUER	TERRAIN CORRECTION	COMPLETE BOUGUER
MH365	38. 38.37	112. 19.64	8112.	53.26	-223.04	3.94	-219.10
MH366	38. 38.85	112. 20.79	8453.	64.02	-223.29	4.68	-218.61
MH367	38. 38.52	112. 20.89	8475.	63.66	-225.00	5.04	-219.96
MH368	38. 38.24	112. 20.64	8516.	61.94	-228.11	6.79	-221.32
MH369	38. 38.03	112. 21.17	8434.	58.98	-228.28	5.18	-223.10
MH370	38. 38.72	112. 21.38	8355.	61.44	-223.13	4.46	-218.67
MH371	38. 38.70	112. 21.92	8166.	57.17	-220.96	3.73	-217.23
MH372	38. 38.35	112. 21.96	8152.	55.28	-222.38	3.87	-218.51
MH373	38. 37.97	112. 22.00	8116.	52.07	-224.16	3.83	-220.33
MH374	38. 37.36	112. 21.76	8024.	46.35	-226.95	3.77	-223.18
MH375	38. 36.94	112. 21.29	8204.	44.64	-234.78	8.60	-226.18
MH376	38. 37.04	112. 22.13	7927.	42.72	-227.27	3.82	-223.45
MH377	38. 36.68	112. 22.14	7942.	39.93	-230.57	4.34	-226.23
MH378	38. 36.46	112. 22.70	7827.	37.10	-229.49	5.04	-224.45
MH379	38. 36.30	112. 22.36	7901.	38.04	-231.07	5.44	-225.63
MH380	38. 36.60	112. 23.21	7350.	26.08	-224.27	3.71	-220.56
MH381	38. 36.79	112. 22.77	7761.	38.23	-226.11	3.93	-222.18
MH382	38. 37.07	112. 22.78	7864.	41.51	-226.34	4.38	-221.96
MH383	38. 37.42	112. 22.63	7970.	45.63	-225.82	3.92	-221.90
MH384	38. 37.70	112. 22.38	8103.	51.37	-224.62	3.95	-220.67
MH385	38. 38.20	112. 22.43	8089.	52.85	-222.66	3.70	-218.96
MH387	38. 39.25	112. 20.76	8483.	67.59	-221.34	4.68	-216.66
MH388	38. 39.72	112. 20.35	8570.	72.27	-219.62	5.47	-214.15
MH390	38. 40.10	112. 20.80	8479.	72.85	-215.95	5.37	-210.58
MH391	38. 40.15	112. 22.32	8024.	60.77	-212.53	3.95	-208.58
MH392	38. 40.31	112. 22.95	7785.	55.53	-209.63	3.75	-205.88
MH393	38. 40.60	112. 21.91	8102.	63.92	-212.04	5.02	-207.02
MH394	38. 41.31	112. 21.61	8387.	71.45	-214.21	8.71	-205.50
MH395	38. 41.40	112. 21.33	8402.	69.96	-216.22	11.46	-204.76
MH396	38. 40.56	112. 19.10	8704.	81.14	-215.32	7.15	-208.17

STATION NUMBER	LATITUDE DEG MIN	LONGITUDE DEG MIN	ELEVATION IN FEET	FREE-AIR ANOMALY	SIMPLE BOUGUER	TERRAIN CORRECTION	COMPLETE BOUGUER
MH397	38. 40.84	112. 19.40	8452.	73.03	-214.85	9.01	-205.84
MH398	38. 40.90	112. 19.63	8373.	70.23	-214.96	8.97	-205.99
MH399	38. 41.30	112. 19.76	8143.	67.45	-209.90	9.29	-200.61
MH400	38. 41.87	112. 19.64	7431.	52.44	-200.66	5.56	-195.10
MH401	38. 41.91	112. 18.91	7609.	59.91	-199.25	4.22	-195.03
MH402	38. 41.92	112. 18.58	7588.	58.75	-199.70	4.42	-195.28
MH403	38. 41.81	112. 17.84	7699.	60.99	-201.24	5.27	-195.97
MH404	38. 41.44	112. 17.42	8072.	68.99	-205.95	5.53	-200.42
MH405	38. 43.13	112. 17.28	7777.	66.23	-198.65	2.95	-195.70
MH406	38. 42.72	112. 17.42	7746.	66.00	-197.83	3.31	-194.52
MH407	38. 42.87	112. 17.79	7700.	65.14	-197.12	3.21	-193.91
MH408	38. 43.44	112. 19.07	6787.	35.87	-195.30	4.94	-190.36
MH409	38. 43.13	112. 19.63	6820.	37.82	-194.47	4.66	-189.81
MH410	38. 43.62	112. 20.19	6182.	15.24	-195.32	6.41	-188.91
MH411	38. 44.40	112. 21.12	5805.	2.60	-195.11	9.20	-185.91
MH412	38. 44.91	112. 21.38	5668.	-1.57	-194.62	9.73	-184.89
MH413	38. 44.79	112. 20.87	5774.	.57	-196.09	9.60	-186.49
MH414	38. 44.74	112. 20.22	5958.	6.79	-196.14	10.29	-185.85
MH415	38. 44.65	112. 19.77	6065.	8.43	-198.15	11.93	-186.22
MH416	38. 36.13	112. 16.57	6105.	-23.56	-231.50	3.66	-227.84
MH417	38. 36.19	112. 17.33	6558.	-7.97	-231.34	3.65	-227.69
MH418	38. 36.44	112. 17.68	6867.	3.93	-229.96	4.26	-225.70
MH419	38. 36.49	112. 18.11	7039.	9.68	-230.07	4.53	-225.54
MH420	38. 37.03	112. 18.24	7614.	27.76	-231.57	6.31	-225.26
MH421	38. 35.61	112. 17.46	6333.	-18.47	-234.17	4.54	-229.63
MH422	38. 35.35	112. 17.52	6202.	-22.66	-233.90	3.77	-230.13
MH423	38. 35.28	112. 16.97	5734.	-36.89	-232.19	4.58	-227.61
MH424	38. 35.31	112. 28.40	6805.	16.58	-215.20	2.44	-212.76
MH425	38. 35.47	112. 29.75	7183.	29.66	-215.00	2.68	-212.32
MH426	38. 34.84	112. 27.75	6694.	8.85	-219.15	2.31	-216.84

STATION NUMBER	LATITUDE DEG MIN	LONGITUDE DEG MIN	ELEVATION IN FEET	FREE-AIR ANOMALY	SIMPLE BOUGUER	TERRAIN CORRECTION	COMPLETE BOUGUER
MH427	38. 34.58	112. 28.08	6842.	13.61	-219.43	1.95	-217.48
MH428	38. 34.81	112. 28.91	6953.	21.02	-215.80	2.21	-213.59
MH430	38. 34.20	112. 29.01	7262.	27.74	-219.61	2.92	-216.69
MH431	38. 34.18	112. 29.65	7521.	36.72	-219.44	3.10	-216.34
MH432	38. 33.87	112. 29.68	7553.	36.24	-221.02	4.64	-216.38
MH433	38. 34.29	112. 27.74	6649.	6.15	-220.32	2.83	-217.49
MH434	38. 33.65	112. 27.98	6971.	17.12	-220.31	2.87	-217.44
MH435	38. 33.42	112. 28.50	6959.	13.42	-223.61	3.50	-220.11
MH436	38. 33.14	112. 28.21	7271.	20.68	-226.97	3.33	-223.64
MH437	38. 32.09	112. 28.62	8057.	42.18	-232.24	6.51	-225.73
MH438	38. 31.58	112. 28.80	8340.	54.41	-229.65	5.66	-223.99
MH439	38. 31.07	112. 29.11	8432.	58.63	-228.56	5.63	-222.93
MH440	38. 30.30	112. 29.49	8381.	52.70	-232.76	8.78	-223.98
MH441	38. 32.56	112. 28.32	7553.	28.22	-229.33	4.41	-224.62
MH442	38. 33.58	112. 26.85	6852.	10.87	-222.51	2.44	-220.07
MH443	38. 34.16	112. 27.25	6753.	8.08	-221.93	1.94	-219.99
MH445	38. 33.86	112. 21.35	6025.	-29.32	-234.53	4.50	-230.03
MH446	38. 33.05	112. 23.34	6639.	1.09	-225.04	3.17	-221.87
MH447	38. 33.75	112. 23.46	6786.	6.00	-225.13	2.07	-223.06
MH448	38. 32.40	112. 24.12	7053.	9.69	-230.53	2.93	-227.60
MH449	38. 32.75	112. 24.96	6957.	10.36	-226.60	2.64	-223.96
MH450	38. 33.17	112. 24.25	6770.	6.60	-223.99	2.19	-221.80
MH451	38. 34.85	112. 16.46	5771.	-31.47	-228.03	4.64	-223.39
MH452	38. 34.31	112. 17.20	6070.	-23.39	-230.14	5.42	-224.72
MH453	38. 33.90	112. 18.50	6538.	-13.91	-236.60	3.04	-233.56
MH454	38. 32.50	112. 19.11	7569.	21.90	-235.96	5.48	-230.42
MH455	38. 32.10	112. 19.09	7728.	26.61	-236.01	5.71	-230.89
MH456	38. 31.80	112. 19.12	8126.	38.65	-238.12	7.18	-230.94
MH457	38. 31.54	112. 19.43	8319.	42.06	-241.28	6.68	-234.60
MH458	38. 31.36	112. 19.11	8481.	49.18	-239.68	7.17	-232.51

STATION NUMBER	LATITUDE DEG MIN	LONGITUDE DEG MIN	ELEVATION IN FEET	FREE-AIR ANOMALY	SIMPLE BOUGUER	TERRAIN CORRECTION	COMPLETE BOUGUER
MH459	38. 30.94	112. 19.06	8808.	56.41	-243.59	8.94	-234.65
MH460	38. 30.31	112. 18.75	8953.	52.82	-252.12	12.73	-239.39
MH461	38. 30.50	112. 19.85	8931.	55.42	-248.77	8.77	-240.00
MH462	38. 30.13	112. 20.14	9277.	63.40	-252.58	11.93	-240.65
MH463	38. 30.94	112. 20.28	8298.	43.06	-239.57	6.84	-232.73
MH465	38. 31.24	112. 20.67	7646.	24.89	-235.54	5.96	-229.58
MH466	38. 31.59	112. 20.53	7519.	19.53	-236.56	5.66	-230.90
MH467	38. 31.88	112. 20.16	7431.	16.47	-236.63	5.42	-231.21
MH468	38. 32.14	112. 19.64	7702.	26.33	-236.01	5.27	-230.74
MH469	38. 32.30	112. 20.40	6787.	-4.00	-235.16	7.43	-227.73
MH470	38. 32.89	112. 20.38	6434.	-24.89	-244.03	7.49	-236.54
MH471	38. 33.48	112. 20.11	6224.	-25.66	-237.65	6.56	-231.09
MH472	38. 33.92	112. 20.13	6071.	-30.51	-237.29	4.16	-233.13
MH473	38. 34.36	112. 20.10	5895.	-35.77	-236.55	4.29	-232.26
MH474	38. 34.30	112. 19.63	5922.	-34.37	-236.07	4.39	-231.68
MH475	38. 34.45	112. 20.54	5921.	-33.88	-235.55	4.47	-231.08
MH476	38. 26.90	112. 14.59	6053.	-48.62	-254.78	5.26	-249.52
MH477	38. 26.96	112. 13.80	5866.	-53.92	-253.71	4.02	-249.69
MH478	38. 26.51	112. 14.13	6015.	-50.14	-255.01	3.95	-251.06
MH479	38. 26.52	112. 13.57	5938.	-52.83	-255.08	3.79	-251.29
MH480	38. 26.44	112. 13.13	5890.	-52.66	-253.27	4.07	-249.20
MH481	38. 26.06	112. 13.63	5950.	-55.14	-257.80	3.82	-253.98
MH482	38. 26.00	112. 14.13	6026.	-51.98	-257.22	4.85	-252.37
MH483	38. 25.20	112. 13.85	6056.	-52.74	-259.01	3.59	-255.42
MH484	38. 25.22	112. 14.41	6168.	-47.78	-257.86	3.87	-253.99
MH485	38. 25.42	112. 14.84	6265.	-43.25	-256.64	4.24	-252.40
MH486	38. 24.77	112. 14.11	6056.	-51.61	-257.88	3.31	-254.57
MH487	38. 24.45	112. 13.83	6020.	-52.06	-257.10	3.95	-253.15
MH488	38. 24.09	112. 14.36	6124.	-47.26	-255.84	4.77	-251.07
MH489	38. 23.25	112. 14.86	6425.	-33.31	-252.14	6.02	-246.12

STATION NUMBER	LATITUDE DEG MIN	LONGITUDE DEG MIN	ELEVATION IN FEET	FREE-AIR ANOMALY	SIMPLE BOUGUER	TERRAIN CORRECTION	COMPLETE BOUGUER
MH490	38. 26.58	112. 14.67	6060.	-47.92	-254.32	4.45	-249.87
MH491	38. 27.45	112. 14.57	6090.	-44.76	-252.19	4.08	-248.11
MH492	38. 25.85	112. 13.16	5838.	-59.57	-258.42	4.18	-254.24
MH493	38. 24.79	112. 12.65	5885.	-57.62	-258.06	4.03	-254.03
MH494	38. 24.52	112. 12.99	6060.	-52.56	-258.96	3.44	-255.52
MH495	38. 22.85	112. 14.59	6485.	-30.10	-250.98	5.48	-245.50
MH496	38. 23.11	112. 13.53	6180.	-42.35	-253.04	3.93	-249.11
MH497	38. 23.65	112. 13.26	6092.	-47.78	-255.28	3.90	-251.38
MH498	38. 23.90	112. 12.10	5910.	-50.62	-252.12	3.62	-248.50
MH499	38. 22.89	112. 11.84	5870.	-44.28	-244.21	3.87	-240.34
MH500	38. 23.34	112. 11.91	5870.	-48.01	-247.94	3.86	-244.08
MH501	38. 23.91	112. 11.33	5865.	-49.89	-249.65	4.12	-245.53
MH502	38. 24.34	112. 11.47	5887.	-51.30	-251.81	4.35	-247.46
MH503	38. 24.70	112. 11.63	5884.	-52.68	-253.09	4.31	-248.78
MH504	38. 25.42	112. 12.00	5865.	-53.66	-253.42	4.41	-249.01
MH505	38. 27.01	112. 13.12	5832.	-52.09	-250.73	4.13	-246.60
MH506	38. 27.24	112. 13.80	5850.	-53.82	-253.35	4.01	-249.34
MH507	38. 27.08	112. 12.73	5919.	-46.67	-248.27	4.37	-243.90
MH508	38. 27.42	112. 12.90	5831.	-49.54	-248.15	4.86	-243.29
MH509	38. 27.85	112. 12.91	5830.	-49.79	-248.36	5.01	-243.35
MH510	38. 28.20	112. 11.95	6234.	-34.97	-247.30	2.85	-244.45
MH511	38. 27.95	112. 11.62	6317.	-31.83	-246.99	3.78	-243.21
MH512	38. 27.39	112. 11.31	6362.	-29.53	-246.22	3.47	-242.75
MH513	38. 27.15	112. 10.67	6555.	-22.49	-245.75	2.83	-242.92
MH514	38. 27.34	112. 10.27	6790.	-13.05	-244.32	4.36	-239.96
MH515	38. 26.79	112. 11.08	6410.	-28.59	-247.12	3.49	-243.63
MH516	38. 25.59	112. 11.09	6125.	-42.03	-250.65	3.77	-246.88
MH517	38. 24.33	112. 10.43	6203.	-37.26	-248.54	3.42	-245.12
MH518	38. 23.89	112. 9.56	6385.	-31.37	-248.85	3.32	-245.53
MH519	38. 23.96	112. 10.56	6076.	-40.85	-247.80	3.98	-243.82

STATION NUMBER	LATITUDE DEG MIN	LONGITUDE DEG MIN	ELEVATION IN FEET	FREE-AIR ANOMALY	SIMPLE BOUGUER	TERRAIN CORRECTION	COMPLETE BOUGUER
MH520	30. 23.29	112. 14.16	5840.	-51.71	-250.83	5.15	-245.68
MH521	30. 29.27	112. 14.69	6110.	-44.88	-252.99	6.10	-246.89
MH522	30. 28.20	112. 13.03	5925.	-46.71	-248.52	4.49	-244.03
MH523	30. 28.92	112. 12.51	6076.	-42.69	-249.64	3.86	-245.78
MH525	30. 29.05	112. 13.46	5915.	-50.32	-251.79	4.43	-247.36
MH526	30. 29.55	112. 13.80	5970.	-49.89	-253.23	5.09	-248.14
MH527	30. 29.37	112. 12.38	6275.	-36.18	-249.91	3.96	-245.95
MH528	30. 29.52	112. 12.88	6786.	-22.26	-253.39	6.69	-246.70
MH529	30. 29.29	112. 11.85	6310.	-33.61	-248.53	3.96	-244.57
MH530	30. 29.65	112. 11.59	6509.	-26.26	-247.95	3.70	-244.25
MH531	30. 29.80	112. 11.23	6596.	-23.21	-247.87	3.50	-244.37
MH532	30. 29.74	112. 10.26	6728.	-18.57	-247.73	4.33	-243.40
MH533	30. 24.44	112. 9.70	6572.	-27.36	-251.20	4.00	-247.20
MH534	30. 25.58	112. 9.15	7274.	-37	-248.12	5.52	-242.60
MH535	30. 25.27	112. 9.27	6945.	-12.51	-249.06	4.20	-244.86
MH536	30. 24.94	112. 8.64	6870.	-12.68	-246.68	4.61	-242.07
MH537	30. 24.71	112. 8.00	6850.	-10.36	-243.67	4.82	-238.85
MH538	30. 24.38	112. 8.14	6865.	-11.68	-245.50	4.17	-241.33
MH539	30. 23.73	112. 8.60	6465.	-26.51	-246.71	4.80	-241.91
MH540	30. 23.42	112. 9.06	6257.	-32.84	-245.96	3.80	-242.16
MH541	30. 23.20	112. 9.65	6225.	-35.77	-247.79	3.27	-244.52
MH542	30. 23.46	112. 10.21	6176.	-35.53	-245.89	3.21	-242.68
MH543	30. 23.11	112. 8.90	6215.	-34.19	-245.87	4.00	-241.87
MH544	30. 22.82	112. 7.75	6494.	-20.61	-241.80	4.58	-237.22
MH545	30. 22.19	112. 8.29	6289.	-27.71	-241.92	3.72	-238.20
MH546	30. 21.29	112. 8.44	6242.	-28.77	-241.37	3.25	-238.12
MH547	30. 20.85	112. 9.10	6271.	-26.84	-240.43	2.69	-237.74
MH548	30. 21.40	112. 11.28	5893.	-39.38	-240.09	3.76	-236.33
MH549	30. 21.98	112. 11.85	5914.	-40.10	-241.53	3.79	-237.74
MH550	30. 22.44	112. 12.10	5870.	-43.77	-243.71	4.35	-239.36

STATION NUMBER	LATITUDE DEG MIN	LONGITUDE DEG MIN	ELEVATION IN FEET	FREE-AIR ANOMALY	SIMPLE BOUGUER	TERRAIN CORRECTION	COMPLETE BOUGUER
MH551	38. 27.96	112. 10.69	6674.	-19.67	-246.99	3.54	-243.45
MH552	38. 28.09	112. 10.29	6820.	-13.51	-246.00	3.93	-242.07
MH553	38. 27.99	112. 9.77	7024.	-6.42	-245.65	4.64	-241.01
MH554	38. 28.24	112. 9.39	7207.	-.57	-246.04	4.67	-241.37
MH555	38. 28.79	112. 8.60	7726.	14.54	-248.61	6.39	-242.22
MH556	38. 29.43	112. 8.41	7934.	21.80	-248.43	6.03	-242.40
MH557	38. 29.16	112. 9.84	7755.	12.28	-251.86	9.52	-242.34
MH558	38. 29.17	112. 9.15	8095.	24.53	-251.18	8.85	-242.33
MH559	38. 29.76	112. 8.80	7870.	17.87	-250.18	5.95	-244.23
MH560	38. 30.05	112. 9.02	7620.	10.09	-249.45	5.35	-244.10
MH561	38. 30.07	112. 7.70	8707.	46.98	-249.58	9.35	-240.23
MH563	38. 28.18	112. 8.57	7644.	10.17	-250.19	7.83	-242.36
MH564	38. 27.45	112. 8.76	7543.	11.45	-245.47	4.55	-240.92
MH565	38. 26.74	112. 9.12	7696.	16.35	-245.77	6.10	-239.67
MH566	38. 27.44	112. 7.68	8007.	26.57	-246.15	7.75	-238.40
MH567	38. 26.79	112. 8.02	7535.	13.00	-243.64	5.01	-238.63
MH568	38. 26.50	112. 7.68	7487.	11.99	-243.01	5.56	-237.45
MH569	38. 25.85	112. 7.40	7119.	.82	-241.65	7.01	-234.64
MH570	38. 24.65	112. 5.81	8544.	51.81	-239.20	8.01	-231.19
MH571	38. 23.98	112. 5.71	8430.	49.96	-237.17	7.88	-229.29
MH572	38. 23.41	112. 5.22	8702.	59.76	-236.63	7.59	-229.04
MH573	38. 23.20	112. 6.06	8561.	49.07	-242.52	13.41	-229.11
MH574	38. 24.65	112. 6.58	7820.	28.97	-237.38	6.78	-230.60
MH575	38. 25.25	112. 7.84	6870.	-8.89	-242.89	5.40	-237.49
MH576	38. 24.29	112. 7.35	7308.	8.03	-240.86	5.46	-235.42
MH577	38. 22.32	112. 9.55	6128.	-36.05	-244.77	3.27	-241.50
MH578	38. 21.72	112. 9.55	6212.	-32.18	-243.76	2.85	-240.91
MH579	38. 22.44	112. 10.95	5929.	-41.15	-243.09	4.55	-238.54
MH580	38. 22.46	112. 10.24	6009.	-39.64	-244.30	3.76	-240.54
MH581	38. 22.80	112. 10.43	6119.	-36.90	-245.31	3.08	-242.23

STATION NUMBER	LATITUDE DEG MIN	LONGITUDE DEG MIN	ELEVATION IN FEET	FREE-AIR ANOMALY	SIMPLE BOUGUER	TERRAIN CORRECTION	COMPLETE BOUGUER
MH582	38. 22.83	112. 9.66	6125.	-37.18	-245.86	3.37	-242.43
MH583	38. 22.06	112. 13.43	6206.	-33.93	-245.37	4.37	-241.00
MH584	38. 21.12	112. 13.18	6267.	-27.24	-240.69	4.35	-236.34
MH585	38. 21.66	112. 13.92	6622.	-16.48	-242.02	5.31	-236.71
MH586	38. 20.54	112. 13.80	6889.	-6.05	-240.69	5.89	-234.80
MH587	38. 20.26	112. 12.97	6351.	-22.17	-238.49	3.63	-234.86
MH588	38. 19.57	112. 13.09	6301.	-22.51	-237.12	3.72	-233.40
MH589	38. 19.24	112. 11.97	6077.	-29.66	-236.64	3.80	-232.84
MH591	38. 20.04	112. 12.58	6215.	-25.75	-237.44	3.48	-233.96
MH592	38. 19.77	112. 11.86	6101.	-29.26	-237.07	3.44	-233.63
MH593	38. 19.46	112. 11.43	5996.	-31.64	-235.87	3.86	-232.01
MH594	38. 18.49	112. 12.71	6029.	-31.56	-236.91	3.93	-232.98
MH595	38. 18.57	112. 13.37	6045.	-32.56	-238.45	3.55	-234.90
MH596	38. 17.07	112. 13.45	6088.	-30.88	-238.24	3.85	-234.39
MH597	38. 17.44	112. 13.48	6117.	-29.64	-237.99	3.89	-234.10
MH598	38. 18.15	112. 14.08	6462.	-15.65	-235.74	4.42	-231.32
MH599	38. 18.29	112. 13.36	6185.	-26.57	-237.24	4.15	-233.09
MH600	38. 18.63	112. 13.70	6410.	-18.05	-236.38	4.43	-231.95
MH601	38. 16.94	112. 14.71	6425.	-19.78	-238.62	4.58	-234.04
MH602	38. 16.01	112. 14.01	6181.	-28.76	-239.28	3.43	-235.85
MH603	38. 15.59	112. 13.20	6063.	-32.02	-238.52	3.08	-235.44
MH604	38. 15.14	112. 12.89	6035.	-31.91	-237.46	2.90	-234.56
MH605	38. 15.03	112. 14.30	6181.	-26.96	-237.48	3.42	-234.06
MH606	38. 15.71	112. 14.98	6377.	-19.35	-236.55	3.77	-232.78
MH607	38. 17.77	112. 11.72	6055.	-29.33	-235.57	5.09	-230.48
MH608	38. 17.39	112. 11.70	6078.	-27.94	-234.96	4.39	-230.57
MH609	38. 16.86	112. 11.78	6076.	-27.66	-234.60	3.86	-230.74
MH610	38. 15.96	112. 11.13	6144.	-25.73	-234.99	4.27	-230.72
MH611	38. 15.22	112. 10.96	6119.	-25.79	-234.20	3.79	-230.41
MH613	38. 39.37	112. .15	9839.	97.71	-237.41	14.84	-222.57

STATION NUMBER	LATITUDE DEG MIN	LONGITUDE DEG MIN	ELEVATION IN FEET	FREE-AIR ANOMALY	SIMPLE BOUGUER	TERAIN CORRECTION	COMPLETE BOUGUER
MH014	30. 37.52	112. .89	11223.	130.98	-251.28	30.93	-220.35
MH015	30. 37.38	112. .30	11162.	134.95	-245.23	23.78	-221.45
MH016	30. 15.43	112. 7.85	7548.	22.57	-234.51	3.18	-231.33
MH017	30. 16.14	112. 8.20	7798.	30.17	-235.43	3.16	-232.27
MH018	30. 19.47	112. 8.48	7841.	29.72	-237.34	3.36	-233.98
MH019	30. 16.74	112. 8.78	7985.	33.36	-238.61	4.59	-234.02
MH020	30. 17.33	112. 9.20	7421.	14.82	-237.94	4.30	-233.64
MH021	30. 18.12	112. 9.06	6846.	-5.41	-238.58	2.81	-235.77
MH022	30. 18.52	112. 8.96	6668.	-13.21	-240.33	2.82	-237.51
MH023	30. 19.12	112. 9.05	6460.	-20.33	-240.35	2.73	-237.62
MH025	30. 18.63	112. 10.33	6457.	-15.38	-235.31	2.96	-232.35
MH026	30. 19.32	112. 9.79	6858.	-7.08	-240.66	4.06	-236.60
MH027	30. 19.16	112. 8.49	6368.	-23.79	-240.69	3.20	-237.49
MH028	30. 18.81	112. 8.49	6445.	-20.50	-240.02	3.25	-236.77
MH029	30. 18.31	112. 8.09	6731.	-9.08	-238.34	3.33	-235.01
MH030	30. 19.17	112. 7.70	6405.	-20.31	-238.47	3.79	-234.68
MH031	30. 20.42	112. 7.52	6360.	-22.01	-238.63	4.06	-234.57
MH032	30. 21.10	112. 5.95	6986.	8.45	-229.50	6.93	-222.57
MH033	30. 21.29	112. 6.43	6757.	-3.32	-233.46	5.34	-228.12
MH034	30. 21.29	112. 6.96	6575.	-12.09	-236.03	4.27	-231.76
MH035	30. 20.90	112. 6.58	6660.	-7.14	-233.98	5.84	-228.14
MH036	30. 18.15	112. 6.87	6835.	.99	-231.81	5.62	-226.19
MH037	30. 17.70	112. 7.60	7434.	14.61	-238.59	6.24	-232.35
MH038	30. 17.27	112. 6.24	7438.	21.10	-232.24	5.85	-226.39
MH039	30. 16.49	112. 7.16	7531.	22.17	-234.34	3.24	-231.10
MH040	30. 16.47	112. 7.79	7684.	25.68	-236.04	2.75	-233.29
MH041	30. 17.16	112. 8.00	7908.	29.24	-240.11	5.21	-234.90
MH042	30. 16.04	112. 7.70	7528.	21.27	-235.13	3.43	-231.70
MH043	30. 29.90	112. 3.69	9780.	93.21	-239.90	6.38	-233.52
MH044	30. 29.04	112. 2.99	9937.	101.63	-236.83	7.24	-229.59

STATION NUMBER	LATITUDE DEG MIN	LONGITUDE DEG MIN	ELEVATION IN FEET	FREE-AIR ANOMALY	SIMPLE BOUGUER	TERRAIN CORRECTION	COMPLETE BOUGUER
MH045	38. 29.10	112. 4.33	9735.	90.52	-241.06	7.14	-233.92
MH046	38. 29.05	112. 5.15	10119.	100.56	-244.09	10.03	-234.06
MH047	38. 28.44	112. 4.34	9553.	86.06	-239.31	6.59	-232.72
MH048	38. 28.71	112. 6.27	10761.	101.23	-265.29	28.62	-236.67
MH049	38. 28.37	112. 5.25	9958.	94.96	-244.21	10.06	-234.15
MH050	38. 27.45	112. 3.28	9314.	79.36	-237.88	4.89	-232.99
MH051	38. 27.37	112. 2.13	9238.	79.11	-235.53	3.97	-231.56
MH052	38. 26.97	112. 1.50	9022.	72.24	-235.05	3.95	-231.10
MH053	38. 27.55	112. 1.62	9140.	75.79	-235.51	3.88	-231.63
MH054	38. 27.55	112. 1.05	9013.	71.15	-235.83	3.09	-232.14
MH055	38. 27.27	112. .84	8902.	68.29	-234.91	3.59	-231.32
MH056	38. 27.70	112. .37	9024.	72.18	-235.18	3.90	-231.28
MH057	38. 28.25	112. .33	9087.	73.22	-236.29	4.14	-232.15
MH058	38. 28.71	112. .14	8882.	66.53	-235.99	3.79	-232.20
MH059	38. 29.02	112. .09	8992.	71.04	-235.23	4.05	-231.18
MH060	38. 20.49	112. 1.24	9076.	74.24	-234.89	3.90	-230.99
MH061	38. 25.90	112. 1.27	9067.	75.44	-233.39	4.13	-229.26
MH062	38. 25.81	112. .70	9009.	72.82	-234.03	4.01	-230.02
MH063	38. 26.31	112. .05	8742.	65.10	-232.65	3.87	-228.78
MH064	38. 26.06	112. 2.20	9376.	84.41	-234.94	4.68	-230.26
MH065	38. 20.40	112. 2.98	9428.	84.55	-236.57	4.85	-231.72
MH066	38. 25.88	112. 3.77	9510.	85.89	-238.02	5.99	-232.03
MH067	38. 25.80	112. 3.10	9262.	79.69	-235.77	5.06	-230.71
MH068	38. 24.38	112. 4.72	9737.	89.38	-242.26	11.05	-231.21
MH069	38. 23.61	112. 4.66	9825.	82.33	-252.30	21.50	-230.80
MH070	38. 24.90	112. 3.94	9912.	93.79	-243.81	12.25	-231.56
MH071	38. 25.71	112. 2.43	9147.	76.41	-235.13	5.24	-229.89
MH072	38. 24.91	112. 2.31	8774.	67.94	-230.90	5.36	-225.54
MH073	38. 24.63	112. 1.09	9210.	85.82	-227.88	4.81	-223.07
MH074	38. 23.49	112. 1.96	9754.	95.46	-236.76	8.49	-228.27

STATION NUMBER	LATITUDE DEG MIN	LONGITUDE DEG MIN	ELEVATION IN FEET	FREE-AIR ANOMALY	SIMPLE BOUGUER	TERRAIN CORRECTION	COMPLETE BOUGUER
MH075	30. 22.30	112. 2.50	9700.	95.39	-234.99	8.98	-226.01
MH076	30. 21.10	112. 1.60	9205.	81.58	-231.94	8.98	-222.96
MH077	30. 20.60	112. 2.20	9300.	85.14	-231.62	8.14	-223.48
MH078	30. 18.90	112. 3.11	8700.	68.92	-227.40	4.58	-222.82
MH079	30. 18.70	112. 3.87	8302.	70.57	-229.22	5.42	-223.80
MH080	30. 18.71	112. 4.27	8810.	69.55	-230.52	8.41	-222.11
MH081	30. 18.22	112. 4.26	8971.	71.42	-234.13	6.17	-227.96
MH082	30. 18.14	112. 5.01	9073.	72.23	-236.79	9.83	-226.96
MH083	30. 17.10	112. 5.35	8724.	61.20	-235.94	8.01	-227.93
MH084	30. 17.07	112. 4.25	8705.	64.18	-232.32	5.74	-226.58
MH085	30. 16.68	112. 4.12	8754.	65.33	-232.83	5.31	-227.52
MH086	30. 15.99	112. 4.04	8820.	67.24	-233.17	5.09	-228.08
MH087	30. 15.40	112. 4.61	9500.	82.77	-240.80	10.47	-230.33
MH088	30. 15.11	112. 4.75	9441.	81.79	-239.77	10.17	-229.60
MH089	30. 15.71	112. 3.33	8775.	64.69	-234.19	4.87	-229.32
MH090	30. 15.70	112. 2.73	8618.	59.64	-233.89	4.93	-228.96
MH091	30. 15.21	112. 2.66	8713.	59.77	-236.99	5.61	-231.38
MH092	30. 27.51	112. 16.00	6253.	-43.68	-256.66	7.86	-248.80
MH093	30. 27.50	112. 16.76	6442.	-37.85	-257.27	9.01	-248.26
MH094	30. 27.57	112. 17.19	6504.	-34.88	-256.41	10.40	-246.01
MH095	30. 27.70	112. 17.78	6689.	-26.99	-254.82	10.62	-244.20
MH096	30. 28.14	112. 18.91	7942.	17.85	-252.65	8.78	-243.87
MH097	30. 28.15	112. 20.52	8639.	44.12	-250.13	9.37	-240.76
MH098	30. 27.80	112. 21.55	9405.	70.02	-250.32	11.94	-238.38
MH099	30. 26.53	112. 22.40	9785.	86.89	-246.38	12.58	-233.80
MH100	30. 25.72	112. 23.70	10490.	111.33	-245.96	12.05	-233.91
MH101	30. 25.20	112. 23.71	10448.	109.49	-246.37	11.38	-234.99
MH102	30. 24.70	112. 23.85	10791.	120.14	-247.40	13.25	-234.15
MH103	30. 24.23	112. 23.74	10973.	127.68	-246.06	12.56	-233.50
MH104	30. 23.74	112. 23.59	10690.	124.28	-239.82	10.24	-229.58

STATION NUMBER	LATITUDE DEG MIN	LONGITUDE DEG MIN	ELEVATION IN FEET	FREE-AIR ANOMALY	SIMPLE BOUGUER	TERRAIN CORRECTION	COMPLETE BOUGUER
MH705	38. 23.45	112. 23.93	11227.	137.35	-245.04	15.02	-230.02
MH706	38. 22.50	112. 23.93	10814.	126.89	-241.43	11.07	-230.36
MH707	38. 22.36	112. 23.40	10804.	127.29	-240.69	11.99	-228.70
MH708	38. 21.50	112. 23.55	10404.	115.42	-238.94	9.15	-229.79
MH709	38. 18.04	112. 25.90	8498.	61.47	-227.97	5.01	-222.96
MH710	38. 18.90	112. 25.57	9516.	86.34	-237.77	6.54	-231.23
MH711	38. 19.41	112. 25.44	9564.	90.52	-235.23	6.19	-229.04
MH713	38. 18.14	112. 23.13	9212.	81.48	-232.28	6.99	-225.29
MH714	38. 18.34	112. 22.70	9367.	85.99	-233.05	6.80	-226.25
MH715	38. 18.01	112. 21.99	9991.	105.92	-234.38	8.55	-225.83
MH716	38. 18.46	112. 21.87	10222.	110.21	-237.95	8.75	-229.20
MH717	38. 15.45	112. 19.58	9155.	69.96	-241.86	11.06	-230.80
MH718	38. 15.01	112. 18.74	8100.	37.61	-238.27	7.39	-230.88
MH719	38. 15.92	112. 18.20	7300.	11.56	-237.08	6.98	-230.10
MH720	38. 15.54	112. 17.32	6950.	.73	-235.98	5.46	-230.52
MH721	38. 34.94	112. 15.45	5537.	-40.53	-229.12	4.51	-224.61
MH722	38. 34.33	112. 15.90	5664.	-36.52	-229.43	6.31	-223.12
MH723	38. 33.59	112. 16.31	5668.	-38.81	-231.86	9.50	-222.36
MH724	38. 33.28	112. 16.25	5710.	-38.20	-232.88	9.23	-223.65
MH725	38. 31.81	112. 16.19	5817.	-42.95	-241.08	11.08	-230.00
MH726	38. 31.41	112. 15.88	5808.	-44.10	-241.92	7.86	-234.06
MH727	38. 30.68	112. 15.60	5823.	-48.87	-247.20	8.56	-238.64
MH728	38. 30.45	112. 15.46	5811.	-51.93	-249.86	8.60	-241.26
MH729	38. 30.14	112. 15.75	5876.	-52.86	-252.99	11.42	-241.57
MH730	38. 30.09	112. 16.18	6019.	-48.14	-253.15	11.84	-241.31
MH731	38. 29.71	112. 17.06	7148.	-5.96	-249.42	7.37	-242.05
MH732	38. 30.42	112. 17.27	7744.	19.78	-243.99	7.50	-236.49
MH733	38. 30.73	112. 17.77	7903.	28.45	-240.73	6.90	-233.83
MH734	38. 30.91	112. 17.29	7374.	12.25	-238.91	6.33	-232.58
MH735	38. 26.73	112. 15.44	6401.	-37.22	-255.24	4.45	-250.79

STATION NUMBER	LATITUDE DEG MIN	LONGITUDE DEG MIN	ELEVATION IN FEET	FREE-AIR ANOMALY	SIMPLE BOUGUER	TERRAIN CORRECTION	COMPLETE BOUGUER
MH736	38. 26.87	112. 16.12	6624.	-29.63	-255.24	4.57	-250.67
MH737	38. 26.93	112. 17.03	6935.	-19.37	-255.57	6.23	-249.34
MH738	38. 26.51	112. 17.07	6888.	-19.50	-254.10	5.40	-248.70
MH739	38. 26.51	112. 17.66	7091.	-10.84	-252.36	6.77	-245.59
MH740	38. 26.44	112. 18.61	7846.	19.99	-247.32	9.43	-237.89
MH741	38. 26.27	112. 18.37	6627.	-29.21	-254.93	5.09	-249.84
MH742	38. 26.26	112. 19.81	6420.	-37.12	-255.78	4.39	-251.39
MH743	38. 26.49	112. 15.17	6185.	-45.68	-256.35	4.46	-251.89
MH744	38. 25.80	112. 15.24	6303.	-41.82	-256.50	4.06	-252.44
MH745	38. 25.41	112. 15.25	6295.	-42.15	-256.56	4.41	-252.15
MH746	38. 25.62	112. 15.81	6438.	-36.37	-255.65	4.67	-250.98
MH747	38. 25.44	112. 16.35	6650.	-27.56	-254.05	5.62	-248.43
MH748	38. 25.20	112. 16.98	6894.	-15.93	-250.74	6.74	-244.00
MH749	38. 24.73	112. 16.99	7260.	-2.14	-249.42	7.60	-241.82
MH750	38. 25.18	112. 17.69	6960.	-10.77	-247.83	10.15	-237.68
MH751	38. 25.01	112. 18.46	7240.	-4.55	-251.15	19.58	-231.57
MH752	38. 24.77	112. 19.70	7880.	17.45	-250.94	19.44	-231.50
MH753	38. 24.43	112. 19.10	9067.	62.12	-246.70	14.78	-231.92
MH754	38. 23.7.	112. 18.41	10565.	100.03	-259.81	27.46	-232.35
MH755	38. 23.30	112. 18.93	11005.	121.08	-253.75	23.93	-229.82
MH756	38. 23.69	112. 19.42	10568.	110.74	-249.20	18.77	-230.43
MH757	38. 23.79	112. 20.58	10454.	109.11	-246.96	15.92	-231.04
MH758	38. 21.66	112. 19.52	9494.	84.46	-238.91	10.35	-228.56
MH759	38. 22.67	112. 15.42	6824.	-14.81	-247.24	8.12	-239.12
MH760	38. 23.31	112. 16.31	7318.	.12	-249.13	13.41	-235.72
MH761	38. 29.67	112. 18.54	7453.	6.63	-247.22	10.40	-236.82
MH762	38. 28.79	112. 20.44	8228.	33.17	-247.08	8.49	-238.59
MH763	38. 25.18	112. 24.70	12137.	130.72	-282.66	48.20	-234.46
MH764	38. 24.03	112. 24.19	11368.	131.52	-255.67	21.68	-233.99
MH765	38. 23.62	112. 24.58	11182.	127.50	-253.36	21.36	-232.00

STATION NUMBER	LATITUDE DEG MIN	LONGITUDE DEG MIN	ELEVATION IN FEET	FREE-AIR ANOMALY	SIMPLE BOUGUER	TERRAIN CORRECTION	COMPLETE BOUGUER
MH766	30. 24.86	112. 23.11	10315.	107.51	-243.82	11.05	-232.77
MH767	30. 32.00	112. 23.13	6565.	-4.85	-228.45	4.79	-223.66
MH768	30. 31.69	112. 24.49	7097.	6.51	-235.21	4.49	-230.72
MH769	30. 31.12	112. 25.03	7452.	15.22	-238.60	5.46	-233.14
MH770	30. 30.66	112. 25.51	7892.	29.56	-239.24	4.93	-234.31
MH771	30. 31.11	112. 25.94	7815.	29.02	-237.15	3.82	-233.33
MH772	30. 31.55	112. 26.32	7468.	20.68	-233.68	3.47	-230.21
MH773	30. 31.51	112. 25.93	7510.	21.30	-234.49	3.43	-231.06
MH774	30. 30.41	112. 25.97	8352.	42.25	-242.22	7.25	-234.97
MH775	30. 30.61	112. 26.62	8392.	42.25	-243.58	10.06	-233.52
MH776	30. 30.00	112. 26.55	7492.	17.40	-237.78	7.24	-230.54
MH777	30. 29.26	112. 27.03	7412.	15.81	-236.64	7.66	-228.98
MH778	30. 28.48	112. 27.31	7541.	13.95	-242.90	10.82	-232.08
MH779	30. 28.94	112. 27.30	7448.	14.28	-239.40	9.52	-229.88
MH780	30. 29.61	112. 26.37	7997.	36.59	-235.79	5.40	-230.39
MH781	30. 29.26	112. 24.88	9835.	87.58	-247.40	16.43	-230.97
MH782	30. 30.12	112. 24.66	9037.	59.54	-248.26	12.58	-235.68
MH783	30. 29.17	112. 24.52	9532.	81.24	-243.42	10.39	-233.03
MH784	30. 28.49	112. 24.17	9720.	85.88	-245.18	12.25	-232.93
MH785	30. 28.85	112. 23.40	9288.	70.27	-246.08	10.73	-235.35
MH786	30. 29.59	112. 22.83	9856.	80.09	-255.60	17.38	-238.22
MH787	30. 28.29	112. 23.27	10538.	103.13	-255.79	19.36	-236.43
MH788	30. 29.03	112. 22.58	10020.	87.75	-253.53	15.16	-238.37
MH789	30. 29.76	112. 21.88	9090.	65.40	-244.48	7.97	-236.51
MH790	30. 29.26	112. 21.17	10238.	81.70	-267.01	26.91	-240.10
MH791	30. 29.46	112. 23.57	8626.	51.58	-242.22	9.30	-232.92
MH792	30. 29.85	112. 23.70	8274.	41.83	-239.98	7.77	-232.21
MH793	30. 30.14	112. 23.81	7998.	33.28	-239.13	6.97	-232.16
MH794	30. 30.31	112. 23.40	7776.	24.29	-240.56	9.59	-230.97
MH795	30. 30.72	112. 23.37	7464.	17.61	-236.61	8.53	-228.08

STATION NUMBER	LATITUDE DEG MIN	LONGITUDE DEG MIN	ELEVATION IN FEET	FREE-AIR ANOMALY	SIMPLE BOUGUER	TERRAIN CORRECTION	COMPLETE BOUGUER
MH790	30. 31.10	112. 22.75	8105.	38.35	-237.71	7.05	-230.66
MH797	30. 31.22	112. 23.29	7583.	20.47	-237.81	6.14	-231.67
MH798	30. 21.11	112. 17.65	8717.	58.69	-238.21	8.01	-230.20
MH799	30. 20.49	112. 16.46	9231.	66.71	-247.69	17.05	-230.64
MH800	30. 20.48	112. 16.94	9003.	64.94	-241.87	10.41	-231.46
MH801	30. 21.50	112. 16.37	8505.	47.25	-242.43	8.86	-233.57
MH802	30. 21.54	112. 15.80	8656.	46.39	-248.56	14.41	-234.09
MH803	30. 21.08	112. 15.40	7460.	11.68	-242.41	9.67	-232.74
MH804	30. 19.33	112. 18.85	7678.	24.41	-237.16	10.46	-226.64
MH805	30. 16.40	112. 18.24	7540.	20.07	-236.74	7.06	-229.68
MH806	30. 17.14	112. 17.95	7862.	30.92	-234.82	6.09	-228.73
MH807	30. 17.70	112. 18.12	8222.	45.57	-234.47	7.96	-226.51
MH808	30. 16.32	112. 17.98	8345.	50.52	-233.71	7.48	-226.23
MH809	30. 18.43	112. 17.45	8187.	46.11	-232.74	5.42	-227.32
MH810	30. 18.99	112. 17.36	7809.	32.53	-235.49	7.78	-227.71
MH811	30. 15.20	112. 26.12	9317.	78.32	-239.52	9.67	-229.35
MH812	30. 15.00	112. 22.82	10018.	110.04	-231.17	7.69	-223.48
MH813	30. 16.49	112. 22.85	9910.	105.02	-232.52	7.00	-225.52
MH814	30. 15.84	112. 22.02	10238.	111.20	-237.51	8.91	-228.60
MH815	30. 16.02	112. 21.20	9935.	100.45	-237.94	8.44	-229.50
MH816	30. 16.83	112. 21.14	10207.	108.43	-239.22	9.53	-229.69
MH817	30. 17.67	112. 20.86	10585.	117.66	-242.86	13.61	-229.25
MH818	30. 10.12	112. 29.13	7467.	33.44	-220.89	8.07	-212.82
MH819	30. 10.31	112. 26.69	7698.	38.86	-223.33	9.03	-214.30
MH820	30. 10.31	112. 28.07	7927.	45.09	-224.90	7.61	-217.29
MH821	30. 17.47	112. 26.52	8360.	57.37	-227.57	6.31	-221.26
MH822	30. 17.70	112. 26.29	8424.	59.95	-226.97	5.17	-221.80
MH823	30. 17.64	112. 26.34	9290.	85.06	-231.56	6.22	-225.34
MH824	30. 18.15	112. 26.76	9586.	90.95	-235.55	8.55	-227.00
MH825	30. 18.50	112. 29.44	9773.	94.79	-238.06	10.57	-227.51

STATION NUMBER	LATITUDE DEG MIN	LONGITUDE DEG MIN	ELEVATION IN FEET	FREE-AIR ANOMALY	SIMPLE BOUGUER	TERRAIN CORRECTION	COMPLETE BOUGUER
MH026	30. 18.91	112. 29.88	9676.	88.76	-240.81	11.86	-228.95
MH027	30. 19.38	112. 26.06	9149.	78.94	-232.68	5.21	-227.47
MH028	30. 19.18	112. 24.47	9112.	77.18	-233.18	5.40	-227.78
MH029	30. 20.67	112. 24.61	9673.	90.60	-238.86	5.98	-232.88
MH030	30. 18.55	112. 24.42	9157.	75.92	-235.96	5.61	-230.35
MH031	30. 17.37	112. 25.45	9132.	80.94	-230.10	5.16	-224.94
MH032	30. 15.44	112. 25.86	9514.	96.27	-227.78	6.18	-221.60
MH033	30. 33.61	112. 9.71	5959.	-42.26	-245.23	4.50	-240.73
MH034	30. 32.77	112. 9.88	6201.	-32.33	-243.53	4.38	-239.15
MH035	30. 31.83	112. 9.52	6391.	-30.94	-248.62	5.73	-242.89
MH036	30. 31.99	112. 6.83	6715.	-20.26	-248.91	7.50	-241.41
MH038	30. 31.94	112. 7.70	7109.	-6.12	-248.26	13.96	-234.30
MH039	30. 32.77	112. 8.85	6440.	-27.64	-246.98	6.47	-240.51
MH040	30. 32.73	112. 8.35	7009.	-6.66	-245.36	8.22	-237.16
MH041	30. 32.52	112. 7.73	7859.	22.70	-244.96	9.02	-235.96
MH042	30. 32.30	112. 7.38	8345.	38.73	-245.50	11.04	-234.46
MH043	30. 32.02	112. 6.51	8380.	42.54	-242.88	9.31	-233.57
MH044	30. 32.49	112. 6.25	8624.	50.30	-243.44	9.09	-234.35
MH045	30. 35.20	112. 20.28	6214.	-23.60	-235.25	3.64	-231.61
MH046	30. 30.21	112. 20.35	6933.	4.18	-231.96	3.33	-228.63
MH047	30. 35.84	112. 24.22	6785.	-3.28	-234.38	3.55	-230.83
MH048	30. 33.44	112. 24.47	6857.	9.40	-224.15	2.01	-222.14
MH049	30. 34.14	112. 24.48	6992.	14.02	-224.13	1.89	-222.24
MH050	30. 34.71	112. 24.28	6911.	11.16	-224.23	3.19	-221.04
MH051	30. 33.20	112. 24.99	6788.	8.13	-223.07	2.38	-220.69
MH052	30. 33.18	112. 25.52	6748.	5.81	-224.03	3.08	-220.95
MH053	30. 33.24	112. 26.09	6767.	7.13	-223.36	2.66	-220.70
MH054	30. 33.64	112. 25.93	6410.	-3.12	-221.45	4.94	-216.51
MH055	30. 32.25	112. 26.93	6641.	-3.21	-229.41	6.89	-222.52
MH056	30. 32.71	112. 26.86	6560.	-3.33	-226.76	6.21	-220.55

STATION NUMBER	LATITUDE DEG MIN	LONGITUDE DEG MIN	ELEVATION IN FEET	FREE-AIR ANOMALY	SIMPLE BOUGUER	TERRAIN CORRECTION	COMPLETE BOUGUER
MH057	30. 33.41	112. 21.24	6141.	-26.01	-235.17	4.97	-230.20
MH058	30. 33.74	112. 20.85	6391.	-19.19	-236.87	3.25	-233.62
MH059	30. 34.00	112. 20.69	6249.	-24.02	-236.86	3.87	-232.99
MH060	30. 22.15	112. 22.24	12173.	155.39	-259.22	30.98	-228.24
MH061	30. 38.61	112. 24.19	7052.	27.98	-212.21	2.85	-209.36
MH062	30. 39.49	112. 24.95	7102.	34.19	-207.70	2.33	-205.37
MH064	30. 40.50	112. 25.99	7202.	43.20	-202.10	1.85	-200.25
MH065	30. 39.72	112. 27.79	7656.	56.52	-204.24	3.40	-200.84
MH066	30. 38.23	112. 28.71	8036.	60.98	-212.73	4.86	-207.87
MH067	30. 38.72	112. 28.49	7678.	55.00	-206.52	3.59	-202.93
MH068	30. 39.79	112. 27.01	7302.	43.77	-204.93	2.22	-202.71
MH069	30. 41.75	112. 26.46	6978.	43.66	-194.02	2.79	-191.23
MH070	30. 41.55	112. 27.15	7195.	50.99	-194.07	2.43	-191.64
MH071	30. 41.25	112. 27.56	7031.	46.11	-193.37	2.67	-190.70
MH072	30. 39.93	112. 29.08	7019.	41.17	-197.90	3.47	-194.43
MH074	30. 42.08	112. 25.86	6833.	37.87	-194.86	3.13	-191.73
MH075	30. 42.50	112. 3.64	5292.	-57.19	-237.43	3.73	-233.70
MH076	30. 43.64	112. 2.19	5254.	-58.50	-237.45	5.01	-232.44
MH077	30. 44.17	112. 2.04	5257.	-59.52	-238.57	5.16	-233.41
MH078	30. 44.61	112. 1.69	5256.	-58.14	-237.16	3.86	-233.30
MH079	30. 43.52	112. 23.80	6863.	39.88	-193.88	2.77	-191.11
MH080	30. 42.39	112. 21.94	6926.	35.78	-200.12	3.39	-196.73
MH081	30. 42.00	112. 21.44	7353.	45.98	-204.46	5.33	-199.13
MH082	30. 43.19	112. 21.90	6202.	14.98	-196.26	3.94	-192.32
MH083	30. 43.60	112. 21.90	6359.	23.12	-193.47	2.62	-190.85
MH084	30. 43.80	112. 22.94	6433.	26.56	-192.54	2.65	-189.89
MH085	30. 44.59	112. 24.41	6942.	44.80	-191.64	4.77	-186.87
MH086	30. 44.11	112. 24.86	6912.	42.33	-193.09	4.69	-188.40
MH087	30. 44.30	112. 24.46	6772.	38.44	-192.22	3.98	-188.24
MH088	30. 44.00	112. 23.31	6498.	29.30	-192.02	2.78	-189.24

STATION NUMBER	LATITUDE DEG MIN	LONGITUDE DEG MIN	ELEVATION IN FEET	FREE-AIR ANOMALY	SIMPLE BOUGUER	TERRAIN CORRECTION	COMPLETE BOUGUER
MH889	38. 43.43	112. 21.58	6129.	14.54	-194.21	4.93	-189.26
MH890	38. 43.73	112. 21.09	6025.	11.03	-194.18	5.76	-188.42
MH891	38. 43.19	112. 20.33	6816.	36.46	-195.69	4.81	-190.88
MH892	38. 42.74	112. 20.56	6584.	29.08	-195.17	3.81	-191.36
MH893	38. 43.24	112. 20.78	6225.	16.92	-195.10	5.24	-189.86
MH894	38. 44.20	112. 28.00	5742.	5.26	-190.31	8.14	-182.17
MH895	38. 44.50	112. 28.17	5657.	4.13	-188.55	6.05	-182.50
MH896	38. 26.00	112. 23.73	11086.	120.62	-256.97	21.31	-235.66
MH897	38. 26.54	112. 23.66	11650.	125.38	-271.42	35.70	-235.72
MH898	38. 27.07	112. 23.64	11179.	119.55	-261.21	23.86	-237.35
MH899	38. 27.67	112. 24.01	11306.	117.99	-267.09	31.48	-235.61
MH901	38. 25.38	112. 29.26	7875.	21.70	-246.52	7.06	-239.46
MH902	38. 26.93	112. 28.96	9287.	69.22	-247.09	8.46	-238.63
MH903	38. 26.80	112. 28.74	9595.	73.09	-253.71	15.85	-237.86
MH904	38. 26.63	112. 28.34	9676.	74.55	-255.01	14.96	-240.05
MH905	38. 26.05	112. 26.76	8722.	48.95	-248.12	8.06	-240.06
MH906	38. 33.30	112. 05	9412.	90.94	-229.63	5.83	-223.80
MH907	38. 34.52	112. 1.08	9462.	92.89	-229.39	9.66	-219.73
MH908	38. 35.00	112. 1.11	9990.	106.47	-233.79	15.66	-218.13
MH909	38. 35.39	112. 0.97	9678.	103.82	-225.81	9.40	-216.41
MH910	38. 35.73	112. 1.91	9738.	99.68	-232.06	15.96	-216.04
MH911	38. 36.60	112. 2.28	8956.	79.36	-225.66	11.82	-213.86
MH912	38. 18.90	112. 28.21	9856.	95.27	-240.42	11.97	-228.45
MH913	38. 19.10	112. 27.86	9635.	92.64	-235.53	7.90	-227.63
MH914	38. 19.80	112. 27.46	10136.	98.28	-247.02	16.30	-230.72
MH915	38. 20.00	112. 27.20	10085.	98.19	-245.31	14.13	-231.18
MH916	38. 20.21	112. 26.65	10027.	98.53	-242.99	12.80	-230.19
MH917	38. 20.70	112. 26.37	9861.	95.60	-240.27	9.68	-230.59
MH918	38. 20.90	112. 25.74	10229.	106.48	-241.92	10.78	-231.14
MH919	38. 24.20	112. 29.53	9038.	56.03	-251.81	11.70	-240.11

STATION NUMBER	LATITUDE DEG MIN	LONGITUDE DEG MIN	ELEVATION IN FEET	FREE-AIR ANOMALY	SIMPLE BOUGUER	TERRAIN CORRECTION	COMPLETE BOUGUER
MH920	30. 24.41	112. 29.22	9150.	60.53	-251.39	11.93	-239.46
MH921	30. 24.43	112. 28.63	9530.	70.63	-253.96	14.20	-239.76
MH922	30. 24.45	112. 28.24	9780.	76.86	-256.45	17.62	-238.83
MH923	30. 24.55	112. 27.77	10150.	87.55	-258.16	18.82	-239.34
MH924	30. 24.55	112. 27.45	10460.	94.59	-261.95	22.05	-239.90
MH925	30. 25.05	112. 27.01	10573.	95.51	-264.60	25.15	-239.45
MH926	30. 25.75	112. 27.14	9795.	79.20	-254.42	14.01	-240.41
MH927	30. 26.13	112. 27.18	9560.	73.15	-252.67	13.11	-239.56
MH928	30. 26.85	112. 26.84	9360.	66.10	-252.70	13.81	-238.89
MH929	30. 27.24	112. 26.76	9176.	63.99	-248.55	11.40	-237.15
MH930	30. 27.40	112. 26.70	9050.	59.52	-249.00	11.62	-237.38
MH931	30. 26.03	112. 19.78	9961.	86.60	-252.67	20.18	-232.49
MH933	30. 40.94	112. 10.48	5871.	-34.83	-234.79	6.44	-228.35
MH934	30. 40.65	112. 12.04	6067.	-22.37	-229.01	4.31	-224.70
MH935	30. 40.66	112. 14.16	7556.	30.24	-227.12	8.03	-219.09
MH936	30. 40.23	112. 13.90	6805.	5.27	-226.51	6.92	-219.59
MH937	30. 39.65	112. 13.70	6164.	-19.49	-229.43	6.38	-223.05
MH938	30. 39.45	112. 13.46	5738.	-36.94	-232.38	5.41	-226.97
MH939	30. 39.40	112. 12.70	5562.	-42.38	-231.82	4.37.	-227.45
MH940	30. 24.64	112. 25.24	11108.	119.23	-259.11	21.91	-237.20
MH941	30. 24.10	112. 26.00	12075.	126.59	-284.69	51.14	-233.55
MH942	30. 23.41	112. 26.93	10788.	107.12	-260.52	25.00	-235.32
MH943	30. 23.22	112. 27.33	10780.	104.62	-262.55	25.81	-236.74
MH944	30. 23.04	112. 27.81	10843.	106.60	-262.71	28.46	-234.25
MH945	30. 23.13	112. 28.28	10611.	101.23	-260.18	25.22	-234.96
MH946	30. 23.26	112. 28.97	10001.	83.39	-257.24	22.67	-234.57
MH947	30. 23.26	112. 29.44	9328.	66.96	-250.75	13.59	-237.16
MH948	30. 23.43	112. 17.14	8972.	51.97	-253.62	18.41	-235.21
MH949	30. 23.70	112. 16.90	7886.	18.74	-249.86	13.25	-236.61
MH950	30. 20.48	112. 21.18	11053.	134.20	-242.27	14.40	-227.87

STATION NUMBER	LATITUDE DEG MIN	LONGITUDE DEG MIN	ELEVATION IN FEET	FREE-AIR ANOMALY	SIMPLE BOUGUER	TERRAIN CORRECTION	COMPLETE BOUGUER
MH951	38. 20.40	112. 20.64	10606.	124.05	-237.19	11.32	-225.87
MH952	38. 19.89	112. 20.04	10574.	116.10	-244.05	18.69	-225.36
MH953	38. 19.30	112. 21.02	9792.	99.89	-233.62	8.46	-225.16
HF96	38. 15.35	112. 14.60	6248.	-24.85	-237.66	4.04	-233.62
HF100	38. 15.55	112. 16.45	6723.	-7.47	-236.45	5.61	-230.84
HF105	38. 15.43	112. 18.90	8350.	44.19	-240.21	10.16	-230.05
HF512	38. 16.48	112. .20	6754.	5.70	-224.35	3.95	-220.40
HF513	38. 17.00	112. .70	6973.	12.86	-224.64	6.26	-218.38
HF514	38. 17.15	112. 1.80	7327.	21.45	-228.13	9.90	-218.23
HF515	38. 17.35	112. 2.85	7725.	35.16	-227.97	8.16	-219.81
HF519	38. 19.55	112. 2.70	8924.	74.91	-229.04	6.35	-222.69
HF520	38. 20.30	112. 2.45	9262.	82.69	-232.77	8.69	-224.08
HF522	38. 21.60	112. 2.00	9039.	79.32	-228.55	6.34	-222.21
HF524	38. 17.65	112. 4.55	8702.	64.82	-231.57	4.81	-226.76
HF529	38. 25.25	112. 1.30	9193.	81.25	-231.85	4.37	-227.48
HF534	38. 23.90	112. 3.10	8386.	51.82	-233.82	8.42	-225.40
HF539	38. 21.95	112. 7.20	6512.	-14.24	-236.05	4.61	-231.44
HF542	38. 21.15	112. 7.95	6337.	-23.82	-239.66	3.55	-236.11

STATION NUMBER	LATITUDE DEG MIN	LONGITUDE DEG MIN	ELEVATION IN FEET	FREE-AIR ANOMALY	SIMPLE BOUGUER	TERRAIN CORRECTION	COMPLETE BOUGUER
RH010	38. 38.15	112. 5.75	5789.1	-31.11	-228.28	8.52	-219.76
RH020	38. 38.15	112. 5.79	5733.0	-32.70	-227.96	8.69	-219.27
RH030	38. 38.24	112. 5.82	5727.0	-32.85	-227.91	7.71	-220.20
RH040	38. 38.31	112. 5.85	5641.7	-36.33	-228.48	7.47	-221.01
RH050	38. 38.34	112. 5.88	5612.9	-37.89	-229.07	7.35	-221.72
RH060	38. 38.37	112. 5.95	5589.9	-39.56	-229.97	6.94	-223.03
RH070	38. 38.40	112. 5.97	5549.1	-41.59	-230.59	7.08	-223.51
RH080	38. 38.43	112. 6.00	5525.6	-42.85	-231.03	6.73	-224.30
RH090	38. 38.47	112. 6.07	5496.8	-44.29	-231.51	6.61	-224.90
RH100	38. 38.51	112. 6.13	5474.9	-45.53	-232.00	6.39	-225.61
RH110	38. 38.55	112. 6.18	5457.6	-46.58	-232.46	6.30	-226.16
RH120	38. 38.56	112. 6.23	5437.4	-47.71	-232.91	5.84	-227.07
RH130	38. 38.62	112. 6.26	5422.1	-48.74	-233.42	5.69	-227.73
RH140	38. 38.60	112. 6.33	5403.2	-49.91	-233.95	5.61	-228.34
RH150	38. 38.72	112. 6.38	5391.0	-50.95	-234.57	5.55	-229.02
RH160	38. 38.74	112. 6.43	5376.2	-52.08	-235.20	5.41	-229.79
RH170	38. 38.76	112. 6.46	5362.5	-53.23	-235.88	5.33	-230.55
RH180	38. 38.82	112. 6.53	5350.0	-54.35	-236.57	5.26	-231.31
SC000	38. 37.41	112. 5.70	5989.1	-22.21	-226.20	9.10	-217.10
SC010	38. 37.43	112. 5.70	5954.0	-23.27	-226.06	9.16	-216.90
SC020	38. 37.45	112. 5.82	5919.2	-24.51	-226.12	9.07	-217.05
SC030	38. 37.49	112. 5.86	5886.7	-25.59	-226.09	7.46	-218.63
SC040	38. 37.50	112. 5.94	5851.3	-27.18	-226.48	7.00	-218.88
SC050	38. 37.50	112. 6.00	5772.1	-30.36	-226.95	7.55	-219.40
SC060	38. 37.50	112. 6.00	5755.1	-30.83	-226.85	7.18	-219.67
SC070	38. 37.50	112. 6.10	5714.2	-32.46	-227.08	7.25	-219.83
SC080	38. 37.52	112. 6.15	5709.5	-32.86	-227.33	7.37	-219.96
SC090	38. 37.55	112. 6.21	5675.9	-34.33	-227.65	6.90	-220.75
SC100	38. 37.59	112. 6.26	5654.6	-35.58	-228.18	6.82	-221.36
SC110	38. 37.60	112. 6.31	5629.2	-37.15	-228.89	6.64	-222.25

STATION NUMBER	LATITUDE DEG MIN	LONGITUDE DEG MIN	ELEVATION IN FEET	FREE-AIR ANOMALY	SIMPLE BOUGUER	TERRAIN CORRECTION	COMPLETE BOUGUER
SC120	30. 37.67	112. 6.56	5596.7	-38.92	-229.54	6.57	-222.97
SC130	30. 37.71	112. 6.41	5569.5	-40.43	-230.13	6.58	-223.55
SC140	30. 37.74	112. 6.47	5547.2	-41.95	-230.89	6.28	-224.61
SC150	30. 37.75	112. 6.52	5523.1	-43.54	-231.05	5.58	-226.07
SC160	30. 37.81	112. 6.50	5503.0	-44.87	-232.30	5.42	-226.88
SC170	30. 37.85	112. 6.52	5481.5	-46.27	-232.96	5.35	-227.61
SC180	30. 37.85	112. 6.50	5460.5	-47.61	-233.59	5.32	-228.27
SC190	30. 37.91	112. 6.69	5475.3	-47.55	-234.64	5.29	-228.75
MC100	30. 30.42	112. 5.93	5782.4	-31.73	-228.08	10.10	-218.58
MC120	30. 30.40	112. 5.93	5775.7	-31.88	-228.00	9.70	-218.90
MC130	30. 30.50	112. 6.10	5739.5	-33.50	-228.99	9.58	-219.41
MC140	30. 30.50	112. 6.10	5714.1	-34.32	-228.94	9.36	-219.58
MC150	30. 30.60	112. 6.23	5688.0	-35.58	-229.33	9.32	-220.01
MC160	30. 30.60	112. 6.29	5674.4	-36.18	-229.44	8.72	-220.72
MC170	30. 30.65	112. 6.30	5656.0	-37.27	-229.91	8.24	-221.67
MC180	30. 30.60	112. 6.41	5622.3	-38.87	-230.37	8.15	-222.22
MC190	30. 30.72	112. 6.47	5592.6	-40.17	-230.06	7.64	-223.02
MC200	30. 30.74	112. 6.52	5577.1	-41.03	-230.99	6.67	-224.32
MC210	30. 30.70	112. 6.53	5561.7	-41.93	-231.37	6.43	-224.94
MC220	30. 30.81	112. 6.64	5547.2	-42.78	-231.72	6.26	-225.46
MC230	30. 30.84	112. 6.69	5533.2	-43.61	-232.07	6.19	-225.88
MC240	30. 30.87	112. 6.75	5521.2	-44.37	-232.42	6.03	-226.39
MC250	30. 30.91	112. 6.81	5509.1	-45.14	-232.78	5.94	-226.84
MC260	30. 30.93	112. 6.80	5495.1	-45.95	-233.11	5.88	-227.23
MC270	30. 30.96	112. 6.92	5483.2	-46.71	-233.47	5.45	-228.02
MC280	30. 30.98	112. 6.96	5472.4	-47.43	-233.82	5.38	-228.44
MC290	30. 30.93	112. 7.03	5463.9	-48.06	-234.16	5.32	-228.84
MC300	30. 30.95	112. 7.09	5454.3	-48.73	-234.51	5.27	-229.24
MC310	30. 30.93	112. 7.13	5443.0	-49.63	-235.02	5.19	-229.83
J1000	30. 30.57	112. 11.93	5587.7	-41.45	-231.77	3.42	-228.35

STATION NUMBER	LATITUDE DEG MIN	LONGITUDE DEG MIN	ELEVATION IN FEET	FREE-AIR ANOMALY	SIMPLE BOUGUER	TERRAIN CORRECTION	COMPLETE BOUGUER
J1010	30. 36.62	112. 11.93	5608.0	-40.83	-231.65	3.09	-228.76
J1020	30. 36.67	112. 11.99	5582.4	-41.34	-231.47	3.19	-228.23
J1030	30. 36.71	112. 12.02	5561.8	-41.74	-231.17	3.07	-228.10
J1040	30. 36.75	112. 12.06	5512.3	-42.97	-230.73	3.19	-227.54
J1050	30. 36.80	112. 12.09	5498.6	-43.43	-230.72	3.15	-227.57
J1060	30. 36.83	112. 12.11	5482.2	-44.09	-230.81	3.08	-227.73
J1070	30. 36.85	112. 12.13	5455.6	-44.95	-230.77	3.06	-227.71
J1080	30. 36.91	112. 12.16	5441.9	-45.69	-231.04	3.05	-227.99
J1090	30. 36.95	112. 12.21	5427.2	-46.57	-231.42	3.01	-228.41
J1100	30. 37.00	112. 12.25	5424.5	-47.18	-231.94	2.99	-228.95
J1110	30. 37.14	112. 12.29	5422.7	-47.80	-232.50	2.95	-229.55
J1120	30. 37.36	112. 12.35	5422.9	-48.43	-233.11	2.91	-230.20
J1130	30. 37.13	112. 12.37	5423.1	-48.98	-233.69	2.90	-230.79
J1140	30. 37.16	112. 12.41	5422.9	-49.57	-234.28	2.86	-231.42
J2000	30. 36.26	112. 11.95	5576.9	-42.27	-232.22	2.80	-229.42
J2010	30. 36.31	112. 12.00	5576.3	-42.61	-231.94	2.78	-229.16
J2020	30. 36.35	112. 12.05	5566.5	-42.25	-231.85	2.69	-229.16
J2030	30. 36.39	112. 12.10	5556.5	-42.42	-231.75	2.70	-229.05
J2040	30. 36.43	112. 12.15	5557.1	-42.40	-231.68	2.70	-228.98
J2050	30. 36.48	112. 12.20	5530.7	-43.34	-231.72	3.06	-228.66
J2060	30. 36.52	112. 12.25	5456.7	-45.02	-231.55	3.24	-228.31
J2070	30. 36.55	112. 12.30	5447.9	-45.91	-231.46	3.22	-228.24
J2080	30. 36.67	112. 12.34	5440.2	-46.97	-231.36	3.01	-228.35
J2090	30. 36.64	112. 12.38	5434.2	-46.46	-231.55	2.98	-228.57
J2100	30. 36.63	112. 12.43	5432.5	-46.90	-231.93	2.92	-229.01
J2110	30. 36.72	112. 12.45	5431.9	-47.41	-232.42	2.87	-229.55
J2120	30. 36.77	112. 12.53	5435.2	-47.87	-233.00	2.83	-230.17
J2130	30. 36.81	112. 12.56	5432.5	-48.50	-233.53	2.84	-230.69

APPENDIX 6

PRINCIPAL FACTS OF GROUND MAGNETIC DATA

NOTES: 1) Units are as follows:

Station location along profile. meters

- 2) Profiles can be identified by reference to Figures 12 and 13 in the text. Magnetic anomaly values are given with respect to Monroe magnetic base which is arbitrarily assigned a value of zero. "N.D." indicates no data taken due to power line interference.

Profile M77-1

<u>Station</u>	<u>Magnetic Anomaly</u>	<u>Station</u>	<u>Magnetic Anomaly</u>	<u>Station</u>	<u>Magnetic Anomaly</u>
1020SE	-254	180SE	-345	660NW	158
1000SE	-245	160SE	-398	680NW	236
980SE	-219	140SE	-437	700NW	207
960SE	-228	120SE	-449	720NW	222
940SE	-266	100SE	-390	740NW	206
920SE	-271	80SE	-466	760NW	151
900SE	-275	60SE	-456	780NW	133
880SE	-279	40SE	-366	800NW	103
860SE	-263	20SE	-358	820NW	111
840SE	-296	00	-343	840NW	72
820SE	-117	20NW	-431	860NW	89
800SE	-53	40NW	-464	880NW	92
780SE	-69	60NW	-488	900NW	93
760SE	-7	80NW	-506	920NW	31
740SE	+82	100NW	-560	940NW	N.D.
720SE	+104	120NW	-527	960NW	N.D.
700SE	+108	140NW	-676	980NW	N.D.
680SE	-234	160NW	-323	1000NW	N.D.
660SE	-328	180NW	-466	1020NW	N.D.
640SE	-376	200NW	-535	1040NW	N.D.
620SE	-327	220NW	-537	1060NW	N.D.
600SE	-279	240NW	-484	1080NW	N.D.
580SE	-347	260NW	-486	1100NW	N.D.
560SE	-264	280NW	-495	1120NW	64
540SE	-371	300NW	-494	1140NW	59
520SE	-285	320NW	-519	1160NW	67
500SE	-444	340NW	-533	1180NW	49
480SE	-524	360NW	-536	1200NW	49
460SE	-464	380NW	-489	1220NW	40
440SE	-343	400NW	-473	1240NW	58
420SE	-324	420NW	-463	1260NW	62
400SE	-372	440NW	-444	1280NW	98
380SE	-367	460NW	-454	1300NW	137
360SE	-457	480NW	-445	1350NW	113
340SE	-530	500NW	-373	1400NW	95
320SE	-415	520NW	-344	1450NW	156
300SE	-380	540NW	-350	1500NW	178
280SE	-329	560NW	-322	1550NW	200
260SE	-288	580NW	-278	1600NW	206
240SE	-323	600NW	-250	1650NW	160
220SE	-191	620NW	-104	1700NW	156
200SE	-239	640NW	+67	1750NW	139

Profile M77-2

<u>Station</u>	<u>Magnetic Anomaly</u>	<u>Station</u>	<u>Magnetic Anomaly</u>	<u>Station</u>	<u>Magnetic Anomaly</u>
00	-547	620	-406	1240	-312
20	-532	640	-282	1260	-438
40	-555	660	-269	1280	-476
60	-431	680	-108	1300	-514
80	-402	700	-49	1320	-416
100	-436	720	N.D.	1340	-280
120	-420	740	N.D.	1360	-259
140	-459	760	N.D.	1380	-243
160	-447	780	N.D.	1400	-233
180	-398	800	N.D.	1420	-238
200	-458	820	N.D.	1440	-246
220	-398	840	N.D.	1460	-240
240	-599	860	N.D.	1480	-216
260	-452	880	N.D.	1500	-216
280	-483	900	N.D.	1520	-194
300	-359	920	N.D.	1540	-195
320	-313	940	N.D.	1560	-182
340	-292	960	-303	1580	-173
360	-238	980	-332	1600	-152
380	-136	1000	-377	1620	-153
400	-99	1020	-397	1640	-150
420	-268	1040	-453	1660	-152
440	-520	1060	-498	1680	-150
460	-541	1080	-554	1700	-139
480	-577	1100	-527	1720	-160
500	-641	1120	-301	1740	-160
520	-546	1140	-320	1760	-138
540	-513	1160	-465	1780	-133
560	-502	1180	-367	1800	-139
580	-553	1200	-297	1820	-144
600	-447	1220	-215	1840	-145
				1860	-33

Profile M77-3

Profile M77-4

<u>Station</u>	<u>Magnetic Anomaly</u>	<u>Station</u>	<u>Magnetic Anomaly</u>	<u>Station</u>	<u>Magnetic Anomaly</u>
100	-345	100	-297	660	-164
150	-367	120	-333	680	+23
200	-421	140	-332	700	-115
250	-446	160	-288	720	-94
300	-377	180	-212	740	-72
350	-382	200	-5	760	-49
400	-540	220	-238	780	-25
450	-581	240	-241	800	+1
500	-639	260	-294	820	+20
550	-640	280	-364	840	31
600	-508	300	-367	860	55
650	-512	320	-195	880	70
700	-456	340	-475	900	72
750	-448	360	-406	920	82
800	-450	380	-497	940	108
850	-433	400	-390	960	127
900	-383	420	-285	980	142
950	-184	440	-294	1000	155
1000	-95	460	-225	1020	165
1050	-38	480	-284	1040	173
1100	N.D.	500	-312	1060	186
1150	N.D.	520	-300	1080	196
1200	N.D.	540	-304	1100	198
1250	N.D.	560	-296	1120	106
1300	+170	580	-309	1140	204
1350	+178	600	-339	1160	229
1400	163	620	-276	1180	224
1450	197	640	-201	1200	211
1500	198				
1550	222				
1600	212				

Profile M77-5

Profile M77-6

Profile M77-7

<u>Station</u>	<u>Magnetic Anomaly</u>	<u>Station</u>	<u>Magnetic Anomaly</u>	<u>Station</u>	<u>Magnetic Anomaly</u>
00	-487	00	-190	100	+172
50	-649	50	-283	150	+46
100	-578	100	-232	200	-102
150	-251	150	-103	250	+35
200	-296	200	-279	300	+142
250	-344	250	-98	350	92
300	-312	300	-367	400	108
350	-384	350	-225	450	133
400	-378	400	-242	500	184
450	-451	450	-445	550	81
500	-351	500	-347	600	140
550	-226	550	-250	650	181
600	N.D.	600	-131	700	190
650	N.D.	650	+9	750	264
700	-53	700	+30	800	252
750	+3	750	-40	850	266
800	+1	800	+126	900	278
850	+127	850	+276	950	283
900	+197	900	+270	1000	N.D.
950	+295	950	+332	1050	N.D.
1000	298	1000	395	1100	N.D.
1050	275	1050	335	1150	+289
1100	259	1100	N.D.	1200	301
1150	243	1150	N.D.	1250	293
1200	216	1200	+489	1300	292
		1250	493	1350	285
		1300	491	1400	310
		1350	386		
		1400	436		
		1450	419		
		1500	392		
		1550	420		
		1600	411		

Profile M77-8

<u>Station</u>	<u>Magnetic Anomaly</u>
----------------	-------------------------

00	-672
50	-641
100	-486
150	-377
200	-170
250	-285
300	-492
350	-417
400	-177
450	-155
500	-139
550	-95
600	-26
650	-70
700	-2
750	+4
800	+40
850	31
900	64
950	+63
1000	66
1050	104
1100	103
1150	98
1200	108
1250	N.D.
1300	N.D.
1350	N.D.
1400	+103
1450	88
1500	60
1550	44
1600	80
1650	54
1700	53
1750	38
1800	39

Profile M77-10

<u>Station</u>	<u>Magnetic Anomaly</u>
----------------	-------------------------

100	-95
150	-22
200	-23
250	-118
300	-7
350	+13
400	+109
450	142
500	202
550	N.D.
600	N.D.
650	N.D.
700	N.D.
750	321
800	319
850	317
900	311
950	340
1000	335
1050	346
1100	354
1150	349
1200	353
1250	357
1300	365
1350	357
1400	344

Profile M77-14

<u>Station</u>	<u>Magnetic Anomaly</u>
----------------	-------------------------

00	-443
20	-496
40	-545
60	-567
80	-395
100	-322
120	-355
140	-365
160	-229
180	-41
200	-446
220	-435
240	-316
260	-352
280	-313
300	-306
320	-512
340	-580
360	-412
380	-544
400	-333
420	-478
440	-380
460	-537
480	-604
500	-555
520	-470
540	-471
560	-469
580	N.D.
600	N.D.
620	N.D.
640	-347
660	-136
680	-317
700	-378
720	-333
740	-333
760	-361
780	-356
800	-292

Profile M77-14

<u>Station</u>	<u>Magnetic Anomaly</u>
820	+94
840	-377
860	-415
880	-417
900	-383
920	-267
940	-242
960	-265
980	-293
1000	-311
1020	-290
1040	-282
1060	-282
1080	-294
1100	-297
1120	-307
1140	-309
1160	-303
1180	-309
1200	-284
1220	-270
1240	-286
1260	-254
1280	-240
1300	-223
1320	-205
1340	-186
1360	-177
1380	-164
1400	-161
1420	-29
1440	-168
1460	-145
1480	-109
1500	-77
1520	-69
1540	-124
1560	-82
1580	-41
1600	-11
1620	-191

Profile M77-15

<u>Station</u>	<u>Magnetic Anomaly</u>
00	-446
20	-512
40	-467
60	-411
80	-399
100	-397
120	-424
140	-433
160	-415
180	-399
200	-402
220	-444
240	-419
260	-452
280	-450
300	-441
320	-467
340	-503
360	-460
380	-509
400	-287
420	-395
440	-438
460	-565
480	-576
500	-543
520	N.D.

Profile M77-15

<u>Station</u>	<u>Magnetic Anomaly</u>
540	N.D.
560	N.D.
580	N.D.
600	N.D.
620	N.D.
640	N.D.
660	N.D.
680	+227
700	+136
720	+70
740	40
760	34
780	-22
800	-19
820	+19
840	15
860	20
880	29
900	23
920	19
940	52
960	42
980	45
1000	44
1050	66
1100	75
1150	110

Profile M77-16

Profile M77-17

BASE LINE

<u>Station</u>	<u>Magnetic Anomaly</u>	<u>Station</u>	<u>Magnetic Anomaly</u>	<u>Station</u>	<u>Magnetic Anomaly</u>
100	-636	00	-344	00	+67
150	-806	20	-458	50	61
200	-584	40	-471	100	62
250	-502	60	-380	150	53
300	-897	80	-444	200	73
350	-728	100	-317	250	24
400	-597	120	-245	300	6
450	-507	140	-325	350	-34
500	-343	160	-261	400	+16
550	-558	180	-359	450	-13
600	-222	200	-333	500	-98
650	-107	220	-383	550	-143
700	-462	240	-445	600	-122
750	N.D.	260	-392	650	-269
800	-446	280	-328	700	-128
850	-397	300	-527	750	-303
900	-241	320	-547	800	-294
950	-227	340	-529	850	-473
1000	-240	360	-498	900	-251
1050	-193	380	-392	950	-391
1100	-98	400	-322	1000	-428
1150	-99	420	-239	1050	-494
1200	N.D.	440	-202	1100	-493
1250	N.D.	460	-170	1150	(-895)
1300	N.D.	480	-145		
1350	N.D.	500	-107		
1400	-28	520	-80		
1450	+138	540	-44		
1500	+86	560	-40		
1550	131	580	-13		
1600	217	600	+4		
1650	219	620	-9		
1700	227	640	+22		
1750	187	660	+16		
1800	168	680	60		
1850	141	700	39		
1900	126	720	65		
		740	52		
		760	63		
		780	90		
		800	87		

LINE 300

LINE 500

LINE 700

<u>Station</u>	<u>Magnetic Anomaly</u>	<u>Station</u>	<u>Magnetic Anomaly</u>	<u>Station</u>	<u>Magnetic Anomaly</u>
740E	-565	160E	-334	200E	-62
720E	-539	140E	-334	180E	-289
700E	-461	120E	-312	160E	-317
680E	-449	100E	-256	140E	-347
660E	-415	80E	-330	120E	-301
640E	-433	60E	-303	100E	-318
620E	-385	40E	-255	80E	-336
600E	-375	20E	-153	60E	-417
580E	-420	00	-95	40E	-394
560E	-437	20W	-61	20E	-300
540E	-395	40W	-3	00	-115
520E	-491	60W	+14	20W	-454
500E	-273	80W	+31	40W	-474
480E	+173	100W	32	60W	-333
460E	+156	120W	41	80W	-249
440E	0	140W	64	100W	-255
420E	25	160W	51	120W	-288
400E	71	180W	63	140W	-320
380E	60	200W	61		
360E	53	220W	-59		
340E	N.D.	240W	+83		
320E	N.D.	260W	101		
300E	N.D.	280W	105		
280E	N.D.	300W	110		
260E	N.D.	320W	98		
240E	N.D.	340W	93		
220E	49	360W	87		
200E	36	380W	83		
180E	55	400W	75		
160E	+108	420W	61		
140E	-88	440W	64		
120E	+33	460W	51		
100E	-60	480W	60		
80E	+14	500W	62		
60E	-20				
40E	-20				
20E	+1				
00	+12				

LINE 1100		LINE 1300		LINE J1	
<u>Station</u>	<u>Magnetic Anomaly</u>	<u>Station</u>	<u>Magnetic Anomaly</u>	<u>Station</u>	<u>Magnetic Anomaly</u>
480E	-397	200E	-256	00	748
460E	-394	180E	-288	20	743
440E	-422	160E	-320	40	626
420E	-358	140E	-295	60	594
400E	-279	120E	-267	80	445
380E	-252	100E	-241	100	302
360E	-303	80E	-206	120	176
340E	-233	60E	+20	140	-69
320E	-531	40E	+202	160	319
300E	-479	20E	-548	180	492
280E	-466	00	-487	200	588
260E	-473	20W	-352	220	244
240E	-449	40W	-330	240	417
220E	-489	60W	-322	260	648
200E	-535	80W	-256	280	329
180E	-521	100W	-240	300	400
160E	-515	120W	-217	320	412
140E	-425	140W	-205	340	277
120E	-345	160W	-191	360	546
100E	-287	180W	-167	380	632
80E	-257	200W	-151	400	614
60E	-217	220W	-124	420	607
40E	-202	240W	-86	440	658
20E	-172	260W	-101	460	646
00	-140	280W	-76	480	631
20W	-141	300W	-37	500	646
40W	-126	320W	-17		
60W	-141	340W	-34		
80W	-119	360W	-20		
100W	-68	380W	-50		
120W	-108	400W	-32		
140W	-105	420W	-23		
160W	-121	440W	+16		
180W	-117	460W	-1		
200W	-96	480W	+21		
220W	-78	500W	+21		
240W	-67				
260W	-64				

LINE J1		LINE J2		LINE J2	
<u>Station</u>	<u>Magnetic Anomaly</u>	<u>Station</u>	<u>Magnetic Anomaly</u>	<u>Station</u>	<u>Magnetic Anomaly</u>
520	698	00	575	540	335
540	663	25	583	560	301
550	673	50	583	580	239
560	753	75	611	600	392
580	786	100	604	620	491
600	767	120	577	640	470
620	803	140	581	660	451
640	733	160	590	680	452
660	707	180	606	700	492
680	697	200	617	720	494
700	666	220	638	740	498
720	635	240	780	760	494
740	613	260	662	780	476
760	596	280	649	800	478
780	558	300	600	820	486
800	517	320	521	840	482
850	496	340	792	860	502
900	467	360	946	880	494
950	442	380	1049	900	482
1000	407	400	777	950	480
1050	378	420	793	1000	463
1100	459	440	794	1050	443
1150	273	460	706	1100	415
1200	226	480	1793	1150	393
1250	154	500	548	1200	300
1300	132	520	794	1250	342
				1300	315

REFERENCES

- Anderson, J. J., Rowley, P. D., Fleck, R. J., and Nairn, A., 1975, Cenozoic geology of southwestern High Plateaus of Utah: Geol. Soc. America Spec. Paper 160, 88p.
- Armstrong, R. L., 1968, Sevier orogenic belt in Nevada and Utah: Geol. Soc. America Bull., v. 79, p. 429-458.
- Bassett, W. A., Kerr, P. F., Schaeffer, O. A., and Stoenner, R. W., 1963, Potassium-argon dating of the Late Tertiary volcanic rocks and mineralization of Marysvale, Utah: Geol. Soc. America Bull., v. 74, p. 213-220.
- Berry, L. G., and Mason, B., 1959, Mineralogy, W. H. Freeman and Company, San Francisco, 630 p.
- Best, M. T., and Brimhall, W. H., 1974, Late Cenozoic alkalic basaltic magmas in the western Colorado Plateaus and the Basin and Range transition zone, U.S.A., and their bearing on mantle dynamics: Geol. Soc. America Bull., v. 85, p. 1677-90.
- Brown, R. B., 1974, Regional gravity survey of the Sanpete-Sevier Valleys and adjacent areas in Utah: unpublished M.S. thesis, Univ. of Utah, 72 p.
- Brumbaugh, W. D., 1977, Gravity survey of the Cove Fort-Sulphurdale KGRA and the north Mineral Mountains area, Millard and Beaver Counties, Utah: unpublished M.S. thesis, Univ. of Utah, 131 p.
- Butler, B. S., and Gale, H. S., 1912, Alunite - a newly discovered deposit near Marysvale, Utah: U.S. Geol. Survey Bull. 511, 64 p.
- Butler, B. S., Loughlin, G. F., Heikes, V. C., and others, 1920, The ore deposits of Utah: U. S. Geol. Survey Prof. Paper 111, 672 p.
- Callaghan, E., 1938, Preliminary report on the alunite deposits of the Marysvale region, Utah: U.S. Geol. Survey Bull. 886-D, p. 91-134.
- _____, 1939, Volcanic sequence in the Marysvale region in southwest central Utah: Am. Geophys. Union Trans., pt. 3, p. 438-452.
- _____, 1973, Mineral resource potential of Piute County, Utah and adjoining area: Utah Geol. and Mineral Survey Bull. 102, 135 p.

- Callaghan, E. and Parker, R. L., 1961a, Geology of the Monroe quadrangle, Utah: U. S. Geol. Survey Map GQ-155.
- _____, 1961b, Geologic map of part of the Beaver quadrangle, Utah: U. S. Geol. Survey Mineral Inv. Field Studies Map MF-202.
- _____, 1962a, Geology of the Delano Peak quadrangle, Utah: U.S. Geol. Survey Map GQ-153.
- _____, 1962b, Geology of the Sevier Quadrangle, Utah: U.S. Geol. Survey Map GQ-156.
- Carter, J. A., 1978, Regional gravity and aeromagnetic surveys of the Mineral Mountains and vicinity, Millard and Beaver Counties, Utah: unpublished M.S. thesis, Univ. of Utah, 178 p.
- Case, J. E., and Joesting, H. R., 1972, Regional geophysical investigations in the central Colorado Plateau: U. S. Geol. Survey Prof. Paper 736, 31 p.
- Caskey, C. F., and Shuey, R. T., 1975, Mid-tertiary volcanic stratigraphy, Sevier-Cove Fort area, central Utah: Geology, v. 2, no. 1, p. 17-25.
- Christiansen, F. W., 1937, The geology and economic possibilities of the alunite deposits in Sevier and Piute Counties, Utah: unpublished M.S. thesis, Univ. of Utah, 97 p.
- Cook, K. L., Montgomery, J. R, Smith, J. T., and Gray, E. F., 1975, Simple Bouguer gravity anomaly map of Utah: Utah Geol. and Mineral Survey Map 37.
- Cook, K. L., Nilsen, T. H., and Lambert, J. F., 1971, Gravity base station network in Utah - 1967: Utah Geol. and Mineral Survey Bull. 92.
- Crebs, T. J., 1976, Gravity and ground magnetic surveys of the central Mineral Mountains, Utah: unpublished M.S. thesis, Univ. of Utah, 129 p.
- Crosby, G. W., 1959, Geology of the South Pavant Range, Millard and Sevier Counties, Utah: Brigham Young Univ. Research Studies, Geology Series, v. 6, No. 3, 59 p.
- _____, 1972, Dual origin of Basin and Range faults, in Plateau-Basin and Range transition zone, central Utah: Utah Geol. Assoc. Publ. no. 2.

- Cunningham, C. G., and Steven, T. A., 1977, Mount Belknap and Red Hills calderas and associated rocks, Marysvale volcanic field, west-central Utah: U.S. Geol. Survey open-file report 77-568, 40 p.
- Cunningham, C. G., Steven, T. A., and Naeser, C. W., 1978, Preliminary structural and mineralogical analysis of the Deer Trail Mountain-Alunite Ridge mining area, Utah: U.S. Geol. Survey open-file report 78-314.
- Dutton, C. E., 1880, Report on the geology of the High Plateaus of Utah: U.S. Geog. and Geol. Survey Rocky Mtn. Region, 307 p.
- Eaton, G. P., Christiansen, R. L., Iyer, H. M., Pitt, A. M., Mabey, D. R., Blank, H. R., Zietz, I., and Gettings, M. E., 1975, Magma beneath Yellowstone National Park: Science, v. 188, p. 787-188.
- Eardley, A. J., and Beutner, E. L., 1934, Geomorphology of Marysvale Canyon and vicinity, Utah: Utah Acad. Sciences Proc., v. 11, p. 149-159.
- Eppich, G. K., 1973, Aeromagnetic survey of south-central Utah: unpublished M.S. thesis, Univ. of Utah, 78 p.
- Fenneman, N. M., 1928, Physiographic divisions of the U.S.: Assoc. Am. Geographers Annals, v. 18, pp. 261-353.
- _____, 1951, Physical divisions of the United States: U.S. Geol. Survey, Physical Div. Map.
- Fishman, H. S., 1976, Geologic structure and regional gravity of a portion of the High Plateaus of Utah: unpublished M.S. thesis, Univ. of Utah, 134p.
- Gardner, S., Williams, J. M., and Brougham, G. W., 1976, Audio magnetotelluric data log and station location map for Monroe-Joseph KGRA, Utah: U.S. Geol. Survey open-file report 76-411.
- Gilbert, G. K., 1875, Report upon the geology of portions of Nevada, Utah, California, and Arizona, examined in the years 1871 and 1872: U. S. Geog. and Geol. Surveys W. 100th Mer., v. 3, p. 21-187.
- _____, 1928, Studies of Basin Range structure: U. S. Geol. Survey Prof. Paper 153, 92p.
- Gregory, H. E., 1944, Geologic observations in the upper Sevier River Valley: Am. Jour. Sci., v. 242, p. 277-606.

- _____, 1945, Post-Wasatch Tertiary formations in southwestern Utah: Jour. Geology, v. 53, p. 105-115.
- _____, 1949, Geologic and geographic reconnaissance of eastern Markagunt Plateau, Utah: Geol. Soc. America Bull., v. 60, p. 969-998.
- _____, 1951, The geology and geography of the Paunsaugunt region, Utah: U.S. Geol. Survey Prof. Paper 226, 115 p.
- Halliday, M. E., Cook, K. L., and Sontag, R. J., 1978, Gravity and magnetic surveys as an aid to geothermal exploration in the Monroe-Marysvale area and vicinity, Utah: Geol. Society of America Abstracts with Programs, v. 10, no. 5, p. 217.
- Hardman, Elwood, 1964, Regional gravity survey of central Iron and Washington Counties, Utah: unpublished M.S. thesis, University of Utah, 107 p.
- Henderson, R. G., and Cordell, L., 1971, Reduction of unevenly spaced potential field data to a horizontal plane by means of finite harmonic series: Geophysics, v. 36, p. 856-866.
- Hilpert, L. S., and Roberts, R. J., 1964, Geology-Economic Geology, in. U. S. Geol. Survey, Mineral and water resources of Utah: U. S. 88th Cong., 2nd sess., p. 28-38.
- Hintze, L. F., 1963, (compiler), Geologic map of southwestern Utah: Utah Geol. and Mineral Survey.
- _____, 1973, Geologic history of Utah: Brigham Young Univ. Geology Studies, v. 20, pt. 3, 181 p.
- Jackson, W. H., and Pakiser, L. C., 1965, Seismic study of crustal structure in the Southern Rocky Mountains: U. S. Geol. Survey Prof. Paper 525-D, p. D85-D92.
- Kane, M. F., 1962, A comprehensive system of terrain corrections using a digital computer: Geophysics, v. 27, p. 455-462.
- Kane, M. F., Mabey, D. R., and Brace, R., 1976, A gravity and magnetic investigation of the Long Valley Caldera, Mono County, California: Jour. Geophy. Research, v. 81, no. 5, p. 754-762.
- Karig, D. E., 1965, Geophysical evidence of a caldera at Bonanza, Colorado: U.S. Geol. Survey Prof. Paper 525-B, p. B9-B12.

- Keller, G. R., Smith, R. B., and Braile, L. W., 1975, Crustal structure along the Great Basin-Colorado Plateau transition from seismic refraction studies: Jour. Geophy. Res., v. 80, p. 1093-1098.
- Kennedy, R. R., 1960, Geology between Pine (Bullion) Creek and Tenmile Creek, eastern Tushar Range, Piute Co., Utah: Brigham Young Univ. Research Studies, Geol. Ser., v. 7, no. 4, 58 p.
- _____, 1963a, Geology of Piute Co., Utah: Ph.D. dissertation, Univ. of Arizona, 282 p.
- _____, 1963b, Sedimentary stratigraphy of the Tushar Range, Piute County, Utah, in Guidebook to Geol. of southwestern Utah, 12th annual field conf., Intermtn. Assoc. Pet. Geologists, p.
- Kerr, P. F., 1963, Geological features of the Marysvale uranium area, Utah, in Guidebook to the Geol. of southwestern Utah, 12th annual field conf., Intermtn. Assoc. Pet. Geologists, p. 125-135.
- Kerr, P. F., Brophy, G. P., Dahl, H. M., Green, J., and Woolard, C. E., 1957, Marysvale, Utah, uranium area: Geol. Soc. America Spec. Paper 64, 212 p.
- Linsser, H., 1967, Investigation of tectonics by gravity detailing: Geophys. Prosp., v. 15, p. 480-515.
- Loughlin, G. F., 1915, Recent alunite developments near Marysvale and Beaver, Utah: U.S. Geol. Survey Bull. 620-K, p. 237-270.
- Mackin, J. H., 1960a, Structural significance of Tertiary volcanic rocks in southwestern Utah: Am. Jour. Sci., v. 258, p. 81-131.
- _____, 1960b, Eruptive tectonic hypothesis for the origin of Basin-Range structure: Geol. Soc. America Bull., v. 71, p. 1921.
- Maxey, G. B., 1946, Geology of part of the Pavant Range, Millard County, Utah: Am. Jour. Sci., v. 244, p. 324-356.
- Mollov, M. W., and Kerr, P. F., 1962, Tushar uranium area, Marysvale, Utah: Geol. Soc. America Bull., v. 73, p. 211-236.
- Montgomery, J. R., 1973, A regional gravity survey of western Utah: unpublished Ph.D. dissertation, Univ. of Utah, 142 p.
- Moody, J. D., 1966, Crustal shear patterns and orogenesis: Tectono-physics, v. 3, p. 479-522.

- Moody, J. D., and Hill, M. J., 1956, Wrench-fault tectonics: Geol. Soc. America Bull., v. 67, p. 1207-1246.
- Moore, J. G., 1960, Curvature of normal faults in the Basin and Range province of western U.S., U. S. Geol. Survey Prof. Paper 400-B, p. B409-B411.
- Mundorff, J. C., 1970, Major thermal springs of Utah: Utah Geol. and Mineral Survey Water Resources Bull. 13.
- Nettleton, L. L., 1976, Gravity and Magnetics in oil prospecting: McGraw-Hill Book Company, New York, 464 p.
- Nolan, T. B., 1943, The Basin and Range province in Utah, Nevada, and California: U. S. Geol. Survey Prof. Paper 197-D, p. 141-196.
- Olson, T. L., 1976, Seismicity of the Roosevelt Hot Springs and Cove Fort areas, Beaver and Millard Counties, Utah: unpublished M.S. thesis, Univ. of Utah.
- Pakiser, L. C., 1964, Gravity, volcanism, and crustal structure in the southern Cascade Range, California: Geol. Soc. America Bull., v. 75, p. 611-620.
- Parry, W. T., Benson, N. L. and Miller, C. D., 1976, Geochemistry and hydrothermal alteration at selected Utah Hot Springs: Final Report NSF Grant GI-43741, v. 3, 131 p.
- Plouff, D., 1977, Preliminary documentation for a FORTRAN program to compute gravity terrain corrections based on topography digitized on a geographic grid: U.S. Geol. Survey open-file report 77-535.
- Plouff, D., and Pakiser, L. C., 1972, Gravity study of the San Juan Mountains, Colorado: U.S. Geol. Survey Prof. Paper 800-B, p. B183-B190.
- Ritzma, H. R., 1972, Six Utah "hingeline" wells, in Plateau-Basin and Range transition zone, central Utah, 1972: Utah Geol. Assoc. Publ. 2, p. 75-80.
- Ross, C. S., and Smith, R. L., 1961, Ash-flow tuffs: their origin, geologic relations, and identification: U.S. Geol. Survey Prof. Paper 366, 81 p.
- Rowley, P. D., 1968, Geology of the southern Sevier Plateau, Utah: Ph.D. dissertation, Univ. of Texas, 327 p.
- Rowley, P. D., Anderson, J. J., and Williams, P. L., 1975, A summary of Tertiary volcanic stratigraphy of the southwestern High Plateaus and adjacent Great Basin, Utah: U. S. Geol. Survey Bull. 1405-B.

- Rowley, P. D., Anderson, J. J., Williams, P. L., and Fleck, R. L., 1978, Age of structural differentiation between the Colorado Plateaus and Basin and Range provinces in southwestern Utah: *Geology*, v. 6, p. 51-55.
- Rowley, P. D., Lipman, P. W., Mehnert, H. H., Lindsey, D. A., and Anderson, J. J., 1978, Blue ribbon lineament, an east-trending structural zone within the Pioche mineral belt of southwestern Utah and eastern Nevada: *U. S. Geol. Survey Jour. Research*, v. 6, no. 2, p. 175-192.
- Sandberg, C. H., 1958, Terrain corrections for an inclined plane in gravity computations: *Geophysics*, v. 23, p. 701-711.
- Sbar, M., Barazangi, M., Dorman, J., Scholz, C. H., and Smith, R., 1972, Tectonics of the Intermountain Seismic Belt, western U. S.: *Geol. Soc. America Bull.*, v. 83, p. 13-27.
- Schellinger, D. K., 1972, Curie-depth determination in the High Plateaus, Utah: unpublished M.S. thesis, Univ. of Utah, 176 p.
- Schneider, M. C., 1964, Geology of the Pavant Mountains west of Richfield, Sevier County, Utah: *Brigham Young Univ. Geology Studies*, v. 11, p. 129-139.
- Selk, D. C., 1976, Crustal and upper-mantle structures in Utah as determined by gravity profiles: unpublished M.S. thesis, Univ. of Utah, 81 p.
- Scholz, C. H., Barazangi, M., and Sbar, M. L., 1971, Late Cenozoic evolution of the Great Basin, Western U.S., as an ensialic interarc basin: *Geol. Soc. America Bull.*, v. 82, p. 2979.
- Shuey, R. T., and Pasquale, A. S., 1973, End corrections in magnetic profile interpretation: *Geophysics*, v. 38, p. 507-512.
- Shuey, R. T., Schellinger, D. K., Johnson, E. H., and Alley, L. B., 1973, Aeromagnetics and the transition between the Colorado Plateau and the Basin and Range province: *Geology*, v. 1, p. 107-112.
- Smith, J. T., 1973, An interpretation of gravity anomalies in north eastern Utah: unpublished M.S. thesis, University of Utah, 74 p.
- Smith, R. B., and Sbar, M. L., 1974, Contemporary tectonics and seismicity of the western United States with emphasis on the Intermountain Seismic Belt: *Geol. Soc. America Bull.*, v. 85, p. 1205-1218.
- Smith, R. B., 1977, Intraplate tectonics of the western North America plate: *Tectonophysics*, v. 37, p. 323-336.

- Smith, R. B., and Eaton, G. P., eds., 1978, Cenozoic Tectonics and regional geophysics of the Western Cordillera: Geol. Soc. America Memoir 152, in press.
- Snow, J. H., 1978, A study of structural and tectonic patterns as interpreted from gravity and aeromagnetic data, unpublished M.S. thesis, Univ. of Utah, 206 p.
- Sontag, R. J., 1965, Regional gravity survey of parts of Beaver, Millard, Piute, and Sevier Counties, Utah: unpublished M.S. thesis, Univ. of Utah, 32 p.
- Spieker, E. M., 1946, Late Mesozoic and early Cenozoic history of central Utah: U.S. Geol. Survey Prof. Paper 205-D, p. 117-161.
- _____, 1949, Transition between the Colorado Plateau and the Great Basin in central Utah: Guidebook to the geology of Utah, no. 4, Utah Geol. Soc., 106 p.
- Steven, T. A., Cunningham, C. G., Naeser, C. W., and Mehnert, H. H., 1977, Revised stratigraphy and radiometric ages of volcanic rocks and mineral deposits in the Marysvale area, west-central Utah: U.S. Geol. Survey open-file report 77-569, 45p.
- Steven, T. A., and Lipman, P. W., 1976, Calderas of the San Juan Volcanic field, southwestern Colorado: U.S. Geol. Survey Prof. Paper 958, 35 p.
- Steven, T. A., Rowley, P. D., and Cunningham, C. G., 1978, Geology of the Marysvale volcanic field, west central Utah: Brigham Young Univ. Geology Studies, v. 25, part 1, p. 67-70.
- Stewart, J. H., 1971, Basin and Range structure: A system of horsts and grabens produced by deep-seated extension: Geol. Soc. America Bull., v. 82, p. 1019-1044.
- Stewart, J. H., Moore, W. J., and Zietz, I., 1977, East-west patterns of Cenozoic igneous rocks, aeromagnetic anomalies, and mineral deposits, Nevada and Utah: Geol. Surv. America Bull., v. 88, p. 67-77.
- Stokes, W. L., 1965, Tectonic history of southwest Utah: Utah Geol. Society Guidebook to the Geol. of Utah No. 19, p. 3-11.
- _____, 1968, Relation of fault trends and mineralization, eastern Great Basin, Utah: Econ. Geology, v. 1, 63, p. 751.
- _____, 1972, Stratigraphic problems of the Triassic and Jurassic sedimentary rocks of Central Utah, in Plateau-Basin and Range transition zone, central Utah: Utah Geol. Assoc. Publication No. 2.

- _____, 1976, What is the Wasatch Line?: in Rocky Mountain Assoc. Geologists - 1976 symposium, p. 11-25.
- _____, 1977, Subdivision of the major physiographic provinces in Utah: Utah Geology, v. 4, no. 1, p. 1-17.
- Stokes, W. L., and Heylmun, E. B., 1963, Tectonic history of south-western Utah: Intermountain Assoc. of Petrol. Geologists 12th annual field conference.
- Swick, C. H., 1942, Pendulum gravity measurements and isostatic reductions: U.S. Coast and Geodetic Survey Spec. Pub. 232.
- Talwani, M., 1965, Computation with help of a digital computer of magnetic anomalies caused by bodies of arbitrary shape: Geophysics, v. 30, p. 797-817.
- Talwani, M., Worzel, J. L., and Landisman, M., 1959, Rapid gravity computations for two-dimensional bodies with application to the Mendocino submarine fracture zone: Jour. Geophys. Research, v. 64, p. 49-59.
- Thompson, G. A., and Burke, D. B., 1974, Regional geophysics of the Basin and Range province: Earth and Planetary Science Annual Review, v. 2, p. 213-238.
- Vajk, R., 1956, Bouguer corrections with varying surface density: Geophysics, v. 21, p. 1004-1020.
- Ward, S. H., 1977, Geothermal exploration architecture: Technical Report ERDA Grant EY-76-S-07-1601, v. 77-2, 19 p.
- Wender, L. E., 1976, Chemical and mineralogical evolution of the Cenozoic volcanics of the Marysvale, Utah area: unpublished M.S. thesis, Univ. of Utah, 57p.
- White, D. E., and Williams, D. L., 1975, Assessment of geothermal resources of the United States - 1975: U.S. Geol. Survey Circ. 726, 155p.
- Willard, M. E., and Callaghan, E., 1962, Geology of the Marysvale quadrangle, Utah: U.S. Geol. Survey Map GQ-154.
- Williams, P. L. and Hackman, R. J., 1971, Geology, structure and uranium deposits of the Salina quadrangle, Utah: U. S. Geol. Survey Map I-591.
- Yokoyama, I., 1958, Gravity survey on Kuttyaro Caldera Lake: Jour. Physics of the Earth, v. 6, p. 75-79.

Zietz, I., Shuey, R. T., and Kirby, J. R., Jr., 1976, Aeromagnetic map
of Utah: U.S. Geol. Survey Map GP-907.

VITA

Name	Mark Everett Halliday
Birthdate	May 9, 1952
Birthplace	Oakland, California
High School	Central Bucks High School Doylestown, Pennsylvania
University 1970-1974	Willamette University Salem, Oregon
Degree 1974	B.S. in Physics Willamette University Salem, Oregon
Professional Organizations 1976-1978	Society of Exploration Geophysicists, student member
Professional Positions summer 1976	Geophysicist Noranda Exploration U.S.A. Anchorage, Alaska
Research Assistant 1977-1978	Department of Geology and Geophysics University of Utah Salt Lake City, Utah
Graduate Study 1975-1978	University of Utah Salt Lake City, Utah
Honors 1976-1977	ASARCO Graduate Fellowship in Geophysics University of Utah

Distribution List - External

James K. Applegate
Department of Geology
Boise State University
Boise, ID 83725

Carl F. Austin
c/o Geothermal Technology
Code 2661, NWC
China Lake, CA 93555

Larry Ball
DOE
Division of Geothermal Energy
3rd Floor
20 Massachusetts Ave., N.W.
Washington, DC 20545

David D. Blackwell
Southern Methodist University
Department of Geological Sciences
Dallas, TX 75275

C. M. Bonar
Director, Geothermal Projects
Atlantic Richfield Co.
P.O. Box 1829
Dallas, TX 75221

William D. Brumbaugh
Geophysics Bldg., Room 12
Interpretation Group
Conoco
Ponca City, OK 74601

Bob Christiansen
U.S. Geological Survey
345 Middlefield Road
Menlo Park, CA 94205

Jim Combs
Geothermal Services, Inc.
10072 Willow Creek Rd.
San Diego, CA 92131

Sam Arentz, Jr., President
Steam Corporation of America
1720 Beneficial Life Tower
Salt Lake City, UT 84111

Lawrence Axtell
Geothermal Services, Inc.
10072 Willow Creek Rd.
San Diego, CA 92131

Ronald Barr
Earth Power Corporation
P.O. Box 1566
Tulsa, OK 74101

Gunnar Bodvarsson
Oregon State University
School of Oceanography
1377 N.W. Alta Vista Dr.
Corvallis, OR 97330

Rudolf A. Black
DOE
Director of Div. of Geothermal Energy
3rd Floor
20 Massachusetts Ave., N.W.
Washington, DC 20545

Glen Campbell
Geothermal Supervisor
Gulf Min. Resource Company
1720 South Bell Aire St.
Denver, CO 80222

Eugene V. Ciancanelli
Consulting Geologist
12352 Escala Drive
San Diego, CA 92128

F. Dale Corman, President
O'Brien Resources, Inc.
49 Toussin Avenue
Kentfield, CA 94904

Ritchie Coryell
Program Manager
National Science Foundation
1800 G Street, N.W.
Washington, DC 20050

Gary Crosby
Phillips Petroleum Company
71-C PRC
Bartlesville, OK 74003

K. R. Davis
Thermal Power Co.
601 California Street
San Francisco, CA 94108

Katie Dixon
3781 Lois Lane
Salt Lake City, UT 84117

John E. Dooley
R. F. Smith Corp.
552 E. 3785 S.
Salt Lake City, UT 84106

Robert C. Edmiston
District Supervisor
Chevron Resources Company
P.O. Box 3722
San Francisco, CA 94119

Val A. Finlayson
Research Engineer
Utah Power and Light Company
1407 West North Temple
Salt Lake City, UT 84110

Ron Forrest, Geologist
Phillips Petroleum Co.
P.O. Box 858
Milford, UT 84751

Gary Galyardt
U.S. Geological Survey
MS 602
Box 25046, Federal Center
Denver, CO 80225

R. Corwin
Dept. Eng. Geoscience
University of California @ Berkeley
Berkeley, CA 94720

C. G. Cunningham
U.S. Geological Survey
Box 25046, Mail Stop 907
Denver Federal Center
Denver, CO 80225

Lucy DeLuke
Main Street
Marysvale, UT 84750

William Dolan
Chief Geophysicist
Amax Exploration Inc.
4704 Harlan Street
Denver, CO 80212

Earth Sciences Division Library
Building 90
University of California
Lawrence Berkeley Laboratory
1 Cyclotron Road
Berkeley, CA 94720

Samuel M. Eisenstat, President
Geothermal Exploration Co., Inc.
400 Park Ave.
New York City, NY 10022

Milton Fisher
295 Madison Avenue
New York City, NY 10017

Frank Frischknecht
Box 25046, Denver Federal Center
U.S. Geological Survey
Denver, CO 80225

N. Sylvia Goeltz
UV Industries, Inc.
19th Floor, University Club Bldg.
Salt Lake City, UT 84111

N. E. Goldstein
Lawrence Berkeley Laboratory
Building 90
University of California, Berkeley
Berkeley, CA 94720

Bob Greider, V. P. Exploration
Intercontinental Energy Co.
P.O. Box 17529
Denver, CO 80217

Glenn Halliday
3043 Brighton Place
Salt Lake City, UT 84121

Dee C. Hansen
Utah State Engineer
442 State Capitol
Salt Lake City, UT 84114

Gerald W. Huttner, Sr. Geologist
Intercontinental Energy Corporation
7503 Marin Dr., Suite 1-C
Englewood, CO 80110

Norris Jensen
General Delivery
Monroe, UT 84754

Richard L. Jodry
P.O. Box 941
Richardson, TX 75080

George Keller
Professor and Head
Department of Geophysics
Colorado School of Mines
Golden, CO 80401

Mark Landisman
Professor of Geophysics
University of Texas, Dallas
Box 688
Richardson, TX 95080

Steven M. Goldstein
The Mitre Corporation
Metrek Division
1820 Dolley Madison Blvd.
McLean, VA 22101

J. H. Hafenbrack
Exxon Co. USA
P.O. Box 120
Denver, CO 80201

Mark Halliday
c/o Resource Associates of Alaska
3230 Airport Way
Fairbanks, AK 99706

Norman Harthill
Executive Vice President
Group Seven, Inc.
1301 Arapahoe St., Suite 300
Golden, CO 80401

Laurence P. James
2525 South Dayton Way #1406
Denver, CO 80231

George R. Jiracek
Department of Geology
University of New Mexico
Albuquerque, NM 87131

Paul Kasameyer
Lawrence Livermore Lab, L-224
P.O. Box 808
Livermore, CA 94550

James B. Koenig
Geothermex
901 Mendocino Avenue
Berkeley, CA 94704

Guy W. Leach, Geologist
Oil Development Company of Texas
Box 12053, American National Bank Bldg.
Amarillo, TX 79101

Dick Lenzer
Phillips Petroleum Company
P.O. Box 752
Del Mar, CA 92014

James O. McClellan, President
Geothermal Electric Systems Corp.
P.O. Box 17574
Salt Lake City, UT 84117

Robert B. McEuen
Woodward Clyde Consultants
Three Embarcadero Center, Suite 700
San Francisco, CA 94111

Don C. McMillan
Utah Geological & Mineral Survey
606 Blackhawk Way, Research Park
Salt Lake City, UT 84108

Skip Matlick
Republic Geothermal
P.O. Box 3388
Santa Fe Springs, CA 90670

Tsvi Meidav
Consultant
40 Brookside Ave.
Berkeley, CA 94705

Frank G. Metcalfe, Pres.
Geothermal Power Corporation
1127 Grant Ave., Suite 6
P.O. Box 1186
Novato, CA 94947

Jerry Montgomery
ASARCO Inc.
Geophysical Office
3422 S. 700 W.
Salt Lake City, UT 84119

Frank Morrison
Professor of Geophysics Eng.
University of California
Hearst Mining Building
Berkeley, CA 94720

L. J. Patrick Muffler
U.S. Geological Survey
345 Middlefield Road
Menlo Park, CA 94205

Clayton Nichols
DOE
Division of Geothermal Energy
3rd Floor
20 Massachusetts Ave., N.W.
Washington, DC 20545

Carel Otte
President of Geothermal Division
Union Oil Company
P.O. Box 7600
Los Angeles, CA 90051

Wayne Peebles
Dept. of Geological Sciences
Southern Methodist University
Dallas, TX 75221

Donald Plouff
U.S. Geological Survey
345 Middlefield Road
Menlo Park, CA 94025

Alan O. Ramo
Sunoco Energy Development Co.
12700 Park Central Pl.
Suite 1500, Box 9
Dallas, TX 75251

Robert W. Rex, President
Republic Geothermal, Inc.
11823 E. Stauson Ave., Suite 1
Santa Fe Springs, CA 90670

Jack Salisbury
DOE
Division of Geothermal Energy
3rd Floor
20 Massachusetts Ave., N.W.
Washington, DC 20545

Konosuke Sato
Metal Mining Agency of Japan
Tokiwa Bldg.
1-24-14 Toranomon
Minato-Ku, Tokyo
JAPAN

John V. A. Sharp
Hydrosearch, Inc.
333 Flint Street
Reno, NV 89501

Wayne Shaw
Getty Oil Company
P.O. Box 5237
Bakersfield, CA 93308

Gregory L. Simay
City of Burbank - Public Service Dept.
164 West Magnolia Blvd.
Burbank, CA 91503

W. P. Sims
DeGolyer and MacNaughton
One Energy Square
Dallas, TX 75206

H. W. Smith
Department of Electrical Engg.
University of Texas, Austin
Austin, TX 78712

T. A. Steven
U.S. Geological Survey
Denver Federal Center
Denver, CO 80225

Paul V. Storm
California Energy Company, Inc.
Wells Fargo Bldg., Suite 300
P.O. Box 3909
Santa Rosa, CA 95402

Chandler Swanberg
New Mexico State University
P.O. Box 4408
University Park Dr.
Las Cruces, NM 88003

Charles M. Swift, Jr.
Chevron Oil Co.-Minerals Staff
P.O. Box 3722
San Francisco, CA 94105

J. B. Syptak
Anadarko Production Co.
P.O. Box 1330
Houston, TX 77001

Bernard Tillement
Aquitaine Co. of Canada
2000 Aquitaine
540 5th Avenue, S.W.
Calgary, Alberta
Canada

Ronald Toms
DOE
Division of Geothermal Energy
3rd Floor
20 Massachusetts Ave., N.W.
Washington, DC 20545

John Tsiaperas
Shell Oil Company
Box 831
Houston, TX 77001

Jack Von Hoene
Davon, Inc.
250 North 100 West
Milford, UT 84751

D. Roger Wall, Geologist
Geothermal Resources Division
Aminoil USA, Inc.
1250 Coddington Center
Santa Rosa, CA 95401

Paul Walton, President
American Geological Enterprises, Inc.
1102 Walker Bank Bldg.
Salt Lake City, UT 84111

Ed Witterholt
City Services Oil Company
Energy Research Laboratory
Box 50408
Tulsa, OK 74150

William B. Wray, Jr.
VanCott, Bagley, Cornwall & McCarthy
141 East 1st South
Salt Lake City, UT 84111

Paul C. Yuen
University of Hawaii @ Manoa
2540 Dole Street, Holmes 240
Honolulu, HI 96822

S. H. Yungul
Chevron Resources Co.
P.O. Box 3722
San Francisco, CA 94119

Elliot J. Zais
Elliot Zais & Associates
7915 N.W. Siskin Dr.
Corvallis, OR 97330